Measurement of the production cross-section of #(2S) → [J over #](→μ[superscript +] μ[superscript –]) π[superscript +] π [superscript –] in pp collisions at √s = 7 TeV at ATLAS

Citation: Aad, G., B. Abbott, J. Abdallah, S. Abdel Khalek, O. Abdinov, R. Aben, B. Abi, et al. "Measurement of the Production Cross-Section of ψ(2S) → [J over ψ](→μ[superscript +] μ[superscript –]) π[superscript +] π [superscript –] in Pp Collisions at √s = 7 TeV at ATLAS." J. High Energ. Phys. 2014, no. 9 (September 2014).

As Published: http://dx.doi.org/10.1007/jhep09(2014)079

Publisher: Springer-Verlag

Persistent URL: http://hdl.handle.net/1721.1/92565

Version: Final published version: final published article, as it appeared in a journal, conference proceedings, or other formally published context

Published for SISSA by Springer

Received: *July 22, 2014*
Accepted: *August 16, 2014*
Published: *September 12, 2014*

Measurement of the production cross-section of $\psi(2S) \to J/\psi(\to \mu^+\mu^-)\pi^+\pi^-$ in pp collisions at $\sqrt{s} = 7$ TeV at ATLAS

The ATLAS collaboration

E-mail: atlas.publications@cern.ch

Abstract: The prompt and non-prompt production cross-sections for $\psi(2S)$ mesons are measured using 2.1 fb^{-1} of pp collision data at a centre-of-mass energy of 7 TeV recorded by the ATLAS experiment at the LHC. The measurement exploits the $\psi(2S) \to J/\psi(\to \mu^+\mu^-)\pi^+\pi^-$ decay mode, and probes $\psi(2S)$ mesons with transverse momenta in the range $10 \leq p_T < 100$ GeV and rapidity $|y| < 2.0$. The results are compared to other measurements of $\psi(2S)$ production at the LHC and to various theoretical models for prompt and non-prompt quarkonium production.

Keywords: Hadron-Hadron Scattering

ArXiv ePrint: 1407.5532

doi:10.1007/JHEP09(2014)079

JHEP09(2014)079

Contents

JHEP09(2014)079

1 Introduction

The production of quarkonium states in hadronic collisions has been the subject of intense theoretical and experimental study for many decades, especially since measurements of prompt J/ψ and Υ production at the Tevatron [1–7] exposed order-of-magnitude differences between data and theoretical expectations [8]. Despite these being among the most studied heavy-quark bound states, there is still no satisfactory understanding of the mechanisms of their formation. Quarkonium production acts as a unique and important testing ground for quantum chromodynamics (QCD) in its own right. While the production of a heavy quark pair occurs at a hard scale and is generally well-described by QCD, its subsequent evolution into a bound state includes many non-perturbative effects at much softer scales that pose a challenge to current theoretical methods. With the data obtained from the Large Hadron Collider (LHC), it is possible to perform stringent tests of theoretical models across a large range of momentum transfer.

Studies of heavy quarkonia were conducted previously by ATLAS in the $J/\psi \to \mu^+\mu^-$ [9] and $\Upsilon(nS) \to \mu^+\mu^-$ [10, 11] decay modes. The measurements described here are based on an analysis of 2.1 fb^{-1} of pp collision data at $\sqrt{s} = 7$ TeV, and study the prompt and non-prompt production of the ψ(2S) meson through its decay to $J/\psi(\to\mu^+\mu^-)\pi^+\pi^-$. The prompt production arises from direct QCD production mechanisms and the non-prompt production arises from weak decays of b-hadrons. The $J/\psi(\to\mu^+\mu^-)\pi^+\pi^-$ final

state offers improvements in $\psi(2S)$ mass resolution and background discrimination over exclusive dilepton channels. Unlike prompt J/ψ production, which can occur through either direct QCD production of J/ψ or the production of excited states that subsequently decay into $J/\psi + X$ final states, no appreciable prompt production of excited states decaying into $\psi(2S)$ has been established in hadron collisions. In this respect the $\psi(2S)$ is a unique state with no significant feed-down from higher quarkonium resonances, which decay predominantly to $D\overline{D}$ pairs.

The measurement presented here, when combined with a concurrent measurement of the prompt and non-prompt production of P-wave χ_{cJ} states [12] and existing measurements of the production cross-section of the J/ψ [9], provides a rather comprehensive picture of the production of both prompt and non-prompt charmonia. These $\psi(2S)$ cross-sections are compared with the results from LHCb [13] and CMS [14] and with a variety of theoretical models for both prompt and non-prompt production, and complement recent measurements from ALICE [15] at low p_{T}.

2 The ATLAS detector

The ATLAS detector [16] is composed of an inner tracking system, calorimeters, and a muon spectrometer. The inner detector (ID) surrounds the proton-proton collision point and consists of a silicon pixel detector, a silicon microstrip detector, and a transition radiation tracker, all of which are immersed in a 2 T axial magnetic field. The inner detector spans the pseudorapidity[1] range $|\eta| < 2.5$ and is enclosed by a system of electromagnetic and hadronic calorimeters. Surrounding the calorimeters is the muon spectrometer (MS) consisting of three large air-core superconducting magnets (each with eight coils) providing a toroidal field, a system of precision tracking chambers, and fast detectors for triggering. This spectrometer is equipped with monitored drift tubes and cathode-strip chambers that provide precision measurements in the bending plane of muons within the pseudorapidity range $|\eta| < 2.7$. Resistive-plate and thin-gap chambers with fast response are primarily used to make fast trigger decisions in the ranges $|\eta| < 1.05$ and $1.05 < |\eta| < 2.4$ respectively, and also provide position measurements in the non-bending plane and improve overall pattern recognition and track reconstruction. Momentum measurements in the muon spectrometer are based on track segments formed in at least two of the three precision chamber planes.

The ATLAS detector employs a three-level trigger system [17], which reduces the 20 MHz proton bunch collision rate to the several-hundred Hz transfer rate to mass storage. The level-1 muon trigger searches for hit coincidences between different muon trigger detector layers inside pre-programmed geometrical windows that bound the path of muon candidates over a given transverse momentum (p_{T}) threshold and provide a rough estimate

[1] ATLAS uses a right-handed coordinate system with its origin at the nominal interaction point (IP) in the centre of the detector and the z-axis along the beam pipe. The x-axis points from the IP to the centre of the LHC ring, and the y-axis points upward. Cylindrical coordinates (r, ϕ) are used in the transverse plane, ϕ being the azimuthal angle around the z-axis. The pseudorapidity η is defined in terms of the polar angle θ as $\eta = -\ln\tan(\theta/2)$ and the transverse momentum p_{T} is defined as $p_{\mathrm{T}} = p\sin\theta$. The rapidity is defined as $y = 0.5\ln\left((E + p_{\mathrm{z}})/(E - p_{\mathrm{z}})\right)$, where E and p_{z} refer to energy and longitudinal momentum, respectively. The η–ϕ distance between two particles is defined as $\Delta R = \sqrt{(\Delta\eta)^2 + (\Delta\phi)^2}$.

JHEP09(2014)079

of its position within the pseudorapidity range $|\eta| < 2.4$. At level-1, muon candidates are reported in "regions of interest" (RoI). Only a single muon can be associated with a given RoI of spatial extent $\Delta\phi \times \Delta\eta \approx 0.1 \times 0.1$. This limitation has a small effect on the trigger efficiency for $\psi(2S)$ mesons, which is corrected in the analysis using a data-driven method based on analysis of $J/\psi \to \mu^+\mu^-$ and $\Upsilon \to \mu^+\mu^-$ decays. There are two subsequent higher-level, software-based trigger selection stages. Muon candidates reconstructed at these higher levels incorporate, with increasing precision, information from both the muon spectrometer and the inner detector, reaching position and momentum resolutions close to those provided by the offline muon reconstruction.

In this analysis, muon candidates are reconstructed using algorithms reliant on the combination of both an MS track and an ID track. Because of this ID coverage requirement, muon reconstruction is possible only within $|\eta| < 2.5$. The muons selected for this analysis are further restricted to $|\eta| < 2.3$. This ensures high-quality tracking and triggering, and reduces the number of fake muon candidates. It also removes regions of strongly varying efficiency and acceptance.

3 Data and event selection

Data for this analysis were collected in 2011, during LHC proton-proton collisions at a centre-of-mass energy of 7 TeV. The data sample was collected using a trigger requiring two oppositely charged muon candidates with no explicit requirement on the transverse momentum at level-1 of the trigger. The higher-level trigger stage subsequently requires each muon to have transverse momentum satisfying $p_{\mathrm{T}} > 4$ GeV. Muon candidates are also required to fulfil additional quality criteria and the dimuon pair must be consistent with having originated from a common vertex, and have invariant mass $2.5 < m_{\mu^+\mu^-} < 4.3$ GeV. The data collected with this trigger configuration corresponded to a total integrated luminosity of $2.09 \pm 0.04\,\mathrm{fb}^{-1}$ [18] in the full 7 TeV dataset.

The $\psi(2S) \to J/\psi\,\pi^+\pi^-$ candidates are reconstructed with a technique similar to the one used by ATLAS for $B_s \to J/\psi\phi$ [19] candidates. The selected events contain at least two oppositely charged muons, identified by the muon spectrometer and with associated tracks reconstructed in the inner detector. The two muon tracks are considered a $J/\psi \to \mu^+\mu^-$ candidate if they can be fitted to a common vertex with a dimuon invariant mass between 2.8 GeV and 3.4 GeV. The muon track parameters are taken from the ID measurement alone, since the MS does not improve the precision in the momentum range relevant for the $\psi(2S)$ measurements presented here. To ensure accurate inner detector measurements, each muon track must contain at least six hits in the silicon microstrip detector and at least one hit in the pixel detector. Muon candidates satisfying these criteria are required to have $p_{\mathrm{T}} > 4$ GeV, $|\eta| < 2.3$, and a successful fit to a common vertex. Good spatial matching, $\Delta R < 0.01$, between each reconstructed muon candidate and a trigger identified candidate is required to accurately correct for trigger inefficiencies. The dimuon pair is further required to satisfy $p_{\mathrm{T}} > 8$ GeV and $|y| < 2.0$ to ensure that the J/ψ candidates are reconstructed in a fiducial region where acceptance and efficiency

JHEP09(2014)079

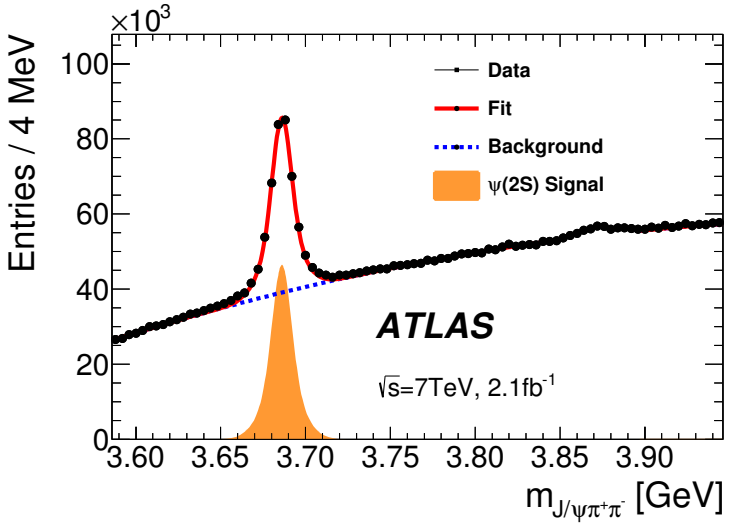

Figure 1. The uncorrected $J/\psi\,\pi^+\pi^-$ mass spectrum between 3.586 GeV and 3.946 GeV. Superimposed on the data points is the result of a fit using a double Gaussian distribution to describe the $J/\psi\,\pi^+\pi^-$ signal peak, and a second-order Chebyshev polynomial to model the background, where the region within ±25 MeV of the $X(3872)$ ($m_{J/\psi\,\pi^+\pi^-} = 3.872$ GeV) is excluded from the fit.

corrections do not vary too rapidly. An additional requirement on the dimuon vertex-fit χ^2 helps to remove spurious dimuon combinations.

The two pions in the $\psi(2S) \to J/\psi\,\pi^+\pi^-$ decay are reconstructed by taking all pairs of the remaining oppositely charged tracks with $p_T > 0.5$ GeV and $|\eta| < 2.5$ and assigning the pion mass hypothesis to each reconstructed track. A constrained four-particle vertex fit is performed to all $\psi(2S)$ candidates, where the $J/\psi \to \mu^+\mu^-$ candidates have their invariant mass constrained to the world average value for the J/ψ mass (3096.916 MeV) [20]. A χ^2 probability requirement of $\mathcal{P}(\chi^2) > 0.005$ is applied to the vertex fit quality, which considerably reduces combinatorial background from incorrect dipion candidate assignment. The constrained vertex fit also provides significantly improved invariant mass resolution for the $J/\psi\,\pi^+\pi^-$ system over that attainable from momentum resolution alone. Corrections are made for signal selection inefficiencies ($\sim$ 5%–8%) arising from the dimuon invariant mass, p_T, and rapidity selections, the vertex requirements on dimuon candidates, and the constrained-fit quality criterion of the four-particle vertex.

Figure 1 shows the $J/\psi\,\pi^+\pi^-$ invariant mass distribution after the above selection criteria are applied. A clear peak of the $\psi(2S)$ is observed near 3.69 GeV. At larger invariant mass, a further structure is also observed, identified as the $X(3872)$.

The cross-section measurements are presented in three $\psi(2S)$ rapidity intervals: $|y| < 0.75$, $0.75 \le |y| < 1.5$, and $1.5 \le |y| < 2.0$, and in ten p_T intervals for each of the rapidity intervals, spanning $10 \le p_T < 100$ GeV. Figure 2 illustrates the uncorrected yields and the invariant mass resolutions of the dimuon and $J/\psi\,\pi^+\pi^-$ systems in the three rapidity regions, which comprise about 96 000, 66 000 and 41 000 $\psi(2S)$ candidates respectively. For both the dimuon and the $J/\psi\,\pi^+\pi^-$ invariant mass fits, a double Gaussian is used to describe the signal shape, and a second-order Chebyshev polynomial to model the background.

JHEP09(2014)079

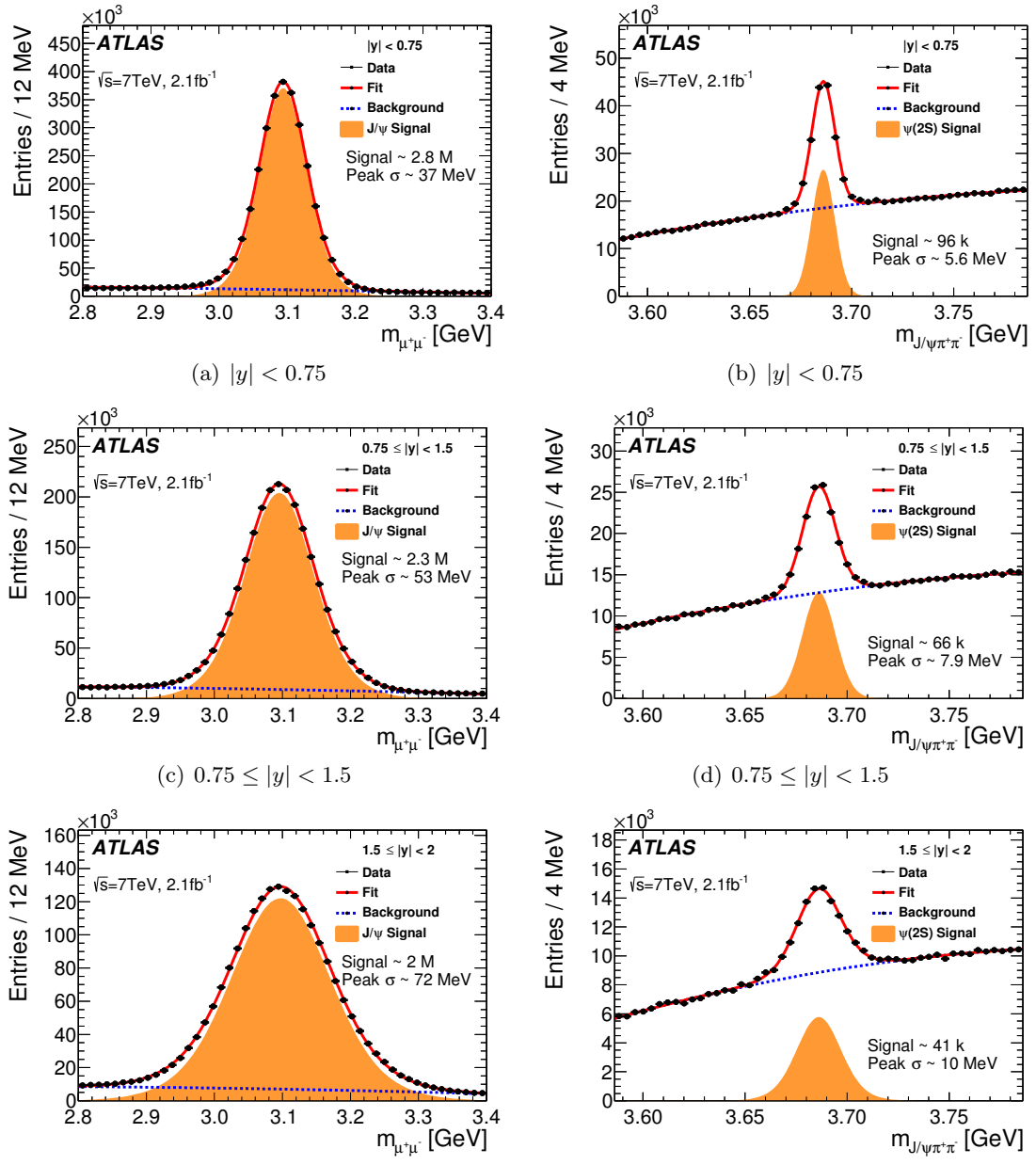

(a) $|y| < 0.75$ (b) $|y| < 0.75$

(c) $0.75 \leq |y| < 1.5$ (d) $0.75 \leq |y| < 1.5$

(e) $1.5 \leq |y| < 2.0$ (f) $1.5 \leq |y| < 2.0$

Figure 2. Invariant mass distributions for the dimuon (left) and $J/\psi\,\pi^+\pi^-$ system after the dimuon mass-constrained fit (right) in the three rapidity ranges of the measurement. The data distributions are fitted with a combination a double Gaussian distribution (for the signals) and a second-order Chebyshev polynomial (for backgrounds).

4 Cross-section determination

The differential production cross-section for $\psi(2S)$ can be apportioned between prompt production and non-prompt production. Non-prompt $\psi(2S)$ production processes are distinguished from prompt processes by their longer apparent lifetimes, with production oc-

JHEP09(2014)079

curring through the decay of a b-hadron. To distinguish between these prompt and non-prompt processes, a parameter called the pseudo-proper lifetime τ is constructed using the $J/\psi\,\pi^+\pi^-$ transverse momentum:

$$\tau = \frac{L_{xy}\, m_{J/\psi\,\pi^+\pi^-}}{p_{\mathrm{T}}}, \tag{4.1}$$

with L_{xy} defined by the equation:

$$L_{xy} \equiv \vec{L} \cdot \vec{p}_{\mathrm{T}}/p_{\mathrm{T}}, \tag{4.2}$$

where $\vec{L}$ is the vector from the primary vertex to the $J/\psi\,\pi^+\pi^-$ decay vertex and $\vec{p}_{\mathrm{T}}$ is the transverse momentum vector of the $J/\psi\,\pi^+\pi^-$ system. The primary vertex is defined as the vertex with the largest scalar sum of associated charged-particle track p_{T}^2, and identified as the location of the primary proton-proton interaction. The presence of additional simultaneous proton-proton collisions, and the effect of associating the final-state particles with the wrong collision was found [19] to have a negligible impact on the discrimination and extraction of short and long-lived components of the signal.

To obtain a measurement of the production cross-sections, the reconstructed candidates are individually weighted to correct for detector effects, such as acceptance, muon reconstruction efficiency, pion reconstruction efficiency and trigger efficiency, which are discussed below in detail. The candidates in each $\psi(2\mathrm{S})$ p_{T} and $|y|$ intervals are then fitted using a weighted two-dimensional unbinned maximum likelihood method, performed on the invariant mass and pseudo-proper lifetime distributions to isolate signal candidates from the backgrounds and separate the prompt signal from the non-prompt signal. The corrected prompt and non-prompt signal yields ($N_{\mathrm{P}}^{\psi(2\mathrm{S})}$, $N_{\mathrm{NP}}^{\psi(2\mathrm{S})}$) are then used to calculate the prompt and non-prompt differential cross-section (σ_{P}, σ_{NP}) times branching ratio, using the equation:

$$\mathcal{B}\left(\psi(2\mathrm{S}) \to J/\psi(\to\mu^+\mu^-)\pi^+\pi^-\right) \times \frac{\mathrm{d}^2\sigma_{\mathrm{P,NP}}^{\psi(2\mathrm{S})}}{\mathrm{d}p_{\mathrm{T}}\mathrm{d}y} = \frac{N_{\mathrm{P,NP}}^{\psi(2\mathrm{S})}}{\Delta p_{\mathrm{T}} \Delta y \int \mathcal{L}\mathrm{d}t}, \tag{4.3}$$

where $\int \mathcal{L}\mathrm{d}t$ is the total integrated luminosity, Δp_{T} and Δy represent the intervals in $\psi(2\mathrm{S})$ transverse momentum and rapidity, respectively, and $\mathcal{B}\left(\psi(2\mathrm{S}) \to J/\psi(\to\mu^+\mu^-)\pi^+\pi^-\right)$ is the total branching ratio of the signal decay, taken to be $(2.02 \pm 0.03)\%$, obtained by combining the world average values for $\mathcal{B}\left(J/\psi \to \mu^+\mu^-\right)$ and $\mathcal{B}\left(\psi(2\mathrm{S}) \to J/\psi\,\pi^+\pi^-\right)$ [20].

In addition to the prompt and non-prompt production cross-sections, the non-prompt $\psi(2\mathrm{S})$ production fraction $f_B^{\psi(2\mathrm{S})}$ is simultaneously extracted from the maximum likelihood fits in the same kinematic intervals. This fraction is defined as the corrected yield of non-prompt $\psi(2\mathrm{S})$ divided by the corrected total yield of produced $\psi(2\mathrm{S})$, as given in the equation:

$$f_B^{\psi(2\mathrm{S})} \equiv \frac{N_{\mathrm{NP}}^{\psi(2\mathrm{S})}}{N_{\mathrm{P}}^{\psi(2\mathrm{S})} + N_{\mathrm{NP}}^{\psi(2\mathrm{S})}}. \tag{4.4}$$

Measurement of this fraction benefits from improved precision over absolute cross-section measurements through cancellation or reduction of overall acceptance and efficiency corrections in the ratio.

JHEP09(2014)079

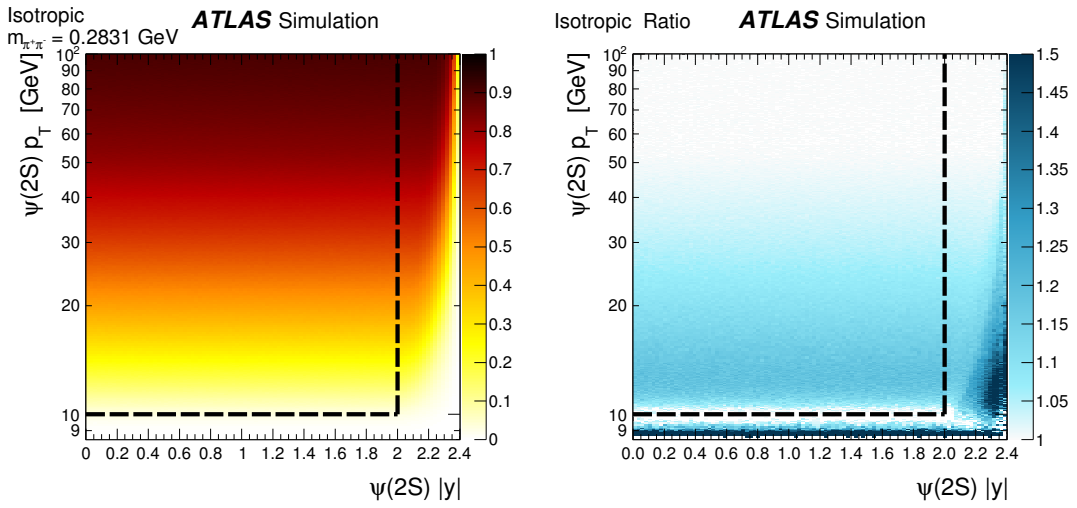

(a) (b)

Figure 3. (a) Example of $\psi(2S) \to J/\psi(\to\mu^+\mu^-)\pi^+\pi^-$ acceptance for isotropic $\psi(2S)$ production for the lowest dipion mass, $m_{\pi^+\pi^-} = 2m_\pi$, and (b) the ratio of the acceptance at the lowest dipion masses to that at the highest dipion masses. Dashed lines show the p_T–y bounds of the measurement.

Acceptance. The acceptance $\mathcal{A}(p_T, y, m_{\pi\pi})$ is defined as the probability that the decay products in $\psi(2S) \to J/\psi(\to\mu^+\mu^-)\pi^+\pi^-$ fall within the fiducial volume ($p_T(\mu^\pm) > 4\,\text{GeV}$, $|\eta(\mu^\pm)| < 2.3$, $p_T(\pi^\pm) > 0.5\,\text{GeV}$, $|\eta(\pi^\pm)| < 2.5$). The acceptance depends on the spin-alignment of $\psi(2S)$. For the central results obtained in this analysis, the $\psi(2S)$ decay was assumed to be isotropic, with variations corresponding to a number of extreme spin-alignment scenarios described below.

Acceptance maps are created using a large sample of generator-level Monte Carlo (MC) simulation, which randomly creates and decays $\psi(2S) \to J/\psi(\to\mu^+\mu^-)\pi^+\pi^-$, as a function of the $\psi(2S)$ transverse momentum and rapidity, in finely binned intervals of the dipion invariant mass $m_{\pi^+\pi^-}$ covering the allowed range, $2m_\pi < m_{\pi^+\pi^-} < m_{\psi(2S)} - m_{J/\psi}$. An example of the acceptance map for the lowest dipion mass ($m_{\pi^+\pi^-} \simeq 2m_\pi$) is shown in figure 3(a) for the isotropic $\psi(2S)$ assumption. The variation of acceptance with dipion mass is illustrated by the ratio of the acceptance at the lowest dipion mass $m_{\pi^+\pi^-} \simeq 2m_\pi$ to the acceptance at the highest dipion mass $m_{\pi^+\pi^-} \simeq m_{\psi(2S)} - m_{J/\psi}$, shown in figure 3(b). The largest variations are observed at low p_T and at high rapidity, reaching $\pm 20\%$ within the p_T–y range of this measurement ($\psi(2S)$ rapidity $|y| < 2.0$ and transverse momentum between 10 GeV and 100 GeV).

It has been shown [21] that the dipion state is largely dominated by the angular momentum configuration where the two pions are in a relative S-wave state, and the J/ψ and dipion system are in an S-wave state as well. The spin-alignment of J/ψ from $\psi(2S)$ decay is thus assumed to be fully transferred from the spin-alignment of $\psi(2S)$ and hence, in its decay frame, the angular dependence of the decay $J/\psi \to \mu^+\mu^-$ is given by

$$\frac{\mathrm{d}^2N}{\mathrm{d}\cos\theta^*\mathrm{d}\phi^*} \propto \left(\frac{1}{3+\lambda_\theta}\right)\left(1 + \lambda_\theta\cos^2\theta^* + \lambda_\phi\sin^2\theta^*\cos 2\phi^* + \lambda_{\theta\phi}\sin 2\theta^*\cos\phi^*\right), \quad (4.5)$$

JHEP09(2014)079

	Angular coefficients		
	λ_θ	λ_ϕ	$\lambda_{\theta\phi}$
Isotropic *(central value)*	0	0	0
Longitudinal	−1	0	0
Transverse positive	+1	+1	0
Transverse zero	+1	0	0
Transverse negative	+1	−1	0
Off-(λ_θ-λ_ϕ)-plane positive	0	0	+0.5
Off-(λ_θ-λ_ϕ)-plane negative	0	0	−0.5

Table 1. Values of angular coefficients describing spin-alignment scenarios with maximal effect on the measured rate for a given total production cross-section.

where the λ_i are coefficients related to the spin density matrix elements of the $\psi(2S)$ wavefunction [22]. The polar angle θ^* and the azimuthal angle ϕ^* are defined by the momentum of the positive muon in the $J/\psi \to \mu^+\mu^-$ decay frame with respect to the direction of the $\psi(2S)$ momentum in the lab frame. In the default case of isotropic $\psi(2S)$ decay, all three λ_i coefficients in eq. (4.5) are equal to zero. This assumption is compatible with measurements for prompt [23, 24] and non-prompt [25] production.

In certain areas of the phase space, the acceptance $\mathcal{A}$ may depend quite strongly on the values of the λ_i coefficients in eq. (4.5). Seven extreme cases that lead to the largest possible variations of acceptance within the phase space of this measurement are identified. These cases, described in table 1, are used to define a range in which the results may vary under any physically allowed spin-alignment assumptions.

Figures 4 and 5 illustrate the variation of the acceptance correction weights with p_{T} and rapidity of $\psi(2S)$ and J/ψ from the $\psi(2S) \to J/\psi(\to \mu^+\mu^-)\pi^+\pi^-$ decay, for the six anisotropic spin-alignment scenarios described above, relative to the isotropic case. There is a clear dependence on the spin-alignment scenario. This can be as large as $(+62\%, -32\%)$ for strong polarisations at the lowest p_{T} probed, but the effect is limited to $(+8\%, -12\%)$ at the highest p_{T} probed. Since spin-alignment is regarded as an ultimately resolvable model-dependence issue rather than an intrinsic experimental shortcoming, the associated uncertainties are handled here differently from purely experimental systematic uncertainties. The range of variation of our cross-section results due to possible spin-alignment scenarios is documented in appendix A.

Dimuon reconstruction efficiency. The dimuon reconstruction efficiency, determined via a data-driven tag-and-probe method [11] from $J/\psi \to \mu^+\mu^-$ decays, is given by:

$$\epsilon^{\mu}_{\mathrm{reco}} = \epsilon_{\mathrm{trk}}(p_{\mathrm{T}}^{\mu 1}, \eta^{\mu 1}) \cdot \epsilon_{\mathrm{trk}}(p_{\mathrm{T}}^{\mu 2}, \eta^{\mu 2}) \cdot \epsilon_{\mu}(p_{\mathrm{T}}^{\mu 1},\, q^{\mu 1} \cdot \eta^{\mu 1}) \cdot \epsilon_{\mu}(p_{\mathrm{T}}^{\mu 2},\, q^{\mu 2} \cdot \eta^{\mu 2}), \tag{4.6}$$

where q is the charge of the muon, ϵ_{trk} is the muon track reconstruction efficiency in the ID, while ϵ_μ is the efficiency of the muon reconstruction algorithm given that the muon track has been reconstructed in the ID. The dependence on charge is due to the effect of the toroidal field bending particles into or out of the detector at low momenta and high

JHEP09(2014)079

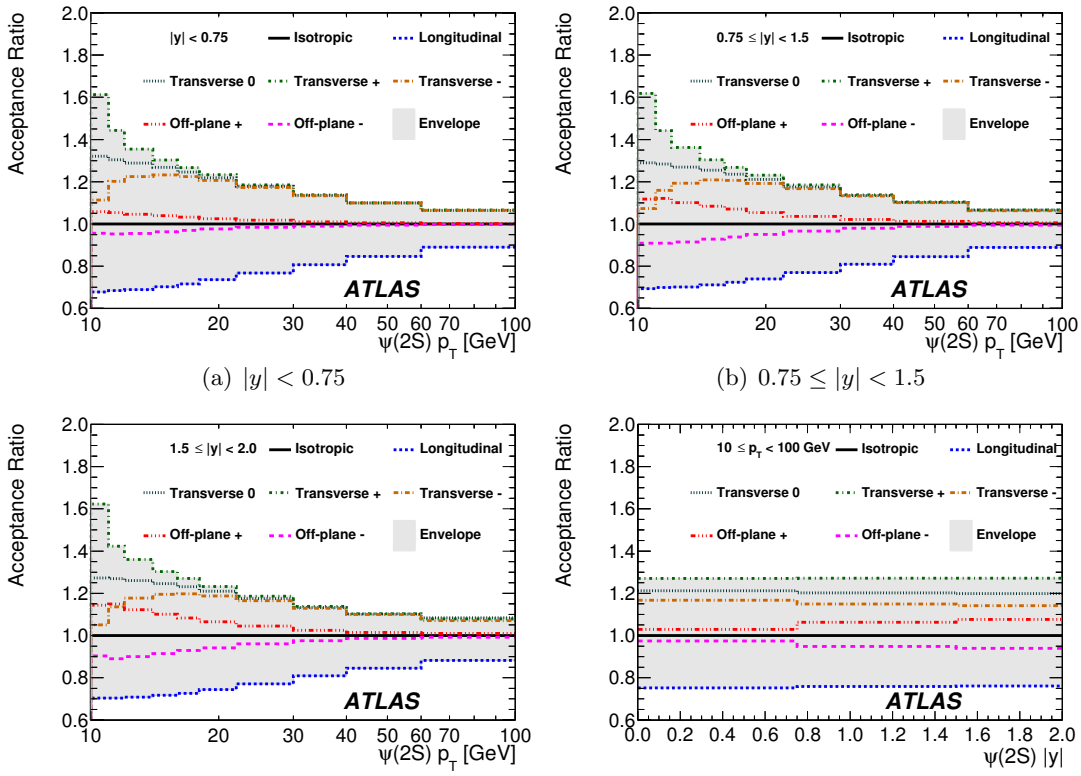

(a) $|y| < 0.75$ (b) $0.75 \leq |y| < 1.5$

(c) $1.5 \leq |y| < 2.0$ (d) $10 \leq p_{\mathrm{T}} < 100$ GeV

Figure 4. Average acceptance correction relative to the isotropic scenario for the six extreme spin-alignment scenarios described in the text, (a)-(c) as a function of $\psi(2S)$ transverse momentum in the three rapidity regions, and (d) versus $\psi(2S)$ rapidity for $10 < p_{\mathrm{T}} < 100\,\mathrm{GeV}$.

rapidities. The muon track reconstruction efficiency ϵ_{trk} is determined [11] to be $(99 \pm 1)\%$ per muon candidate within the kinematic range of interest. Possible correlation effects were found to be negligible due to the large spatial separation of the two reconstructed muon candidates relative to the spatial resolution of the detector.

Dipion reconstruction efficiency. The dipion reconstruction efficiency $\epsilon^{\pi}_{\mathrm{reco}}$ is given by:

$$\epsilon^{\pi}_{\mathrm{reco}} = \epsilon_{\pi}(p_{\mathrm{T}}^{\pi 1},\, \eta^{\pi 1}) \cdot \epsilon_{\pi}(p_{\mathrm{T}}^{\pi 2},\, \eta^{\pi 2}), \tag{4.7}$$

where the two ϵ_{π} are individual pion reconstruction efficiencies. These are determined using techniques derived for tracking-efficiency measurements [26]. Pions produced in MC event simulation using a PYTHIA6 [27] sample of $\psi(2S) \to J/\psi(\to\mu^+\mu^-)\pi^+\pi^-$ decays were used to determine the efficiencies in the interval $p_{\mathrm{T}} > 0.5\,\mathrm{GeV}$ and $|\eta| < 2.5$. The MC sample was produced using the ATLAS 2011 MC tuning [28] and simulated using the ATLAS GEANT4 [29] detector simulation [30]. The pion track reconstruction efficiencies are calculated in intervals of track pseudorapidity and transverse momentum. In addition to the statistical uncertainties on the efficiency due to the size of the MC sample, each efficiency value also contains an additional uncertainty to account for any possible mismodelling in

JHEP09(2014)079

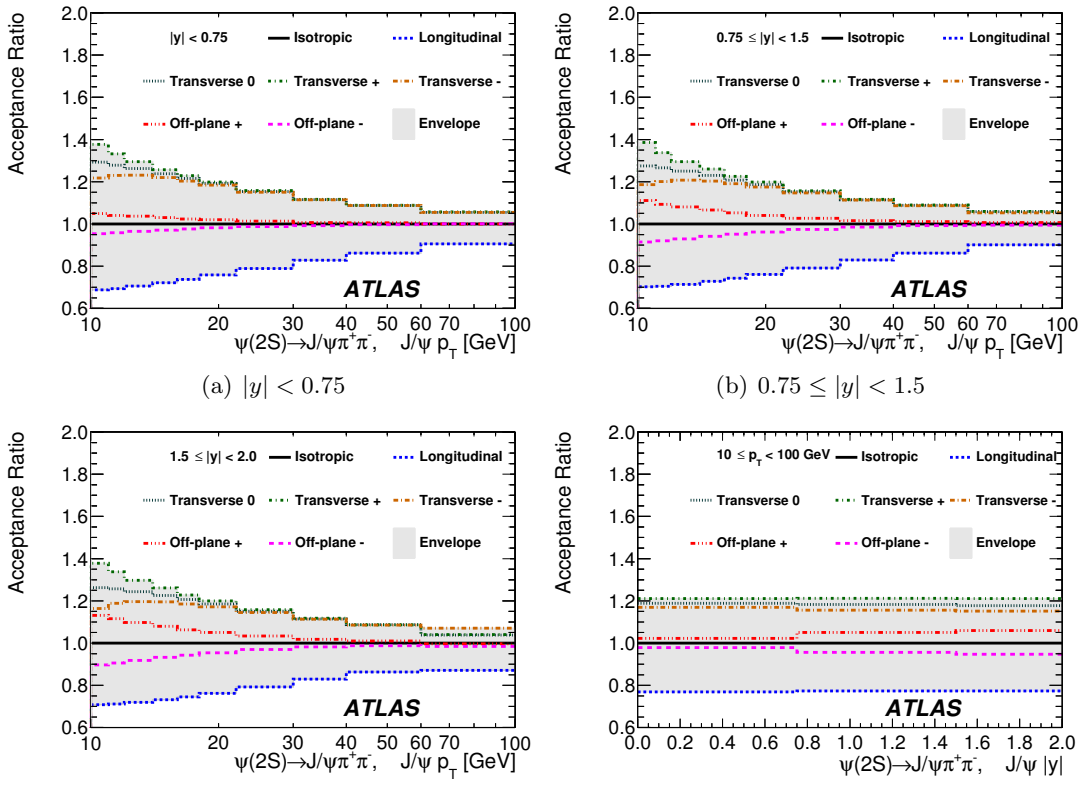

(a) $|y| < 0.75$ (b) $0.75 \leq |y| < 1.5$

(c) $1.5 \leq |y| < 2.0$ (d) $10 \leq p_{\mathrm{T}} < 100$ GeV

Figure 5. Average acceptance correction relative to the isotropic scenario for the six extreme spin-alignment scenarios described in the text, as a function of the transverse momentum of the J/ψ in $\psi(2\mathrm{S}) \to J/\psi(\to\mu^+\mu^-)\pi^+\pi^-$ decays in (a)-(c) the three rapidity regions, and (d) versus J/ψ rapidity for $10 \leq p_{\mathrm{T}} < 100\,\mathrm{GeV}$.

the simulations. Pion candidates were found to have spatial separations sufficient to not require additional corrections for correlations in reconstruction efficiency.

Trigger efficiency. The efficiency of the dimuon trigger used in this analysis was measured in a previous analysis [11] from $J/\psi \to \mu^+\mu^-$ and $\Upsilon \to \mu^+\mu^-$ decays using a data-driven method. The trigger efficiency is the efficiency for the trigger system to select signal events that also pass the reconstruction-level analysis selection, and is parameterised as:

$$\epsilon_{\mathrm{trig}} = \epsilon_{\mathrm{RoI}}(p_{\mathrm{T}}^{\mu 1},\, q^{\mu 1},\, \eta^{\mu 1}) \cdot \epsilon_{\mathrm{RoI}}(p_{\mathrm{T}}^{\mu 2},\, q^{\mu 2},\, \eta^{\mu 2}) \cdot c_{\mu\mu}(\Delta R, |y_{\mu\mu}|), \tag{4.8}$$

where ϵ_{RoI} is the efficiency of the trigger system to find an RoI for a single muon and $c_{\mu\mu}$ is a correction term taking into account muon-muon correlations, dependent on the angular separation ΔR between the two muons, and the absolute rapidity of the dimuon system, $|y_{\mu\mu}|$. The invariant mass requirement of the trigger was found to be fully efficient, with a correction for an efficiency of $(99.7 \pm 0.3)\%$ applied to account for possible signal loss as determined from MC simulation.

JHEP09(2014)079

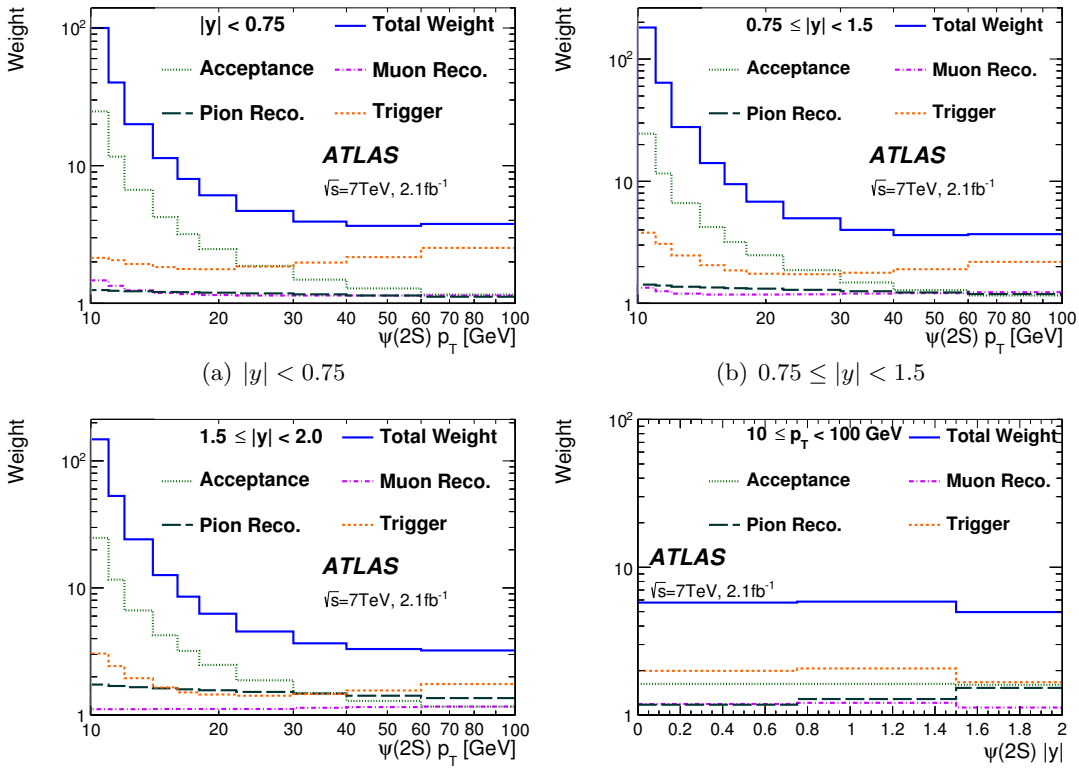

(a) $|y| < 0.75$ (b) $0.75 \leq |y| < 1.5$

(c) $1.5 \leq |y| < 2.0$ (d) $10 \leq p_{\mathrm{T}} < 100$ GeV

Figure 6. Average correction weights (a)-(c) for the three rapidity regions versus p_{T} and (d) for the full p_{T} region versus $|y|$.

Total weight. The total weight w for each $J/\psi\,\pi^+\pi^-$ candidate was calculated as the inverse of the product of acceptance and efficiency corrections, as described by:

$$w^{-1} = \mathcal{A}(p_{\mathrm{T}}, y, m_{\pi\pi}) \cdot \epsilon^{\mu}_{\mathrm{reco}} \cdot \epsilon^{\pi}_{\mathrm{reco}} \cdot \epsilon_{\mathrm{trig}}. \tag{4.9}$$

No lifetime dependence was observed in any of the efficiency corrections. While weights are applied to the data on a candidate-by-candidate basis, the average of the total weight and its breakdown into individual sources is shown in figure 6 for the three rapidity regions and in each p_{T} bin of the measurement, and as an average over the full transverse momentum range ($10 \leq p_{\mathrm{T}} < 100\,\mathrm{GeV}$) versus rapidity. The inverse of these weights illustrate a representative average efficiency correction in each measurement interval.

Fitting procedure. The corrected prompt and non-prompt $\psi(2\mathrm{S})$ signal yields are extracted from two-dimensional weighted unbinned maximum likelihood fits performed on the $J/\psi\,\pi^+\pi^-$ invariant mass (m) and pseudo-proper lifetime (τ) in each p_{T}–$|y|$ interval. The probability density function (PDF) for the fit is defined as a normalised sum, where each term is factorised into mass- and lifetime-dependent functions. The PDF can be written in a compact form as

$$\mathrm{PDF}(m, \tau) = \sum_{i=1}^{5} \kappa_i f_i(m) \cdot h_i(\tau) \otimes G(\tau), \tag{4.10}$$

JHEP09(2014)079

i	Type	Source	$f_i(m)$	$h_i(\tau)$
1	S	P	$\omega G_1(m) + (1-\omega)G_2(m)$	$\delta(\tau)$
2	S	NP	$\omega G_1(m) + (1-\omega)G_2(m)$	$E_1(\tau)$
3	B	P	$C_1(m)$	$\delta(\tau)$
4	B	NP	$C_2(m)$	$\rho E_2(\tau) + (1-\rho)E_3(\tau)$
5	B	NP	$C_3(m)$	$E_4(\lvert\tau\rvert)$

Table 2. Components of the probability density function used to extract the prompt (P) and non-prompt (NP) contributions for signal (S) and background (B).

where κ_i represents the relative normalisation of the i^{th} term (such that $\sum_i \kappa_i \equiv 1$), $f_i(m)$ is the mass-dependent term, and $\otimes$ represents the convolution of the lifetime-dependent function $h_i(\tau)$ with the lifetime resolution term, $G(\tau)$. The latter is modelled by a Gaussian distribution with mean fixed to zero and resolution determined from the fit.

Table 2 shows the five contributions to the overall PDF with the corresponding f_i and h_i functions. Here G_1 and G_2 are Gaussian distributions with the same mean, but different width parameters (see below), while C_1, C_2 and C_3 are different linear combinations of Chebyshev polynomials up to second order. The exponential functions E_1, E_2, E_3 and E_4 have different slope parameters, where $E_1(\tau)$, $E_2(\tau)$ and $E_3(\tau)$ are required to vanish for $\tau < 0$, whereas $E_4(|\tau|)$ is a double-sided exponential with the same slope parameter on either side of $\tau = 0$. The parameters ω and ρ represent the fractional contributions of the components shown, while $\delta(\tau)$ is the Dirac delta function modelling the lifetime distribution of prompt candidates.

To better constrain the fit model at high p_{T}, the widths of the Gaussian distributions G_1 and G_2 are required to satisfy the relation $\sigma_2 = s\sigma_1$. The values of σ_1 and s are obtained as a function of p_{T}, for each $|y|$ range, from separate one-dimensional mass fits. A value of $s = 1.5$ is used for the central fit results, and its variation considered within the systematics. The relative normalisations, κ_i, ρ, and ω, are kept free in all fits, and any autocorrelation effects are accounted for as part of the systematic uncertainties in the fit procedure. Projections of the fit results, for three representative p_{T}–$|y|$ intervals, are presented in figure 7.

5 Systematic uncertainties

Various sources of systematic uncertainties in the measurement are considered and are outlined below.

Acceptance corrections. The acceptance maps were generated using large event samples from MC simulation. Statistical uncertainties in the maps are assigned as a systematic effect on the acceptance correction (a sub-1% effect). Possible deviation of the spin-alignment from an isotropic configuration is accounted for separately (see figures 4 and 5). Other effects, such as smearing of the primary vertex position and momentum resolution causing migrations between particle-level and reconstruction-level kinematic intervals were studied using methods discussed in previous publications [9, 11]. Corrections

JHEP09(2014)079

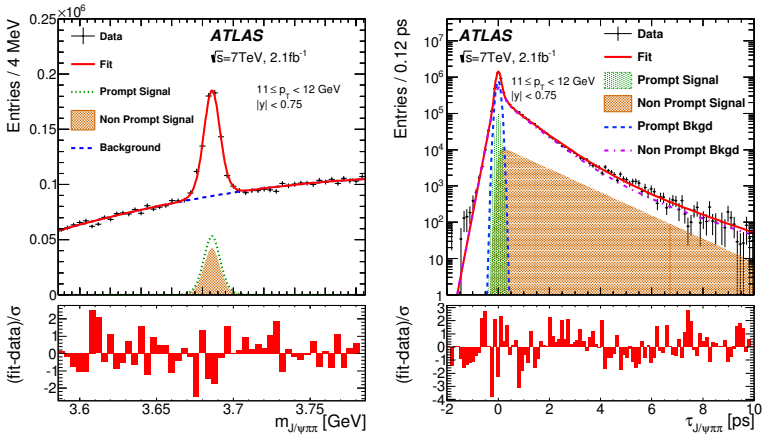

(a) $|y| < 0.75$, $11 \leq p_{\mathrm{T}} < 12\,\mathrm{GeV}$

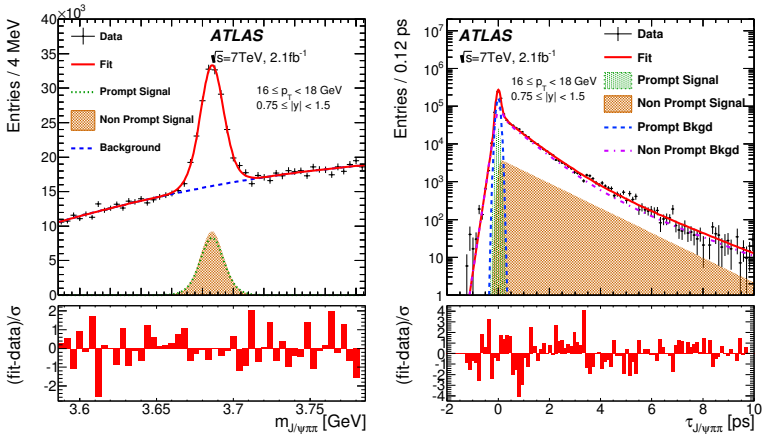

(b) $0.75 \leq |y| < 1.5$, $16 \leq p_{\mathrm{T}} < 18\,\mathrm{GeV}$

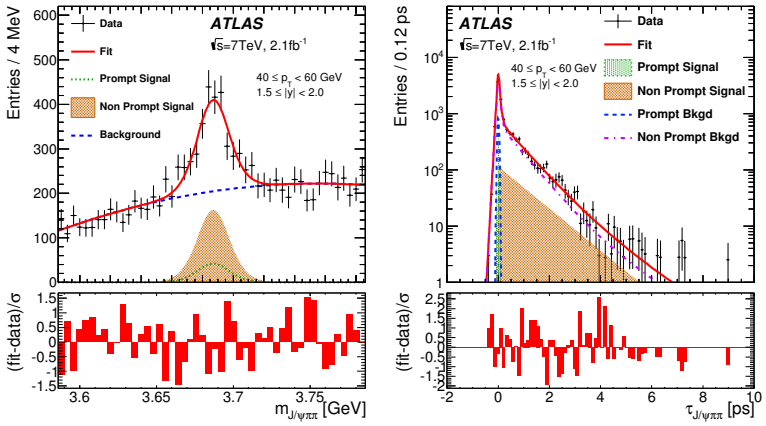

(c) $1.5 \leq |y| < 2.0$, $40 \leq p_{\mathrm{T}} < 60\,\mathrm{GeV}$

Figure 7. Unbinned maximum likelihood fit and data projections onto the invariant mass and pseudo-proper lifetimes of the $\psi(2S)$ candidates for three representative kinematic intervals studied in this measurement. Total signal-plus-background fits to the data are shown, along with the breakdown by prompt/non-prompt production for the $\psi(2S)$ signal. The bottom panel shows the pull distribution between the fit and the data.

JHEP09(2014)079

Variation	
	Mass PDF variation $[f_i(m)]$
1	$\omega G_1 + (1-\omega)G_2$ (fit σ_1, $\sigma_2 = 1.5 \times \sigma_1$) $\rightarrow$ (fit σ_1, $\sigma_2 = \mathbf{1.2} \times \sigma_1$)
2	$\omega G_1 + (1-\omega)G_2$ (fit σ_1, $\sigma_2 = 1.5 \times \sigma_1$) $\rightarrow$ (fit σ_1, $\sigma_2 = \mathbf{2.0} \times \sigma_1$)
3	$\omega G_1 + (1-\omega)G_2$ (fit σ_1, $\sigma_2 = 1.5 \times \sigma_1$) $\rightarrow$ (**free** σ_1, $\sigma_2 = 1.5 \times \sigma_1$)
4	$\omega G_1 + (1-\omega)G_2 \rightarrow$ **CB**(fit σ, fixed α, n)
5	$C_{1,2,3}$ second-order $\rightarrow$ **third-order**
6	$C_{1,2,3} \rightarrow$ **Gaussian**
	Lifetime PDF variation $[h_i(\tau)$ and $G(\tau)]$
7	Resolution $G(\tau) \rightarrow$ **Double Gaussian** ($\sigma_2 = 2.0 \times \sigma_1$)
8	$E_1 \rightarrow \rho' \mathbf{E_5} + (\mathbf{1} - \rho')\mathbf{E_6}$
9	$\rho E_2 + (1-\rho)E_3 \rightarrow \mathbf{E_7}$

Table 3. Fit models used to test the variation from the central model, where the changes made are highlighted in bold. Definitions of the symbols are described in the text.

due to migration effects were found to be negligible ($< 1\%$), largely because of improved momentum resolution due to the vertex-constrained and mass-constrained fits.

Fit model variations. The uncertainty due to the fit procedure was determined by changing one component at a time in the fit model described in section 4, creating a set of new fit models. For each new fit model, the cross-section was recalculated, and in each p_{T} and $|y|$ interval the maximal variation from the central fit model was used as its systematic uncertainty. Table 3 shows the changes made to the mass and lifetime PDFs in the central fit model, as defined in eq. (4.10) and table 2, where CB is a Crystal Ball function [31–33], with parameters α and n fixed, $\alpha = 2.0, n = 2.0$, as determined from test fits. In table 3, "fit σ" means that the result is obtained using the fitted σ (defined in section 4) while "free σ" means that the width σ is completely free in the fit. Fit model changes cause signal yield variations of up to 5%–10% and form one of the dominant uncertainties in the cross-section measurement, however no single variation was found to dominate the total systematic variation in the whole kinematic range.

ID tracking efficiency for muons. The ID tracking efficiency for muon tracks varies as a function of track transverse momentum and pseudorapidity in the kinematic intervals studied in this analysis. The tracking efficiency also has a small dependence on the number of proton-proton collisions that contribute to the event. These variations are contained within a band of $\pm 1.0\%$ around the nominal value of 99.0% determined for the efficiency per-track, and this band is directly assigned as a systematic uncertainty in measured cross-sections.

Muon reconstruction and trigger efficiencies. Uncertainties in the muon reconstruction and muon trigger efficiencies arise predominantly from statistical uncertainties due to

JHEP09(2014)079

the size of the data samples used to determine the efficiencies. The uncertainties in the $\psi(2S)$ yields are determined for each efficiency map independently by fluctuating each entry in the efficiency maps according to their uncertainty independently from bin-to-bin to create a series of toy efficiency maps through many such trials. These fluctuated maps are used to recalculate the corrected signal yields in each kinematic bin of the measurement. A fit of a Gaussian distribution to the resultant yields (relative to the nominal extraction) allows determination of the $\pm 1\sigma$ variations of these yields up and down due to the uncertainties in the individual efficiencies, that affect the measurement at the 3%–5% level.

Pion track reconstruction efficiency. The pion track reconstruction uncertainty contains the contributions from statistical uncertainties in the pion efficiency maps, which are estimated using the same procedure as for the muon efficiency maps. Systematic uncertainties in the efficiencies are assigned based on tracking efficiency variations observed in alternative detector material and geometry simulations [26]. The total uncertainties are determined to be 2%–3% per pion in the p_{T} ranges considered, varying with rapidity, with an additional 1% contribution per pion from the hadronic track reconstruction uncertainties.

Selection criteria. The efficiency of the constrained $J/\psi\,\pi^+\pi^-$ vertex-fit quality criterion, $\mathcal{P}(\chi^2) > 0.005$, was estimated from data and MC studies to vary between 93% and 97% as a function of rapidity and p_{T}, with an uncertainty of about 2%, determined from data/MC comparison and the variation of the efficiency with transverse momentum.

Additional inefficiencies from the other selection criteria described in section 3 and their corresponding uncertainties were estimated using simulations, and were found to be less than 1% in the first two rapidity regions and less than 2% in the highest rapidity region. These were combined with the efficiencies of the constrained-fit quality requirement to calculate the total selection efficiency, which was found to vary between 92% and 95% with a 2% uncertainty.

Luminosity. The uncertainty in the integrated luminosity for the dataset used in this analysis was determined [18] to be $\pm 1.8\%$. This systematic uncertainty does not affect the measurement of the non-prompt production fraction.

Total uncertainties. Figures 8–10 summarise the total systematic and statistical uncertainties in the measurement of the non-prompt production fraction and the prompt/non-prompt cross-sections.

6 Production of $\psi(2S)$ as a function of J/ψ p_{T} and rapidity

In order to better understand the various feed-down contributions to J/ψ production it is important to measure the differential cross-section of the production of J/ψ mesons from prompt and non-prompt $\psi(2S) \to J/\psi\,\pi^+\pi^-$ decays, as a function of the transverse momentum of the J/ψ. The procedure is very similar to the measurement of $\psi(2S)$ production: the invariant mass distributions of all $\psi(2S) \to J/\psi\,\pi^+\pi^-$ candidates (selected and fully corrected for acceptance and efficiency, according to eq. (4.9)), are fitted again to extract the yield of $\psi(2S)$ mesons, but this time in bins of J/ψ p_{T} and rapidity. Fitting and

JHEP09(2014)079

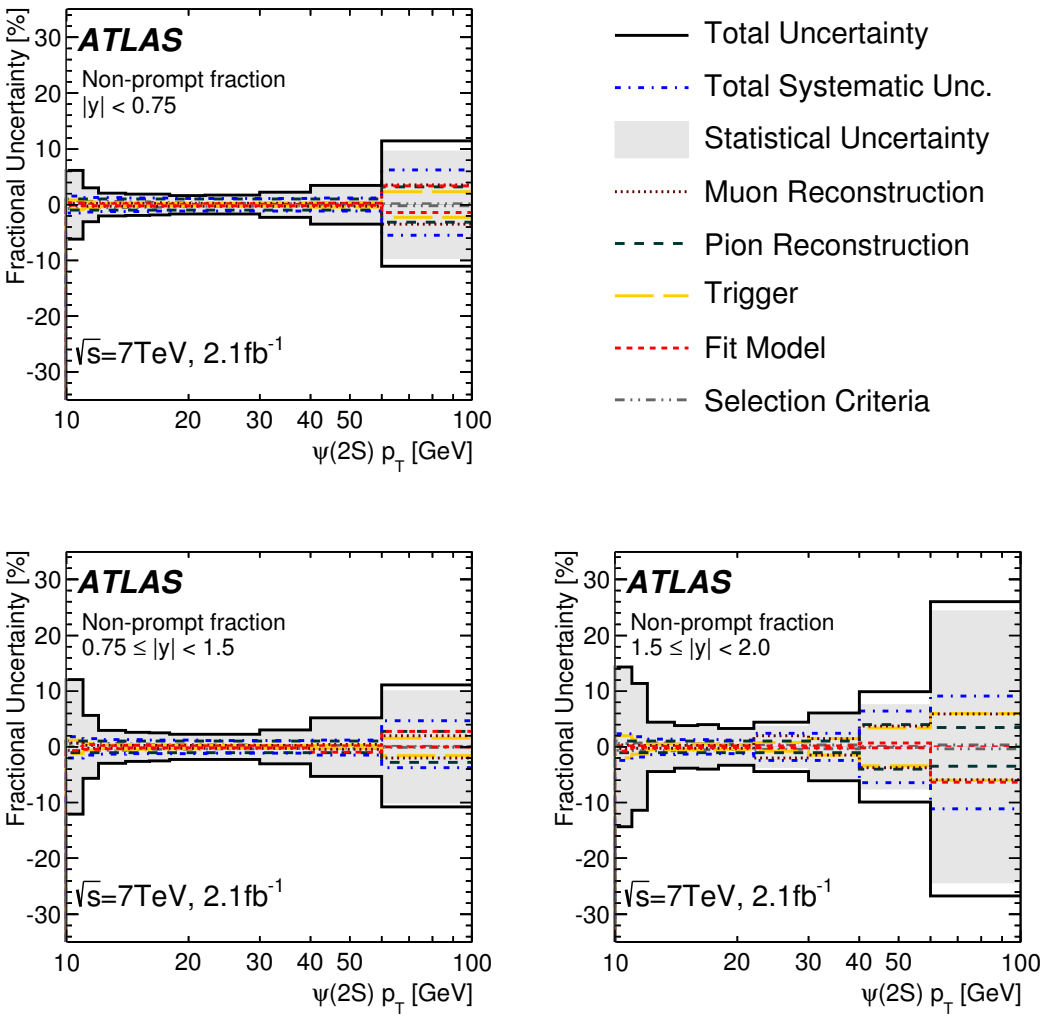

Figure 8. Summary of the positive and negative uncertainties for the non-prompt fraction measurement in three $\psi(2S)$ rapidity intervals. The plots do not include the spin-alignment uncertainty.

uncertainty estimation procedures remain the same. As the fiducial volume from which $J/\psi\,\pi^+\pi^-$ candidates are reconstructed extends well beyond the kinematic range over which the measurements are presented, no additional corrections are needed to present the data as a function of J/ψ kinematic variables. The absence of any need for additional corrections was cross-checked using MC simulations.

7 Results and discussion

The corrected non-prompt $\psi(2S)$ production fraction, and the prompt and non-prompt $\psi(2S)$ production cross-sections are measured in intervals of $\psi(2S)$ transverse momentum and three ranges of $\psi(2S)$ rapidity. All measurements are presented assuming the $\psi(2S)$ decays isotropically. Figure 11 shows the fully corrected measured non-prompt production fraction $f_B^{\psi(2S)}$ as a function of p_T. A rise in the relative non-prompt production rate

JHEP09(2014)079

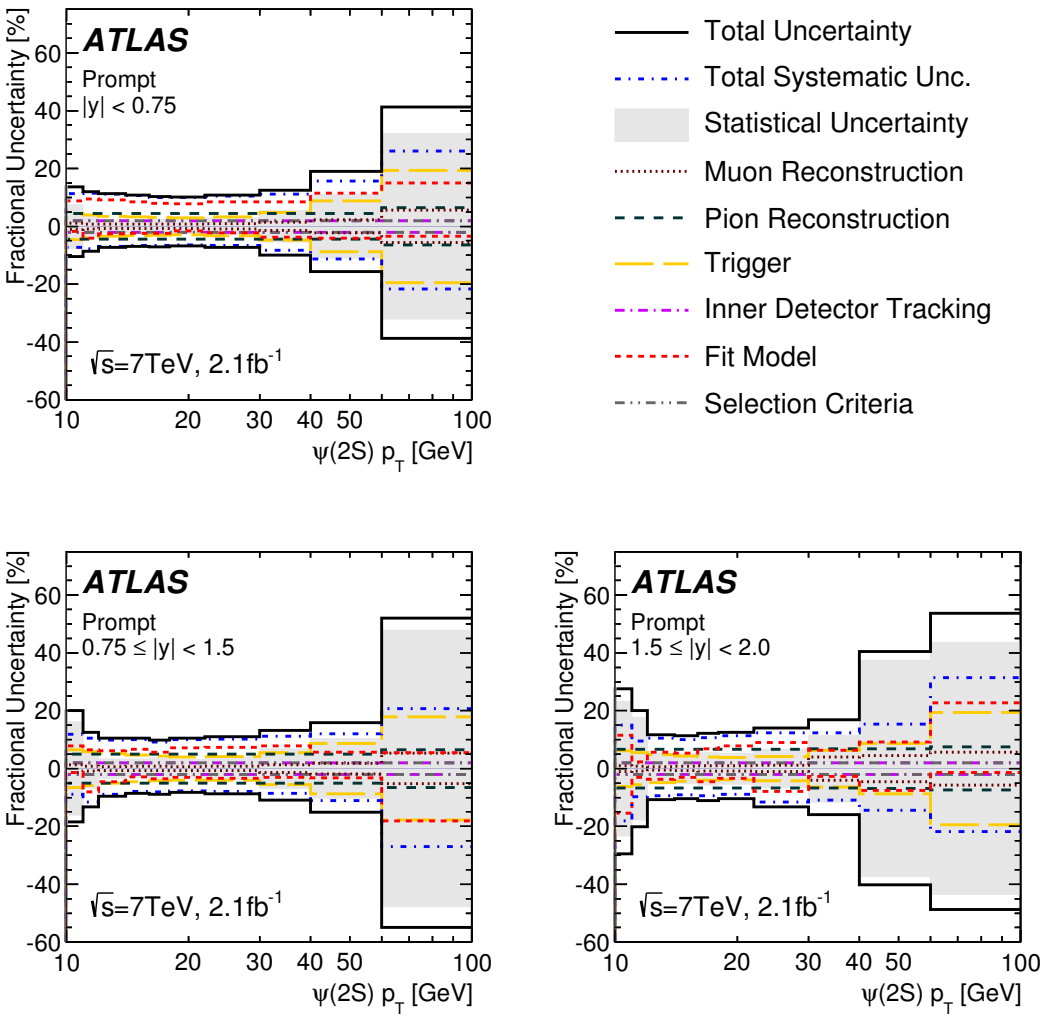

Figure 9. Summary of the positive and negative uncertainties for the prompt cross-section measurement in three ψ(2S) rapidity intervals. The plots do not include the constant 1.8% luminosity uncertainty or the spin-alignment uncertainty.

is observed with increasing p_{T} for all three rapidity intervals. This behaviour is similar to that seen for the non-prompt J/ψ production fraction [9]. Whereas at large $p_{\mathrm{T}}(>$ 50 GeV) the non-prompt ψ(2S) fraction approaches that of the J/ψ, at low p_{T} the non-prompt fraction for ψ(2S) is somewhat larger than is observed for J/ψ. The data shows no significant dependence on rapidity at the lowest transverse momenta probed, but a systematic reduction in the non-prompt fraction with increasing rapidity is observed as the ψ(2S) transverse momentum increases. The data are tabulated in table 4.

Fully corrected measurements of the differential prompt and non-prompt cross-sections as functions of ψ(2S) p_{T} and rapidity are presented in figures 12(a) and 12(b) and are tabulated in table 5. These results are compared to results from CMS [14] and LHCb [13] in similar or neighbouring rapidity intervals (the LHCb and CMS data are also presented assuming isotropic ψ(2S) production). The measured differential cross-sections of prompt

JHEP09(2014)079

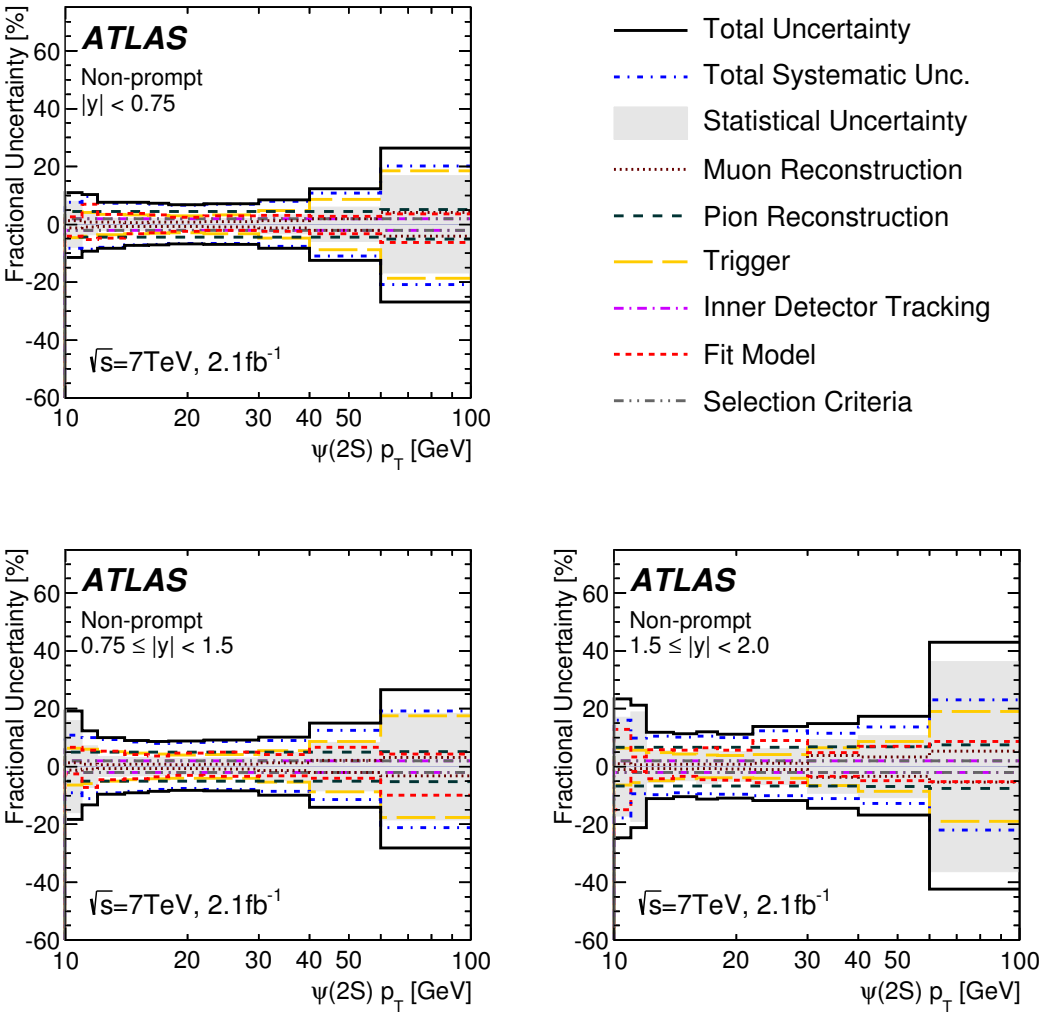

Figure 10. Summary of the positive and negative uncertainties for the non-prompt cross-section measurement in three $\psi(2S)$ rapidity intervals. The plots do not include the constant 1.8% luminosity uncertainty or the spin-alignment uncertainty.

and non-prompt production of J/ψ mesons from $\psi(2S) \to J/\psi\,\pi^+\pi^-$ decays are presented as functions of J/ψ transverse momentum and rapidity in figures 12(c) and 12(d) and in table 6.

The effects of the various polarisation scenarios described in section 4 on the measured J/ψ cross-sections were also studied. The corresponding correction factors for all J/ψ and $\psi(2S)$ p_{T} —$|y|$ bins are tabulated in appendix A.

Prompt cross-section measurement versus theory. In figure 13, the measured prompt production cross-sections are compared to predictions from colour-singlet [34–40] perturbative QCD calculations at partial next-to-next-to-leading-order (NNLO*) [41] using the CTEQ6M [42] parton distribution function set, leading-order (LO) and next-to-leading-order (NLO) non-relativistic QCD (NRQCD) [43] (or 'colour-octet' approach), the colour evaporation model [44–46], and a k_{T}-factorisation approach [47].

JHEP09(2014)079

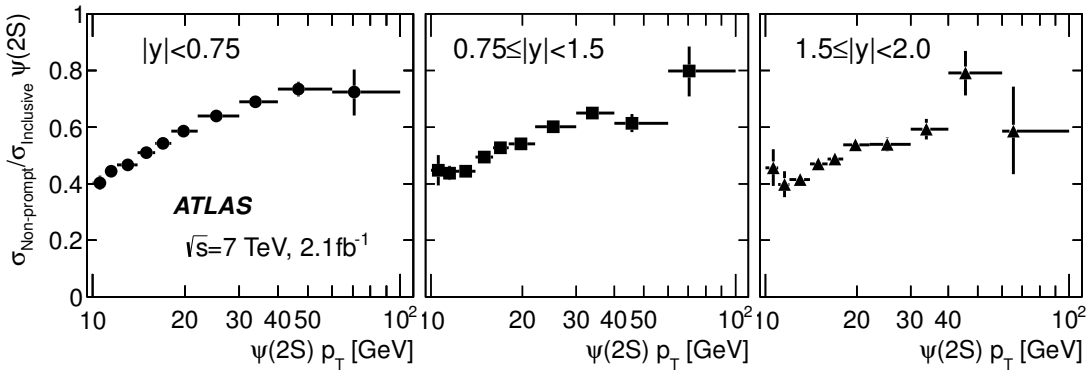

Figure 11. Non-prompt $\psi(2S)$ production fraction is calculated using eq. (4.4), and is shown here as a function of $\psi(2S)$ transverse momentum in three intervals of $\psi(2S)$ rapidity. The data points are at the mean of the efficiency and acceptance corrected p_T distribution in each p_T interval, indicated by the horizontal error bars, and the vertical error bars represent the total statistical and systematic uncertainty (see figure 8).

The colour-singlet NNLO* predictions have no free parameters constrained from experimental data. Uncertainties in these predictions are assessed by variation of renormalisation and factorisation scales (which dominate the total uncertainty), and the charm quark mass used in the calculation as discussed in ref. [41]. The central values of the NNLO* predictions underestimate the observed cross-sections by a factor of five, significantly outside the variation permitted by the associated scale uncertainties. Deviations from the data are enhanced at high p_T pointing to the need for further large singlet corrections or a sizeable colour octet contribution at these momenta.

The NRQCD predictions presented here are derived using HELAC-ONIA [48–51], an automatic matrix-element generator for the calculation of the heavy quarkonium helicity amplitudes in the framework of NRQCD factorisation. Uncertainties in the predictions come from the uncertainties due to the choice of scale, charm quark mass and long-distance matrix elements (LDME) as discussed in ref. [49]. NLO colour-octet LDME values from ref. [43] are used. NLO predictions do well in describing the shape and normalisation of prompt production data over the full range of transverse momenta probed, with the agreement particularly notable at large p_T where prior constraints on the LDME were not available. The ratio of theory to data is also shown in figure 13.

Uncertainties in the colour evaporation model (CEM) [52–54] predictions from factorisation and renormalisation scale dependencies are estimated according to the prescription discussed in ref. [55], using a central value for the charm quark mass of 1.27 GeV. The predictions of the CEM are found to describe $\psi(2S)$ production well, and tend to follow the same behaviour as the NLO NRQCD predictions, but at the highest p_T probed, there is a tendency for CEM to predict a somewhat harder spectrum than is observed in the data.

Parameter settings for the predictions of the k_T-factorisation approach shown here are described in ref. [47], take a parton-level cross-section prediction from the colour-singlet model [37, 38, 56] and make use of the CCFM A0 unintegrated gluon parameterisation [57] that incorporates initial-state radiation dependencies. Comparison with data shows that

JHEP09(2014)079

$0 \le \lvert y \rvert < 0.75$		
p_{T} interval [GeV]	$\langle p_{\mathrm{T}} \rangle$ [GeV]	Non-prompt fraction
10.0–11.0	10.6	$0.404 \pm 0.024 \pm 0.006$
11.0–12.0	11.5	$0.445 \pm 0.012 \pm 0.006$
12.0–14.0	13.0	$0.466 \pm 0.007 \pm 0.006$
14.0–16.0	15.0	$0.509 \pm 0.007 \pm 0.006$
16.0–18.0	17.0	$0.543 \pm 0.008 \pm 0.006$
18.0–22.0	19.8	$0.586 \pm 0.007 \pm 0.007$
22.0–30.0	25.2	$0.639 \pm 0.008 \pm 0.007$
30.0–40.0	33.8	$0.690 \pm 0.014 \pm 0.008$
40.0–60.0	46.6	$0.735 \pm 0.024 \pm 0.009$
60.0–100.0	70.8	$0.724 \pm 0.070 \pm 0.042$
$0.75 \le \lvert y \rvert < 1.5$		
p_{T} interval [GeV]	$\langle p_{\mathrm{T}} \rangle$ [GeV]	Non-prompt fraction
10.0–11.0	10.6	$0.448 \pm 0.053 \pm 0.009$
11.0–12.0	11.5	$0.438 \pm 0.024 \pm 0.006$
12.0–14.0	13.0	$0.445 \pm 0.012 \pm 0.006$
14.0–16.0	15.0	$0.495 \pm 0.011 \pm 0.006$
16.0–18.0	16.9	$0.527 \pm 0.012 \pm 0.006$
18.0–22.0	19.8	$0.542 \pm 0.010 \pm 0.006$
22.0–30.0	25.2	$0.602 \pm 0.012 \pm 0.007$
30.0–40.0	33.8	$0.649 \pm 0.018 \pm 0.007$
40.0–60.0	45.6	$0.614 \pm 0.031 \pm 0.008$
60.0–100.0	70.4	$0.798 \pm 0.081 \pm 0.034$
$1.5 \le \lvert y \rvert < 2$		
p_{T} interval [GeV]	$\langle p_{\mathrm{T}} \rangle$ [GeV]	Non-prompt fraction
10.0–11.0	10.6	$0.457 \pm 0.064 \pm 0.011$
11.0–12.0	11.5	$0.398 \pm 0.045 \pm 0.007$
12.0–14.0	13.0	$0.414 \pm 0.018 \pm 0.006$
14.0–16.0	14.9	$0.471 \pm 0.017 \pm 0.006$
16.0–18.0	16.9	$0.488 \pm 0.018 \pm 0.006$
18.0–22.0	19.8	$0.537 \pm 0.016 \pm 0.007$
22.0–30.0	25.1	$0.539 \pm 0.020 \pm 0.013$
30.0–40.0	33.9	$0.593 \pm 0.033 \pm 0.014$
40.0–60.0	45.5	$0.791 \pm 0.059 \pm 0.051$
60.0–100.0	65.3	$0.587 \pm 0.143 \pm 0.069$

Table 4. Non-prompt $\psi(2S)$ production fraction as a function of $\psi(2S)$ p_{T} for three $\psi(2S)$ rapidity intervals. The first uncertainty is statistical, the second is systematic. Spin-alignment uncertainties are not included.

the k_{T}-factorisation approach significantly underestimates the prompt $\psi(2S)$ production rate. The theory-to-data ratio in figure 13 highlights that this underestimation also has a p_{T}-dependent shape. This underestimation may be related to the observation [12] that the same model overestimates the production of C-even (χ_c) charmonium states.

JHEP09(2014)079

$\mathcal{B}(\psi(2S) \to J/\psi(\to \mu^+\mu^-)\pi^+\pi^-) \cdot \mathrm{d}^2\sigma^{\psi(2S)}/\mathrm{d}p_\mathrm{T}\,\mathrm{d}y$					
$0 \le \lvert y \rvert < 0.75$					
p_T interval [GeV]	$\langle p_\mathrm{T} \rangle$ [GeV]	Prompt [pb/GeV]		Non-prompt [pb/GeV]	
10.0–11.0	10.6	89 ± 7	$^{+10}_{-7}$	60.4 ± 4.8	$^{+4.6}_{-5.0}$
11.0–12.0	11.5	61.6 ± 2.1	$^{+7.1}_{-4.8}$	49.4 ± 1.7	$^{+4.8}_{-4.2}$
12.0–14.0	13.0	34.1 ± 0.7	$^{+3.8}_{-2.4}$	29.8 ± 0.6	$^{+2.2}_{-2.4}$
14.0–16.0	15.0	15.4 ± 0.3	$^{+1.6}_{-1.0}$	16.0 ± 0.3	$^{+1.2}_{-1.1}$
16.0–18.0	17.0	7.84 ± 0.19	$^{+0.79}_{-0.52}$	9.30 ± 0.20	$^{+0.65}_{-0.64}$
18.0–22.0	19.8	3.21 ± 0.07	$^{+0.32}_{-0.20}$	4.54 ± 0.08	$^{+0.30}_{-0.30}$
22.0–30.0	25.2	0.822 ± 0.024	$^{+0.086}_{-0.055}$	1.46 ± 0.03	$^{+0.10}_{-0.10}$
30.0–40.0	33.8	0.171 ± 0.009	$^{+0.019}_{-0.014}$	0.381 ± 0.012	$^{+0.030}_{-0.029}$
40.0–60.0	46.6	0.0241 ± 0.0026	$^{+0.0038}_{-0.0027}$	0.0670 ± 0.0040	$^{+0.0072}_{-0.0073}$
60.0–100.0	70.8	0.00106 ± 0.00034	$^{+0.00028}_{-0.00023}$	0.00279 ± 0.00047	$^{+0.00056}_{-0.00058}$
$\mathcal{B}(\psi(2S) \to J/\psi(\to \mu^+\mu^-)\pi^+\pi^-) \cdot \mathrm{d}^2\sigma^{\psi(2S)}/\mathrm{d}p_\mathrm{T}\,\mathrm{d}y$					
$0.75 \le \lvert y \rvert < 1.5$					
p_T interval [GeV]	$\langle p_\mathrm{T} \rangle$ [GeV]	Prompt [pb/GeV]		Non-prompt [pb/GeV]	
10.0–11.0	10.6	70 ± 11	$^{+8}_{-6}$	57 ± 9	$^{+6}_{-5}$
11.0–12.0	11.5	60.7 ± 4.1	$^{+6.4}_{-7.0}$	47.3 ± 3.4	$^{+4.8}_{-5.2}$
12.0–14.0	13.0	33.6 ± 1.1	$^{+3.3}_{-3.0}$	26.9 ± 0.9	$^{+2.5}_{-2.4}$
14.0–16.0	15.0	14.0 ± 0.5	$^{+1.4}_{-1.1}$	13.7 ± 0.4	$^{+1.2}_{-1.2}$
16.0–18.0	16.9	6.92 ± 0.25	$^{+0.64}_{-0.56}$	7.72 ± 0.25	$^{+0.62}_{-0.62}$
18.0–22.0	19.8	2.97 ± 0.09	$^{+0.30}_{-0.23}$	3.51 ± 0.10	$^{+0.30}_{-0.27}$
22.0–30.0	25.2	0.712 ± 0.028	$^{+0.073}_{-0.056}$	1.075 ± 0.031	$^{+0.094}_{-0.084}$
30.0–40.0	33.8	0.145 ± 0.010	$^{+0.016}_{-0.012}$	0.269 ± 0.013	$^{+0.024}_{-0.023}$
40.0–60.0	45.6	0.0259 ± 0.0027	$^{+0.0031}_{-0.0029}$	0.0412 ± 0.0035	$^{+0.0052}_{-0.0047}$
60.0–100.0	70.4	0.00068 ± 0.00032	$^{+0.00014}_{-0.00018}$	0.00269 ± 0.00050	$^{+0.00052}_{-0.00057}$
$\mathcal{B}(\psi(2S) \to J/\psi(\to \mu^+\mu^-)\pi^+\pi^-) \cdot \mathrm{d}^2\sigma^{\psi(2S)}/\mathrm{d}p_\mathrm{T}\,\mathrm{d}y$					
$1.5 \le \lvert y \rvert < 2$					
p_T interval [GeV]	$\langle p_\mathrm{T} \rangle$ [GeV]	Prompt [pb/GeV]		Non-prompt [pb/GeV]	
10.0–11.0	10.6	70 ± 16	$^{+11}_{-13}$	59 ± 10	$^{+9}_{-11}$
11.0–12.0	11.5	51.2 ± 9.1	$^{+4.9}_{-5.0}$	33.9 ± 6.4	$^{+3.3}_{-3.2}$
12.0–14.0	13.0	29.0 ± 1.5	$^{+3.0}_{-2.7}$	20.5 ± 1.1	$^{+2.2}_{-2.0}$
14.0–16.0	14.9	12.3 ± 0.6	$^{+1.2}_{-1.1}$	11.0 ± 0.5	$^{+1.1}_{-1.0}$
16.0–18.0	16.9	6.23 ± 0.36	$^{+0.67}_{-0.59}$	5.94 ± 0.35	$^{+0.63}_{-0.56}$
18.0–22.0	19.8	2.35 ± 0.13	$^{+0.27}_{-0.21}$	2.73 ± 0.14	$^{+0.27}_{-0.26}$
22.0–30.0	25.1	0.636 ± 0.042	$^{+0.078}_{-0.074}$	0.74 ± 0.05	$^{+0.09}_{-0.07}$
30.0–40.0	33.9	0.108 ± 0.012	$^{+0.013}_{-0.012}$	0.157 ± 0.015	$^{+0.018}_{-0.017}$
40.0–60.0	45.5	0.0095 ± 0.0035	$^{+0.0014}_{-0.0014}$	0.0358 ± 0.0038	$^{+0.0049}_{-0.0046}$
60.0–100.0	65.3	0.00072 ± 0.00031	$^{+0.00023}_{-0.00016}$	0.00103 ± 0.00037	$^{+0.00024}_{-0.00023}$

Table 5. Prompt and non-prompt production cross-section times branching ratio as a function of ψ(2S) p_T for three ψ(2S) rapidity intervals. The first uncertainty is statistical, the second is systematic. Spin-alignment and luminosity ($\pm 1.8\%$) uncertainties are not included.

JHEP09(2014)079

$\mathcal{B}(\psi(2S) \to J/\psi(\to \mu^+\mu^-)\pi^+\pi^-) \cdot \mathrm{d}^2\sigma^{\psi(2S)}/\mathrm{d}p_\mathrm{T}\,\mathrm{d}y$					
$0 \le \lvert y \rvert < 0.75$					
p_T interval [GeV]	$\langle p_\mathrm{T} \rangle$ [GeV]	Prompt [pb/GeV]		Non-prompt [pb/GeV]	
10.0–11.0	10.6	46.5 ± 1.7	$^{+6.1}_{-3.5}$	39.4 ± 1.5	$^{+3.2}_{-3.6}$
11.0–12.0	11.5	29.3 ± 0.9	$^{+3.4}_{-2.1}$	27.4 ± 0.8	$^{+2.2}_{-2.2}$
12.0–14.0	13.0	15.4 ± 0.3	$^{+1.6}_{-1.0}$	16.3 ± 0.3	$^{+1.2}_{-1.2}$
14.0–16.0	15.0	6.59 ± 0.18	$^{+0.65}_{-0.43}$	8.79 ± 0.19	$^{+0.61}_{-0.58}$
16.0–18.0	17.0	3.54 ± 0.11	$^{+0.36}_{-0.23}$	4.80 ± 0.13	$^{+0.32}_{-0.32}$
18.0–22.0	19.8	1.50 ± 0.05	$^{+0.15}_{-0.10}$	2.40 ± 0.06	$^{+0.16}_{-0.16}$
22.0–30.0	25.2	0.353 ± 0.015	$^{+0.039}_{-0.025}$	0.762 ± 0.019	$^{+0.054}_{-0.053}$
30.0–40.0	33.8	0.0602 ± 0.0054	$^{+0.0095}_{-0.0052}$	0.157 ± 0.008	$^{+0.013}_{-0.013}$
40.0–60.0	46.6	0.0086 ± 0.0015	$^{+0.0018}_{-0.0014}$	0.0203 ± 0.0020	$^{+0.0028}_{-0.0030}$
60.0–100.0	70.8	0.00030 ± 0.00017	$^{+0.00030}_{-0.00010}$	0.0010 ± 0.0006	$^{+0.0009}_{-0.0003}$
$\mathcal{B}(\psi(2S) \to J/\psi(\to \mu^+\mu^-)\pi^+\pi^-) \cdot \mathrm{d}^2\sigma^{\psi(2S)}/\mathrm{d}p_\mathrm{T}\,\mathrm{d}y$					
$0.75 \le \lvert y \rvert < 1.5$					
p_T interval [GeV]	$\langle p_\mathrm{T} \rangle$ [GeV]	Prompt [pb/GeV]		Non-prompt [pb/GeV]	
10.0–11.0	10.6	44.5 ± 2.2	$^{+4.9}_{-4.2}$	36.3 ± 1.9	$^{+3.8}_{-3.5}$
11.0–12.0	11.5	27.0 ± 1.2	$^{+2.7}_{-2.5}$	22.4 ± 1.2	$^{+2.3}_{-2.1}$
12.0–14.0	13.0	14.8 ± 0.5	$^{+1.5}_{-1.3}$	13.8 ± 0.5	$^{+1.2}_{-1.2}$
14.0–16.0	15.0	5.95 ± 0.23	$^{+0.62}_{-0.48}$	7.32 ± 0.25	$^{+0.63}_{-0.60}$
16.0–18.0	16.9	3.14 ± 0.16	$^{+0.30}_{-0.24}$	3.84 ± 0.17	$^{+0.33}_{-0.29}$
18.0–22.0	19.8	1.34 ± 0.06	$^{+0.12}_{-0.11}$	1.71 ± 0.06	$^{+0.15}_{-0.14}$
22.0–30.0	25.2	0.316 ± 0.017	$^{+0.033}_{-0.026}$	0.544 ± 0.022	$^{+0.049}_{-0.046}$
30.0–40.0	33.8	0.0636 ± 0.0060	$^{+0.0073}_{-0.0061}$	0.107 ± 0.008	$^{+0.010}_{-0.010}$
40.0–60.0	45.6	0.0078 ± 0.0015	$^{+0.0011}_{-0.0010}$	0.0165 ± 0.0020	$^{+0.0024}_{-0.0023}$
60.0–100.0	70.4	0.00023 ± 0.00014	$^{+0.00010}_{-0.00017}$	0.00070 ± 0.00042	$^{+0.00046}_{-0.00017}$
$\mathcal{B}(\psi(2S) \to J/\psi(\to \mu^+\mu^-)\pi^+\pi^-) \cdot \mathrm{d}^2\sigma^{\psi(2S)}/\mathrm{d}p_\mathrm{T}\,\mathrm{d}y$					
$1.5 \le \lvert y \rvert < 2$					
p_T interval [GeV]	$\langle p_\mathrm{T} \rangle$ [GeV]	Prompt [pb/GeV]		Non-prompt [pb/GeV]	
10.0–11.0	10.6	36 ± 14	$^{+5}_{-6}$	27 ± 12	$^{+4}_{-5}$
11.0–12.0	11.5	22.9 ± 2.2	$^{+3.4}_{-4.2}$	17.7 ± 1.8	$^{+2.5}_{-3.0}$
12.0–14.0	13.0	11.7 ± 0.7	$^{+1.6}_{-2.1}$	10.2 ± 0.6	$^{+1.3}_{-1.8}$
14.0–16.0	14.9	5.01 ± 0.28	$^{+0.61}_{-0.77}$	5.37 ± 0.28	$^{+0.67}_{-0.80}$
16.0–18.0	16.9	2.38 ± 0.19	$^{+0.26}_{-0.37}$	2.93 ± 0.21	$^{+0.32}_{-0.45}$
18.0–22.0	19.8	1.18 ± 0.09	$^{+0.15}_{-0.17}$	1.25 ± 0.09	$^{+0.15}_{-0.17}$
22.0–30.0	25.1	0.251 ± 0.024	$^{+0.027}_{-0.024}$	0.343 ± 0.029	$^{+0.036}_{-0.033}$
30.0–40.0	33.9	0.0318 ± 0.0004	$^{+0.0040}_{-0.0036}$	0.095 ± 0.001	$^{+0.012}_{-0.011}$
40.0–60.0	45.5	0.0031 ± 0.0006	$^{+0.0011}_{-0.0018}$	0.0115 ± 0.0008	$^{+0.0016}_{-0.0026}$
60.0–100.0	65.3	0.00034 ± 0.00032	$^{+0.00009}_{-0.00015}$	0.00031 ± 0.00023	$^{+0.00008}_{-0.00015}$

Table 6. Prompt and non-prompt production cross-section times branching ratio as a function of J/ψ p_T for three J/ψ rapidity intervals. The first uncertainty is statistical, the second is systematic. Spin-alignment and luminosity (±1.8%) uncertainties are not included.

JHEP09(2014)079

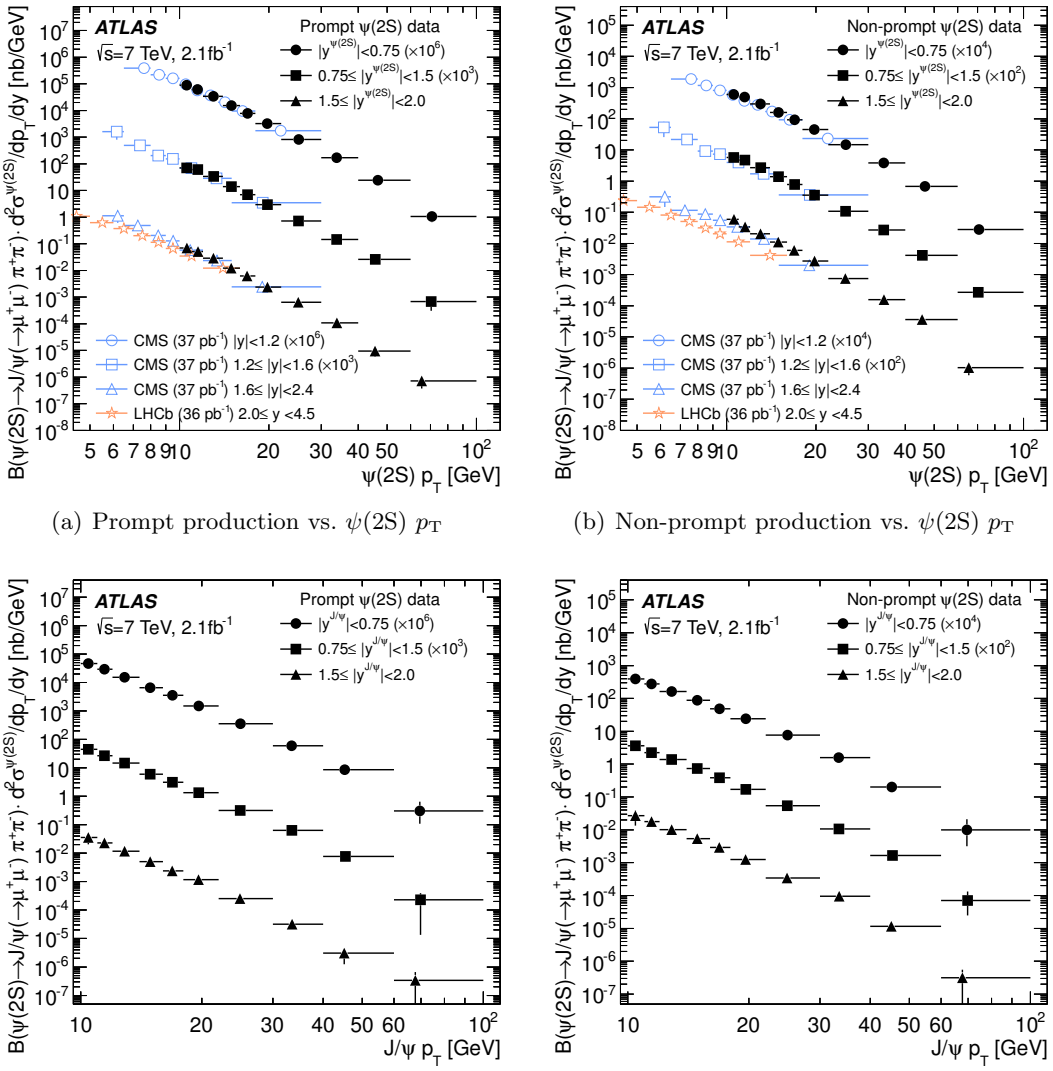

(a) Prompt production vs. $\psi(2S)$ p_T

(b) Non-prompt production vs. $\psi(2S)$ p_T

(c) Prompt production vs. J/ψ p_T

(d) Non-prompt production vs. J/ψ p_T

Figure 12. Measured differential cross-sections for (a) prompt $\psi(2S)$ production and (b) non-prompt $\psi(2S)$ production as a function of $\psi(2S)$ transverse momentum for three $\psi(2S)$ rapidity intervals. Also shown are (c) prompt and (d) non-prompt cross-sections expressed as a function of the transverse momentum of the J/ψ from the $\psi(2S) \to J/\psi(\to\mu^+\mu^-)\pi^+\pi^-$ decay for three J/ψ rapidity intervals. The results in the various rapidity intervals are scaled by powers of ten for clarity of presentation. The data points are at the mean of the efficiency and acceptance corrected p_T distribution in each p_T interval, indicated by the horizontal error bars, and the vertical error bars represent the total statistical and systematic uncertainty (see figures 9 and 10). Overlaid on the results presented as a function of $\psi(2S)$ p_T are measurements from the CMS and LHCb experiments.

Regarding the impact of possible spin-alignment variation on the prompt cross-section extracted (see figure 4 and appendix A), it is clear that even in the most extreme cases disfavoured by available data [23, 24], the maximum impact on the total reported cross-section is $(+62\%, -32\%)$ at a p_T of 10 GeV and drops to $(+8\%, -12\%)$ at high p_T. This range

JHEP09(2014)079

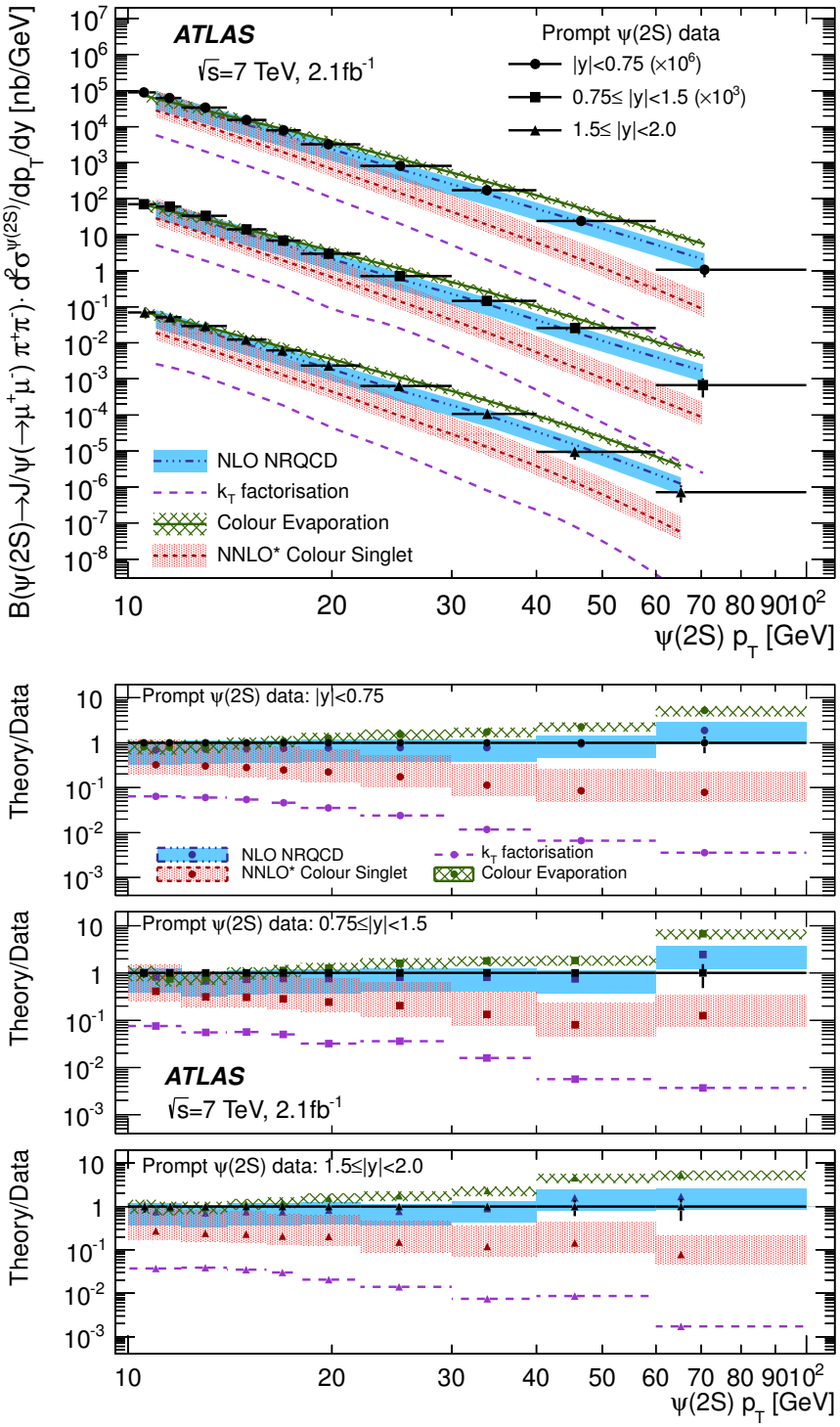

Figure 13. Measured differential cross-sections (top) and ratios of the predicted to measured differential cross-sections (bottom) for prompt $\psi(2S)$ production as a function of $\psi(2S)$ transverse momentum for three $\psi(2S)$ rapidity intervals, with comparison to theoretical predictions in the ATLAS fiducial region. The data points are at the mean of the efficiency and acceptance corrected p_T distribution in each p_T interval, indicated by the horizontal error bars, and the vertical error bars represent the total statistical and systematic uncertainty (see figure 9).

JHEP09(2014)079

of variation is significantly smaller than the observed differences between some theories and data.

Non-prompt cross-section measurement versus theory. For non-prompt production, comparison is made to theoretical predictions from fixed-order next-to-leading-logarithm (FONLL) calculations [58, 59], which have been successful in describing J/ψ [9] and B-meson production [60] at the LHC, and NLO predictions in the general-mass variable-flavour-number scheme (GM-VFNS), which have also proved reliable at describing production of non-prompt J/ψ at low p_{T} and central rapidities [61].

Comparison of the non-prompt spectra is made to FONLL predictions obtained by first determining the b-hadron production spectrum from a next-to-leading order QCD calculation matched with an all-order resummation to next-to-leading-logarithm accuracy in the limit where the transverse momentum of the b-quark is much larger than its mass. This distribution is then convolved with a phenomenological spectrum, obtained from experimental data that describe the momentum distribution of the $\psi(2S)$ in B-meson decays. The parton distribution function set CTEQ 6.6 [42] is used and the renormalisation and factorisation scales are chosen to be $\mu = \sqrt{m^2 + p_T^2}$, where m and p_{T} refer to the mass and transverse momentum of the b-quark, where a b-quark mass of 4.75 GeV is used. The Kartvelishvili-Likhoded-Petrov fragmentation function parameterisation [62] is used for determination of the b-quark fragmentation distribution. Uncertainties on the predictions are assessed by varying the b-quark mass (by ± 0.25 GeV), evaluating the parton distribution function uncertainties and varying the renormalisation and factorisation scales independently up and down by a factor of two from their nominal values, with the additional constraint that the ratio of two scales must be in the range 0.5–2.0.

NLO GM-VFNS predictions also use the CTEQ 6.6 parton distribution function set, the same choice of renormalisation and factorisation scales and variation as for FONLL, with a c-quark mass of 1.3 GeV and b-quark mass of 4.5 GeV. The NLO predictions make use of a fragmentation function derived from NLO fits to LEP data [63].

Figure 14 shows a comparison of FONLL and NLO GM-VFNS predictions to the non-prompt experimental data. Also shown is a comparison of NLO predictions using the FONLL fragmentation functions. At small and moderate transverse momenta, near and not significantly larger than the b-quark mass, NLO approaches are expected to do well, and scale uncertainties from the GM-VFNS approach are smaller than those from FONLL.

Both the FONLL and NLO GM-VFNS predictions describe the data well over the transverse momentum range studied but tend to predict a slightly harder p_{T} spectrum than observed in the data. This tendency is more noticeable in NLO predictions using the FONLL fragmentation functions. The differences observed between data and theoretical expectations are significantly larger than can be expected from any modification to the acceptance of $\psi(2S)$ due to a non-isotropic spin-alignment. Our data supports hints of a similar trend observed in CMS data [14], and extends the comparison with theory to higher momenta. Given that FONLL is able to describe reasonably well the production of fully reconstructed charged B mesons in a similar range of transverse momenta [60], the deviation observed in this measurement seems to point towards possible mismodelling in b-hadron composition and decay kinematics, rather than in the b-quark fragmentation.

JHEP09(2014)079

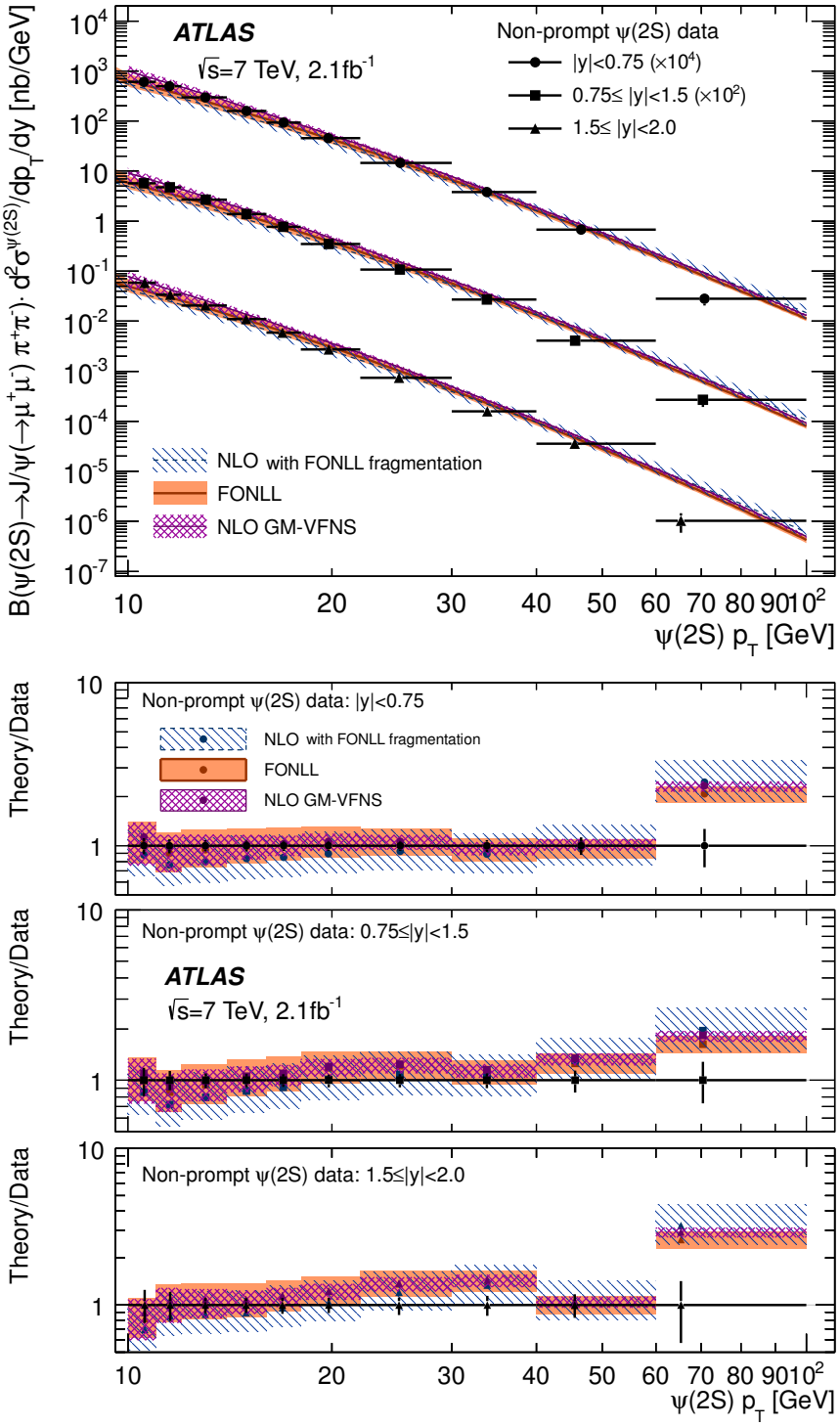

Figure 14. Measured differential cross-sections (top) and ratios of the predicted to measured differential cross-sections (bottom) for non-prompt $\psi(2S)$ production as a function of $\psi(2S)$ transverse momentum for three $\psi(2S)$ rapidity intervals with comparison to theoretical predictions in the ATLAS fiducial region. The data points are at the mean of the efficiency and acceptance corrected p_{T} distribution in each p_{T} interval, indicated by the horizontal error bars, and the vertical error bars represent the total statistical and systematic uncertainty (see figure 10).

JHEP09(2014)079

8 Conclusions

The prompt and non-prompt production cross-sections and the non-prompt production fraction of the $\psi(2S)$ decaying into $J/\psi(\rightarrow \mu^+\mu^-)\pi^+\pi^-$ were measured in the rapidity range $|y| < 2.0$ for transverse momenta between 10 and 100 GeV. This measurement was carried out using 2.1 fb^{-1} of pp collision data at a centre-of-mass energy of 7 TeV recorded by the ATLAS experiment at the LHC. The results presented here significantly extend the range of the measurement to higher transverse momenta with increased precision over previous measurements.

Theoretical models of prompt $\psi(2S)$ production vary significantly in their predictions of overall rate and kinematic dependence. NLO NRQCD predictions were found to describe the data satisfactorily across the full range of transverse momentum studied. Predictions from the colour evaporation model were able to describe all but the the highest p_{T} region, where the production rates were significantly overestimated. NNLO* colour-singlet calculations, in contrast, undershoot the data by an order of magnitude at the highest p_{T} studied. The addition of further large corrections to NNLO* colour-singlet calculations, or a significant colour-octet contribution at high transverse momentum is needed to describe the data. Predictions of the k_{T}-factorisation model exhibit a softer p_{T} spectrum than observed and clearly undershoot the data in overall rate. Together with the recent observation [12] of an overestimate of the production rate of C-even χ_c charmonium states in the k_{T}-factorisation approach, these measurements provide coherent input to improve the k_{T}-dependent approach.

In non-prompt $\psi(2S)$ production, both NLO GM-VFNS and FONLL calculations describe the data well, but a tendency is observed for the theory to predict a slightly harder p_{T} spectrum than is measured in data. This supports trends previously observed in CMS data at lower p_{T}, with the ATLAS and CMS data consistent in the region of overlap.

Acknowledgments

We thank Carlos Lourenço and Hermine Wöhri for pointing out an issue with the preliminary version of the data presented in this paper.

We thank CERN for the very successful operation of the LHC, as well as the support staff from our institutions without whom ATLAS could not be operated efficiently.

We acknowledge the support of ANPCyT, Argentina; YerPhI, Armenia; ARC, Australia; BMWF and FWF, Austria; ANAS, Azerbaijan; SSTC, Belarus; CNPq and FAPESP, Brazil; NSERC, NRC and CFI, Canada; CERN; CONICYT, Chile; CAS, MOST and NSFC, China; COLCIENCIAS, Colombia; MSMT CR, MPO CR and VSC CR, Czech Republic; DNRF, DNSRC and Lundbeck Foundation, Denmark; EPLANET, ERC and NSRF, European Union; IN2P3-CNRS, CEA-DSM/IRFU, France; GNSF, Georgia; BMBF, DFG, HGF, MPG and AvH Foundation, Germany; GSRT and NSRF, Greece; ISF, MINERVA, GIF, I-CORE and Benoziyo Center, Israel; INFN, Italy; MEXT and JSPS, Japan; CNRST, Morocco; FOM and NWO, Netherlands; BRF and RCN, Norway; MNiSW and NCN, Poland; GRICES and FCT, Portugal; MNE/IFA, Romania; MES of Russia and ROSATOM, Russian Federation; JINR; MSTD, Serbia; MSSR, Slovakia; ARRS and MIZŠ,

JHEP09(2014)079

Slovenia; DST/NRF, South Africa; MINECO, Spain; SRC and Wallenberg Foundation, Sweden; SER, SNSF and Cantons of Bern and Geneva, Switzerland; NSC, Taiwan; TAEK, Turkey; STFC, the Royal Society and Leverhulme Trust, United Kingdom; DOE and NSF, United States of America.

The crucial computing support from all WLCG partners is acknowledged gratefully, in particular from CERN and the ATLAS Tier-1 facilities at TRIUMF (Canada), NDGF (Denmark, Norway, Sweden), CC-IN2P3 (France), KIT/GridKA (Germany), INFN-CNAF (Italy), NL-T1 (Netherlands), PIC (Spain), ASGC (Taiwan), RAL (UK) and BNL (USA) and in the Tier-2 facilities worldwide.

A Acceptance correction factors

Tables 7 and 8 document correction factors that can be used to correct measured prompt $\psi(2S)$ production cross-sections from isotropic production cross-sections presented in the main text to an alternative spin-alignment scenario.

p_T [GeV]	10–11	11–12	12–14	14–16	16–18	18–22	22–30	30–40	40–60	60–100
Longitudinal										
$\lvert y\rvert < 0.75$	0.68	0.68	0.69	0.70	0.72	0.74	0.77	0.81	0.85	0.89
$0.75 \leq \lvert y\rvert < 1.50$	0.69	0.70	0.70	0.71	0.72	0.74	0.77	0.81	0.85	0.89
$1.50 \leq \lvert y\rvert < 2.00$	0.70	0.70	0.71	0.72	0.73	0.74	0.77	0.81	0.85	0.88
Transverse zero										
$\lvert y\rvert < 0.75$	1.32	1.30	1.29	1.27	1.25	1.22	1.18	1.14	1.10	1.06
$0.75 \leq \lvert y\rvert < 1.50$	1.29	1.28	1.27	1.25	1.24	1.21	1.18	1.13	1.10	1.07
$1.50 \leq \lvert y\rvert < 2.00$	1.27	1.27	1.26	1.25	1.23	1.21	1.17	1.13	1.10	1.08
Transverse positive										
$\lvert y\rvert < 0.75$	1.61	1.44	1.35	1.30	1.27	1.23	1.18	1.14	1.10	1.07
$0.75 \leq \lvert y\rvert < 1.50$	1.62	1.44	1.36	1.30	1.27	1.23	1.19	1.14	1.10	1.07
$1.50 \leq \lvert y\rvert < 2.00$	1.62	1.42	1.36	1.30	1.27	1.23	1.19	1.14	1.10	1.08
Transverse negative										
$\lvert y\rvert < 0.75$	1.11	1.20	1.22	1.23	1.22	1.21	1.17	1.13	1.10	1.07
$0.75 \leq \lvert y\rvert < 1.50$	1.07	1.16	1.19	1.21	1.21	1.19	1.17	1.13	1.10	1.06
$1.50 \leq \lvert y\rvert < 2.00$	1.05	1.14	1.18	1.20	1.20	1.19	1.16	1.13	1.10	1.07
Off-plane positive										
$\lvert y\rvert < 0.75$	1.06	1.05	1.05	1.04	1.03	1.02	1.02	1.01	1.01	1.00
$0.75 \leq \lvert y\rvert < 1.50$	1.12	1.12	1.10	1.08	1.07	1.05	1.04	1.02	1.01	1.01
$1.50 \leq \lvert y\rvert < 2.00$	1.14	1.15	1.12	1.10	1.08	1.07	1.04	1.02	1.01	1.01
Off-plane negative										
$\lvert y\rvert < 0.75$	0.96	0.95	0.96	0.96	0.97	0.98	0.98	0.99	0.99	1.00
$0.75 \leq \lvert y\rvert < 1.50$	0.91	0.91	0.92	0.93	0.94	0.95	0.97	0.98	0.99	0.99
$1.50 \leq \lvert y\rvert < 2.00$	0.90	0.89	0.90	0.91	0.93	0.94	0.96	0.97	0.99	0.99

Table 7. Multiplicative factors to correct measured production cross-sections measured in $\psi(2S)$ p_T and $|y|$ from isotropic production to an alternative spin-alignment scenario.

p_T [GeV]	10–11	11–12	12–14	14–16	16–18	18–22	22–30	30–40	40–60	60–100
Longitudinal										
$\|y\| < 0.75$	0.69	0.69	0.71	0.72	0.74	0.76	0.79	0.83	0.86	0.91
$0.75 \leq \|y\| < 1.50$	0.70	0.71	0.71	0.73	0.74	0.76	0.79	0.83	0.86	0.90
$1.50 \leq \|y\| < 2.00$	0.71	0.71	0.72	0.73	0.75	0.76	0.79	0.83	0.86	0.87
Transverse zero										
$\|y\| < 0.75$	1.29	1.28	1.26	1.24	1.22	1.19	1.15	1.12	1.09	1.06
$0.75 \leq \|y\| < 1.50$	1.28	1.27	1.25	1.23	1.21	1.19	1.15	1.11	1.09	1.06
$1.50 \leq \|y\| < 2.00$	1.26	1.26	1.24	1.23	1.21	1.19	1.15	1.11	1.09	1.04
Transverse positive										
$\|y\| < 0.75$	1.38	1.33	1.30	1.26	1.23	1.20	1.16	1.12	1.09	1.06
$0.75 \leq \|y\| < 1.50$	1.39	1.34	1.30	1.26	1.23	1.20	1.16	1.12	1.09	1.06
$1.50 \leq \|y\| < 2.00$	1.38	1.34	1.30	1.26	1.23	1.20	1.16	1.12	1.09	1.04
Transverse negative										
$\|y\| < 0.75$	1.22	1.23	1.23	1.22	1.20	1.18	1.15	1.11	1.09	1.05
$0.75 \leq \|y\| < 1.50$	1.19	1.20	1.21	1.20	1.19	1.17	1.15	1.11	1.09	1.05
$1.50 \leq \|y\| < 2.00$	1.16	1.19	1.20	1.20	1.19	1.17	1.15	1.11	1.09	1.07
Off-plane positive										
$\|y\| < 0.75$	1.05	1.04	1.04	1.03	1.02	1.02	1.01	1.01	1.01	1.00
$0.75 \leq \|y\| < 1.50$	1.11	1.09	1.08	1.07	1.05	1.04	1.03	1.02	1.01	1.01
$1.50 \leq \|y\| < 2.00$	1.13	1.12	1.10	1.08	1.06	1.05	1.03	1.02	1.01	1.00
Off-plane negative										
$\|y\| < 0.75$	0.95	0.96	0.97	0.97	0.98	0.98	0.99	0.99	1.00	1.00
$0.75 \leq \|y\| < 1.50$	0.91	0.92	0.93	0.94	0.95	0.96	0.97	0.99	0.99	0.99
$1.50 \leq \|y\| < 2.00$	0.90	0.91	0.92	0.93	0.94	0.95	0.97	0.98	0.99	0.98

Table 8. Multiplicative factors to correct measured production cross-sections measured in p_T and $|y|$ for J/ψ in the $\psi(2S) \to J/\psi(\to\mu^+\mu^-)\pi^+\pi^-$ decay from isotropic production to an alternative spin-alignment scenario.

References

[1] CDF collaboration, F. Abe et al., *J/ψ and $\psi(2S)$ production in $p\bar{p}$ collisions at $\sqrt{s} = 1.8$ TeV*, *Phys. Rev. Lett.* **79** (1997) 572 [INSPIRE].

[2] CDF collaboration, F. Abe et al., *Production of J/ψ mesons from χ_c meson decays in $p\bar{p}$ collisions at $\sqrt{s} = 1.8$ TeV*, *Phys. Rev. Lett.* **79** (1997) 578 [INSPIRE].

[3] CDF collaboration, D. Acosta et al., *Υ production and polarization in $p\bar{p}$ collisions at $\sqrt{s} = 1.8$ TeV*, *Phys. Rev. Lett.* **88** (2002) 161802 [INSPIRE].

[4] CDF collaboration, D. Acosta et al., *Measurement of the J/ψ meson and b-hadron production cross sections in $p\bar{p}$ collisions at $\sqrt{s} = 1960$ GeV*, *Phys. Rev.* **D 71** (2005) 032001 [hep-ex/0412071] [INSPIRE].

JHEP09(2014)079

[5] D0 collaboration, S. Abachi et al., *J/ψ production in $p\bar{p}$ collisions at $\sqrt{s} = 1.8$ TeV*, *Phys. Lett.* **B 370** (1996) 239 [INSPIRE].

[6] D0 collaboration, B. Abbott et al., *Small angle J/ψ production in $p\bar{p}$ collisions at $\sqrt{s} = 1.8$ TeV*, *Phys. Rev. Lett.* **82** (1999) 35 [hep-ex/9807029] [INSPIRE].

[7] D0 collaboration, V.M. Abazov et al., *Measurement of inclusive differential cross sections for Υ_{1S} production in $p\bar{p}$ collisions at $\sqrt{s} = 1.96$ TeV*, *Phys. Rev. Lett.* **94** (2005) 232001 [*Erratum ibid.* **100** (2008) 049902] [hep-ex/0502030] [INSPIRE].

[8] M. Kramer, *Quarkonium production at high-energy colliders*, *Prog. Part. Nucl. Phys.* **47** (2001) 141 [hep-ph/0106120] [INSPIRE].

[9] ATLAS collaboration, *Measurement of the differential cross-sections of inclusive, prompt and non-prompt J/ψ production in proton-proton collisions at $\sqrt{s} = 7$ TeV*, *Nucl. Phys.* **B 850** (2011) 387 [arXiv:1104.3038] [INSPIRE].

[10] ATLAS collaboration, *Measurement of the Υ_{1S} production cross-section in pp collisions at $\sqrt{s} = 7$ TeV in ATLAS*, *Phys. Lett.* **B 705** (2011) 9 [arXiv:1106.5325] [INSPIRE].

[11] ATLAS collaboration, *Measurement of Υ production in 7 TeV pp collisions at ATLAS*, *Phys. Rev.* **D 87** (2013) 052004 [arXiv:1211.7255] [INSPIRE].

[12] ATLAS collaboration, *Measurement of χ_{c1} and χ_{c2} production with $\sqrt{s} = 7$ TeV pp collisions at ATLAS*, *JHEP* **07** (2014) 154 [arXiv:1404.7035] [INSPIRE].

[13] LHCb collaboration, *Measurement of ψ_{2S} meson production in pp collisions at $\sqrt{s} = 7$ TeV*, *Eur. Phys. J.* **C 72** (2012) 2100 [arXiv:1204.1258] [INSPIRE].

[14] CMS collaboration, *J/ψ and ψ_{2S} production in pp collisions at $\sqrt{s} = 7$ TeV*, *JHEP* **02** (2012) 011 [arXiv:1111.1557] [INSPIRE].

[15] ALICE collaboration, *Measurement of quarkonium production at forward rapidity in pp collisions at $\sqrt{s} = 7$ TeV*, arXiv:1403.3648 [INSPIRE].

[16] ATLAS collaboration, *The ATLAS experiment at the CERN Large Hadron Collider*, 2008 *JINST* **3** S08003 [INSPIRE].

[17] ATLAS collaboration, *Performance of the ATLAS trigger system in 2010*, *Eur. Phys. J.* **C 72** (2012) 1849 [arXiv:1110.1530] [INSPIRE].

[18] ATLAS collaboration, *Improved luminosity determination in pp collisions at $\sqrt{s} = 7$ TeV using the ATLAS detector at the LHC*, *Eur. Phys. J.* **C 73** (2013) 2518 [arXiv:1302.4393] [INSPIRE].

[19] ATLAS collaboration, *Time-dependent angular analysis of the decay $B_s^0 \to J/\psi\phi$ and extraction of $\Delta\Gamma_s$ and the CP-violating weak phase ϕ_s by ATLAS*, *JHEP* **12** (2012) 072 [arXiv:1208.0572] [INSPIRE].

[20] Particle Data Group collaboration, J. Beringer et al., *Review of particle physics*, *Phys. Rev.* **D 86** (2012) 010001 [INSPIRE].

[21] BES collaboration, J.Z. Bai et al., *$\psi_{2S} \to \pi^+\pi^- J/\psi$ decay distributions*, *Phys. Rev.* **D 62** (2000) 032002 [hep-ex/9909038] [INSPIRE].

[22] P. Faccioli, C. Lourenco, J. Seixas and H.K. Wohri, *Towards the experimental clarification of quarkonium polarization*, *Eur. Phys. J.* **C 69** (2010) 657 [arXiv:1006.2738] [INSPIRE].

[23] CMS collaboration, *Measurement of the prompt J/ψ and ψ_{2S} polarizations in pp collisions at $\sqrt{s} = 7$ TeV*, *Phys. Lett.* **B 727** (2013) 381 [arXiv:1307.6070] [INSPIRE].

[24] LHCb collaboration, *Measurement of $\psi(2S)$ polarisation in pp collisions at $\sqrt{s} = 7$ TeV*, *Eur. Phys. J.* **C 74** (2014) 2872 [arXiv:1403.1339] [INSPIRE].

JHEP09(2014)079

[25] CDF collaboration, A. Abulencia et al., *Polarization of J/ψ and ψ_{2S} mesons produced in $p\bar{p}$ collisions at $\sqrt{s} = 1.96$ TeV*, *Phys. Rev. Lett.* **99** (2007) 132001 [arXiv:0704.0638] [INSPIRE].

[26] ATLAS collaboration, *Charged-particle multiplicities in pp interactions measured with the ATLAS detector at the LHC*, *New J. Phys.* **13** (2011) 053033 [arXiv:1012.5104] [INSPIRE].

[27] T. Sjöstrand, S. Mrenna and P.Z. Skands, *PYTHIA 6.4 physics and manual*, *JHEP* **05** (2006) 026 [hep-ph/0603175] [INSPIRE].

[28] ATLAS collaboration, *ATLAS tunes of PYTHIA 6 and PYTHIA 8 for MC11*, ATL-PHYS-PUB-2011-009 (2011).

[29] GEANT4 collaboration, S. Agostinelli et al., *GEANT4: a simulation toolkit*, *Nucl. Instrum. Meth.* **A 506** (2003) 250 [INSPIRE].

[30] ATLAS collaboration, *The ATLAS simulation infrastructure*, *Eur. Phys. J.* **C 70** (2010) 823 [arXiv:1005.4568] [INSPIRE].

[31] M. Oreglia, *A study of the reactions $\psi' \to \gamma\gamma\psi$*, Ph.D. thesis, Stanford University, U.S.A. (1980) [SLAC-R-0236].

[32] J. Gaiser, *Charmonium spectroscopy from radiative decays of the J/ψ and ψ'*, Ph.D. thesis, Stanford University, U.S.A. (1982) [SLAC-R-0255].

[33] T. Skwarnicki, *A study of the radiative cascade transitions between the Υ' and Υ resonances*, Ph.D. thesis, Institute of Nuclear Physics, Krakow, Poland (1986) [DESY-F31-86-02].

[34] J.F. Owens, E. Reya and M. Gluck, *Detailed quantum chromodynamic predictions for high p_T processes*, *Phys. Rev.* **D 18** (1978) 1501 [INSPIRE].

[35] V.G. Kartvelishvili, A.K. Likhoded and S.R. Slabospitsky, *D meson and ψ meson production in hadronic interactions*, *Sov. J. Nucl. Phys.* **28** (1978) 678 [INSPIRE].

[36] V.D. Barger, W.-Y. Keung and R.J.N. Phillips, *On ψ and Υ production via gluons*, *Phys. Lett.* **B 91** (1980) 253 [INSPIRE].

[37] C.-H. Chang, *Hadronic production of J/ψ associated with a gluon*, *Nucl. Phys.* **B 172** (1980) 425 [INSPIRE].

[38] E.L. Berger and D.L. Jones, *Inelastic photoproduction of J/ψ and Υ by gluons*, *Phys. Rev.* **D 23** (1981) 1521 [INSPIRE].

[39] R. Baier and R. Ruckl, *On inelastic leptoproduction of heavy quarkonium states*, *Nucl. Phys.* **B 201** (1982) 1 [INSPIRE].

[40] R. Baier and R. Ruckl, *Hadronic collisions: a quarkonium factory*, *Z. Phys.* **C 19** (1983) 251 [INSPIRE].

[41] J.P. Lansberg, *On the mechanisms of heavy-quarkonium hadroproduction*, *Eur. Phys. J.* **C 61** (2009) 693 [arXiv:0811.4005] [INSPIRE].

[42] J. Pumplin et al., *New generation of parton distributions with uncertainties from global QCD analysis*, *JHEP* **07** (2002) 012 [hep-ph/0201195] [INSPIRE].

[43] Y.-Q. Ma, K. Wang and K.-T. Chao, *$J/\psi(\psi')$ production at the Tevatron and LHC at $\mathcal{O}(\alpha_s^4 v^4)$ in nonrelativistic QCD*, *Phys. Rev. Lett.* **106** (2011) 042002 [arXiv:1009.3655] [INSPIRE].

[44] H. Fritzsch, *Producing heavy quark flavors in hadronic collisions: a test of quantum chromodynamics*, *Phys. Lett.* **B 67** (1977) 217 [INSPIRE].

[45] F. Halzen, *CVC for gluons and hadroproduction of quark flavors*, *Phys. Lett.* **B 69** (1977) 105 [INSPIRE].

JHEP09(2014)079

[46] A.D. Frawley, T. Ullrich and R. Vogt, *Heavy flavor in heavy-ion collisions at RHIC and RHIC II*, *Phys. Rept.* **462** (2008) 125 [arXiv:0806.1013] [INSPIRE].

[47] S.P. Baranov, A.V. Lipatov and N.P. Zotov, *Prompt J/Ψ production at LHC: new evidence for the k_t-factorization*, *Phys. Rev.* **D 85** (2012) 014034 [arXiv:1108.2856] [INSPIRE].

[48] H.-S. Shao, *HELAC-Onia: an automatic matrix element generator for heavy quarkonium physics*, *Comput. Phys. Commun.* **184** (2013) 2562 [arXiv:1212.5293] [INSPIRE].

[49] A. Kanaki and C.G. Papadopoulos, *HELAC: a package to compute electroweak helicity amplitudes*, *Comput. Phys. Commun.* **132** (2000) 306 [hep-ph/0002082] [INSPIRE].

[50] C.G. Papadopoulos, *PHEGAS: a phase space generator for automatic cross-section computation*, *Comput. Phys. Commun.* **137** (2001) 247 [hep-ph/0007335] [INSPIRE].

[51] A. Cafarella, C.G. Papadopoulos and M. Worek, *Helac-Phegas: a generator for all parton level processes*, *Comput. Phys. Commun.* **180** (2009) 1941 [arXiv:0710.2427] [INSPIRE].

[52] G.A. Schuler and R. Vogt, *Systematics of quarkonium production*, *Phys. Lett.* **B 387** (1996) 181 [hep-ph/9606410] [INSPIRE].

[53] J.F. Amundson, O.J.P. Eboli, E.M. Gregores and F. Halzen, *Colorless states in perturbative QCD: Charmonium and rapidity gaps*, *Phys. Lett.* **B 372** (1996) 127 [hep-ph/9512248] [INSPIRE].

[54] J.F. Amundson, O.J.P. Eboli, E.M. Gregores and F. Halzen, *Quantitative tests of color evaporation: charmonium production*, *Phys. Lett.* **B 390** (1997) 323 [hep-ph/9605295] [INSPIRE].

[55] R.E. Nelson, R. Vogt and A.D. Frawley, *Narrowing the uncertainty on the total charm cross section and its effect on the J/ψ cross section*, *Phys. Rev.* **C 87** (2013) 014908 [arXiv:1210.4610] [INSPIRE].

[56] R. Baier and R. Ruckl, *Hadronic production of J/ψ and Υ: transverse momentum distributions*, *Phys. Lett.* **B 102** (1981) 364 [INSPIRE].

[57] H. Jung, *Un-integrated PDFs in CCFM*, hep-ph/0411287 [INSPIRE].

[58] M. Cacciari, S. Frixione and P. Nason, *The p_T spectrum in heavy flavor photoproduction*, *JHEP* **03** (2001) 006 [hep-ph/0102134] [INSPIRE].

[59] M. Cacciari et al., *Theoretical predictions for charm and bottom production at the LHC*, *JHEP* **10** (2012) 137 [arXiv:1205.6344] [INSPIRE].

[60] ATLAS collaboration, *Measurement of the differential cross-section of B^+ meson production in pp collisions at $\sqrt{s} = 7$ TeV at ATLAS*, *JHEP* **10** (2013) 042 [arXiv:1307.0126] [INSPIRE].

[61] P. Bolzoni, B.A. Kniehl and G. Kramer, *Inclusive J/ψ and ψ_{2S} production from b-hadron decay in $p\bar{p}$ and pp collisions*, *Phys. Rev.* **D 88** (2013) 074035 [arXiv:1309.3389] [INSPIRE].

[62] V.G. Kartvelishvili, A.K. Likhoded and V.A. Petrov, *On the fragmentation functions of heavy quarks into hadrons*, *Phys. Lett.* **B 78** (1978) 615 [INSPIRE].

[63] B.A. Kniehl, G. Kramer, I. Schienbein and H. Spiesberger, *Finite-mass effects on inclusive B meson hadroproduction*, *Phys. Rev.* **D 77** (2008) 014011 [arXiv:0705.4392] [INSPIRE].

JHEP09(2014)079

The ATLAS collaboration

G. Aad[84], B. Abbott[112], J. Abdallah[152], S. Abdel Khalek[116], O. Abdinov[11], R. Aben[106], B. Abi[113], M. Abolins[89], O.S. AbouZeid[159], H. Abramowicz[154], H. Abreu[137], R. Abreu[30], Y. Abulaiti[147a,147b], B.S. Acharya[165a,165b,a], L. Adamczyk[38a], D.L. Adams[25], J. Adelman[177], S. Adomeit[99], T. Adye[130], T. Agatonovic-Jovin[13a], J.A. Aguilar-Saavedra[125a,125f], M. Agustoni[17], S.P. Ahlen[22], F. Ahmadov[64,b], G. Aielli[134a,134b], H. Akerstedt[147a,147b], T.P.A. Åkesson[80], G. Akimoto[156], A.V. Akimov[95], G.L. Alberghi[20a,20b], J. Albert[170], S. Albrand[55], M.J. Alconada Verzini[70], M. Aleksa[30], I.N. Aleksandrov[64], C. Alexa[26a], G. Alexander[154], G. Alexandre[49], T. Alexopoulos[10], M. Alhroob[165a,165c], G. Alimonti[90a], L. Alio[84], J. Alison[31], B.M.M. Allbrooke[18], L.J. Allison[71], P.P. Allport[73], J. Almond[83], A. Aloisio[103a,103b], A. Alonso[36], F. Alonso[70], C. Alpigiani[75], A. Altheimer[35], B. Alvarez Gonzalez[89], M.G. Alviggi[103a,103b], K. Amako[65], Y. Amaral Coutinho[24a], C. Amelung[23], D. Amidei[88], S.P. Amor Dos Santos[125a,125c], A. Amorim[125a,125b], S. Amoroso[48], N. Amram[154], G. Amundsen[23], C. Anastopoulos[140], L.S. Ancu[49], N. Andari[30], T. Andeen[35], C.F. Anders[58b], G. Anders[30], K.J. Anderson[31], A. Andreazza[90a,90b], V. Andrei[58a], X.S. Anduaga[70], S. Angelidakis[9], I. Angelozzi[106], P. Anger[44], A. Angerami[35], F. Anghinolfi[30], A.V. Anisenkov[108], N. Anjos[125a], A. Annovi[47], A. Antonaki[9], M. Antonelli[47], A. Antonov[97], J. Antos[145b], F. Anulli[133a], M. Aoki[65], L. Aperio Bella[18], R. Apolle[119,c], G. Arabidze[89], I. Aracena[144], Y. Arai[65], J.P. Araque[125a], A.T.H. Arce[45], J-F. Arguin[94], S. Argyropoulos[42], M. Arik[19a], A.J. Armbruster[30], O. Arnaez[82], V. Arnal[81], H. Arnold[48], O. Arslan[21], A. Artamonov[96], G. Artoni[23], S. Asai[156], N. Asbah[42], A. Ashkenazi[154], B. Åsman[147a,147b], L. Asquith[6], K. Assamagan[25], R. Astalos[145a], M. Atkinson[166], N.B. Atlay[142], B. Auerbach[6], K. Augsten[127], M. Aurousseau[146b], G. Avolio[30], G. Azuelos[94,d], Y. Azuma[156], M.A. Baak[30], C. Bacci[135a,135b], H. Bachacou[137], K. Bachas[155], M. Backes[30], M. Backhaus[30], J. Backus Mayes[144], E. Badescu[26a], P. Bagiacchi[133a,133b], P. Bagnaia[133a,133b], Y. Bai[33a], T. Bain[35], J.T. Baines[130], O.K. Baker[177], S. Baker[77], P. Balek[128], F. Balli[137], E. Banas[39], Sw. Banerjee[174], A. Bangert[151], A.A.E. Bannoura[176], V. Bansal[170], H.S. Bansil[18], L. Barak[173], S.P. Baranov[95], E.L. Barberio[87], D. Barberis[50a,50b], M. Barbero[84], T. Barillari[100], M. Barisonzi[176], T. Barklow[144], N. Barlow[28], B.M. Barnett[130], R.M. Barnett[15], Z. Barnovska[5], A. Baroncelli[135a], G. Barone[49], A.J. Barr[119], F. Barreiro[81], J. Barreiro Guimarães da Costa[57], R. Bartoldus[144], A.E. Barton[71], P. Bartos[145a], V. Bartsch[150], A. Bassalat[116], A. Basye[166], R.L. Bates[53], L. Batkova[145a], J.R. Batley[28], M. Battistin[30], F. Bauer[137], H.S. Bawa[144,e], T. Beau[79], P.H. Beauchemin[162], R. Beccherle[123a,123b], P. Bechtle[21], H.P. Beck[17], K. Becker[176], S. Becker[99], M. Beckingham[139], C. Becot[116], A.J. Beddall[19c], A. Beddall[19c], S. Bedikian[177], V.A. Bednyakov[64], C.P. Bee[149], L.J. Beemster[106], T.A. Beermann[176], M. Begel[25], K. Behr[119], C. Belanger-Champagne[86], P.J. Bell[49], W.H. Bell[49], G. Bella[154], L. Bellagamba[20a], A. Bellerive[29], M. Bellomo[85], K. Belotskiy[97], O. Beltramello[30], O. Benary[154], D. Benchekroun[136a], K. Bendtz[147a,147b], N. Benekos[166], Y. Benhammou[154], E. Benhar Noccioli[49], J.A. Benitez Garcia[160b], D.P. Benjamin[45], J.R. Bensinger[23], K. Benslama[131], S. Bentvelsen[106], D. Berge[106], E. Bergeaas Kuutmann[16], N. Berger[5], F. Berghaus[170], E. Berglund[106], J. Beringer[15], C. Bernard[22], P. Bernat[77], C. Bernius[78], F.U. Bernlochner[170], T. Berry[76], P. Berta[128], C. Bertella[84], F. Bertolucci[123a,123b], D. Bertsche[112], M.I. Besana[90a], G.J. Besjes[105], O. Bessidskaia[147a,147b], M.F. Bessner[42], N. Besson[137], C. Betancourt[48], S. Bethke[100], W. Bhimji[46], R.M. Bianchi[124], L. Bianchini[23], M. Bianco[30], O. Biebel[99], S.P. Bieniek[77], K. Bierwagen[54], J. Biesiada[15], M. Biglietti[135a], J. Bilbao De Mendizabal[49], H. Bilokon[47], M. Bindi[54], S. Binet[116], A. Bingul[19c], C. Bini[133a,133b], C.W. Black[151], J.E. Black[144], K.M. Black[22], D. Blackburn[139], R.E. Blair[6], J.-B. Blanchard[137], T. Blazek[145a], I. Bloch[42], C. Blocker[23], W. Blum[82,*], U. Blumenschein[54], G.J. Bobbink[106], V.S. Bobrovnikov[108], S.S. Bocchetta[80], A. Bocci[45], C.R. Boddy[119], M. Boehler[48], J. Boek[176], T.T. Boek[176], J.A. Bogaerts[30], A.G. Bogdanchikov[108], A. Bogouch[91,*], C. Bohm[147a], J. Bohm[126], V. Boisvert[76], T. Bold[38a], V. Boldea[26a], A.S. Boldyrev[98], M. Bomben[79], M. Bona[75], M. Boonekamp[137], A. Borisov[129], G. Borissov[71], M. Borri[83], S. Borroni[42], J. Bortfeldt[99], V. Bortolotto[135a,135b], K. Bos[106], D. Boscherini[20a], M. Bosman[12], H. Boterenbrood[106], J. Boudreau[124], J. Bouffard[2], E.V. Bouhova-Thacker[71],

JHEP09(2014)079

D. Boumediene[34], C. Bourdarios[116], N. Bousson[113], S. Boutouil[136d], A. Boveia[31], J. Boyd[30], I.R. Boyko[64], I. Bozovic-Jelisavcic[13b], J. Bracinik[18], P. Branchini[135a], A. Brandt[8], G. Brandt[15], O. Brandt[58a], U. Bratzler[157], B. Brau[85], J.E. Brau[115], H.M. Braun[176,*], S.F. Brazzale[165a,165c], B. Brelier[159], K. Brendlinger[121], A.J. Brennan[87], R. Brenner[167], S. Bressler[173], K. Bristow[146c], T.M. Bristow[46], D. Britton[53], F.M. Brochu[28], I. Brock[21], R. Brock[89], C. Bromberg[89], J. Bronner[100], G. Brooijmans[35], T. Brooks[76], W.K. Brooks[32b], J. Brosamer[15], E. Brost[115], G. Brown[83], J. Brown[55], P.A. Bruckman de Renstrom[39], D. Bruncko[145b], R. Bruneliere[48], S. Brunet[60], A. Bruni[20a], G. Bruni[20a], M. Bruschi[20a], L. Bryngemark[80], T. Buanes[14], Q. Buat[143], F. Bucci[49], P. Buchholz[142], R.M. Buckingham[119], A.G. Buckley[53], S.I. Buda[26a], I.A. Budagov[64], F. Buehrer[48], L. Bugge[118], M.K. Bugge[118], O. Bulekov[97], A.C. Bundock[73], H. Burckhart[30], S. Burdin[73], B. Burghgrave[107], S. Burke[130], I. Burmeister[43], E. Busato[34], D. Büscher[48], V. Büscher[82], P. Bussey[53], C.P. Buszello[167], B. Butler[57], J.M. Butler[22], A.I. Butt[3], C.M. Buttar[53], J.M. Butterworth[77], P. Butti[106], W. Buttinger[28], A. Buzatu[53], M. Byszewski[10], S. Cabrera Urbán[168], D. Caforio[20a,20b], O. Cakir[4a], P. Calafiura[15], A. Calandri[137], G. Calderini[79], P. Calfayan[99], R. Calkins[107], L.P. Caloba[24a], D. Calvet[34], S. Calvet[34], R. Camacho Toro[49], S. Camarda[42], D. Cameron[118], L.M. Caminada[15], R. Caminal Armadans[12], S. Campana[30], M. Campanelli[77], A. Campoverde[149], V. Canale[103a,103b], A. Canepa[160a], M. Cano Bret[75], J. Cantero[81], R. Cantrill[76], T. Cao[40], M.D.M. Capeans Garrido[30], I. Caprini[26a], M. Caprini[26a], M. Capua[37a,37b], R. Caputo[82], R. Cardarelli[134a], T. Carli[30], G. Carlino[103a], L. Carminati[90a,90b], S. Caron[105], E. Carquin[32a], G.D. Carrillo-Montoya[146c], J.R. Carter[28], J. Carvalho[125a,125c], D. Casadei[77], M.P. Casado[12], M. Casolino[12], E. Castaneda-Miranda[146b], A. Castelli[106], V. Castillo Gimenez[168], N.F. Castro[125a], P. Catastini[57], A. Catinaccio[30], J.R. Catmore[118], A. Cattai[30], G. Cattani[134a,134b], S. Caughron[89], V. Cavaliere[166], D. Cavalli[90a], M. Cavalli-Sforza[12], V. Cavasinni[123a,123b], F. Ceradini[135a,135b], B. Cerio[45], K. Cerny[128], A.S. Cerqueira[24b], A. Cerri[150], L. Cerrito[75], F. Cerutti[15], M. Cerv[30], A. Cervelli[17], S.A. Cetin[19b], A. Chafaq[136a], D. Chakraborty[107], I. Chalupkova[128], K. Chan[3], P. Chang[166], B. Chapleau[86], J.D. Chapman[28], D. Charfeddine[116], D.G. Charlton[18], C.C. Chau[159], C.A. Chavez Barajas[150], S. Cheatham[86], A. Chegwidden[89], S. Chekanov[6], S.V. Chekulaev[160a], G.A. Chelkov[64,f], M.A. Chelstowska[88], C. Chen[63], H. Chen[25], K. Chen[149], L. Chen[33d,g], S. Chen[33c], X. Chen[146c], Y. Chen[35], H.C. Cheng[88], Y. Cheng[31], A. Cheplakov[64], R. Cherkaoui El Moursli[136e], V. Chernyatin[25,*], E. Cheu[7], L. Chevalier[137], V. Chiarella[47], G. Chiefari[103a,103b], J.T. Childers[6], A. Chilingarov[71], G. Chiodini[72a], A.S. Chisholm[18], R.T. Chislett[77], A. Chitan[26a], M.V. Chizhov[64], S. Chouridou[9], B.K.B. Chow[99], D. Chromek-Burckhart[30], M.L. Chu[152], J. Chudoba[126], J.J. Chwastowski[39], L. Chytka[114], G. Ciapetti[133a,133b], A.K. Ciftci[4a], R. Ciftci[4a], D. Cinca[62], V. Cindro[74], A. Ciocio[15], P. Cirkovic[13b], Z.H. Citron[173], M. Citterio[90a], M. Ciubancan[26a], A. Clark[49], P.J. Clark[46], R.N. Clarke[15], W. Cleland[124], J.C. Clemens[84], C. Clement[147a,147b], Y. Coadou[84], M. Cobal[165a,165c], A. Coccaro[139], J. Cochran[63], L. Coffey[23], J.G. Cogan[144], J. Coggeshall[166], B. Cole[35], S. Cole[107], A.P. Colijn[106], J. Collot[55], T. Colombo[58c], G. Colon[85], G. Compostella[100], P. Conde Muiño[125a,125b], E. Coniavitis[167], M.C. Conidi[12], S.H. Connell[146b], I.A. Connelly[76], S.M. Consonni[90a,90b], V. Consorti[48], S. Constantinescu[26a], C. Conta[120a,120b], G. Conti[57], F. Conventi[103a,h], M. Cooke[15], B.D. Cooper[77], A.M. Cooper-Sarkar[119], N.J. Cooper-Smith[76], K. Copic[15], T. Cornelissen[176], M. Corradi[20a], F. Corriveau[86,i], A. Corso-Radu[164], A. Cortes-Gonzalez[12], G. Cortiana[100], G. Costa[90a], M.J. Costa[168], D. Costanzo[140], D. Côté[8], G. Cottin[28], G. Cowan[76], B.E. Cox[83], K. Cranmer[109], G. Cree[29], S. Crépé-Renaudin[55], F. Crescioli[79], W.A. Cribbs[147a,147b], M. Crispin Ortuzar[119], M. Cristinziani[21], V. Croft[105], G. Crosetti[37a,37b], C.-M. Cuciuc[26a], T. Cuhadar Donszelmann[140], J. Cummings[177], M. Curatolo[47], C. Cuthbert[151], H. Czirr[142], P. Czodrowski[3], Z. Czyczula[177], S. D'Auria[53], M. D'Onofrio[73], M.J. Da Cunha Sargedas De Sousa[125a,125b], C. Da Via[83], W. Dabrowski[38a], A. Dafinca[119], T. Dai[88], O. Dale[14], F. Dallaire[94], C. Dallapiccola[85], M. Dam[36], A.C. Daniells[18], M. Dano Hoffmann[137], V. Dao[105], G. Darbo[50a], G.L. Darlea[26c], S. Darmora[8], J.A. Dassoulas[42], A. Dattagupta[60], W. Davey[21], C. David[170], T. Davidek[128], E. Davies[119,c], M. Davies[154], O. Davignon[79], A.R. Davison[77], P. Davison[77], Y. Davygora[58a], E. Dawe[143],

JHEP09(2014)079

I. Dawson[140], R.K. Daya-Ishmukhametova[85], K. De[8], R. de Asmundis[103a], S. De Castro[20a,20b], S. De Cecco[79], N. De Groot[105], P. de Jong[106], H. De la Torre[81], F. De Lorenzi[63], L. De Nooij[106], D. De Pedis[133a], A. De Salvo[133a], U. De Sanctis[165a,165b], A. De Santo[150], J.B. De Vivie De Regie[116], W.J. Dearnaley[71], R. Debbe[25], C. Debenedetti[46], B. Dechenaux[55], D.V. Dedovich[64], J. Degenhardt[121], I. Deigaard[106], J. Del Peso[81], T. Del Prete[123a,123b], F. Deliot[137], C.M. Delitzsch[49], M. Deliyergiyev[74], A. Dell'Acqua[30], L. Dell'Asta[22], M. Dell'Orso[123a,123b], M. Della Pietra[103a,h], D. della Volpe[49], M. Delmastro[5], P.A. Delsart[55], C. Deluca[106], S. Demers[177], M. Demichev[64], A. Demilly[79], S.P. Denisov[129], D. Derendarz[39], J.E. Derkaoui[136d], F. Derue[79], P. Dervan[73], K. Desch[21], C. Deterre[42], P.O. Deviveiros[106], A. Dewhurst[130], S. Dhaliwal[106], A. Di Ciaccio[134a,134b], L. Di Ciaccio[5], A. Di Domenico[133a,133b], C. Di Donato[103a,103b], A. Di Girolamo[30], B. Di Girolamo[30], A. Di Mattia[153], B. Di Micco[135a,135b], R. Di Nardo[47], A. Di Simone[48], R. Di Sipio[20a,20b], D. Di Valentino[29], M.A. Diaz[32a], E.B. Diehl[88], J. Dietrich[42], T.A. Dietzsch[58a], S. Diglio[84], A. Dimitrievska[13a], J. Dingfelder[21], C. Dionisi[133a,133b], P. Dita[26a], S. Dita[26a], F. Dittus[30], F. Djama[84], T. Djobava[51b], M.A.B. do Vale[24c], A. Do Valle Wemans[125a,125g], T.K.O. Doan[5], D. Dobos[30], C. Doglioni[49], T. Doherty[53], T. Dohmae[156], J. Dolejsi[128], Z. Dolezal[128], B.A. Dolgoshein[97,*], M. Donadelli[24d], S. Donati[123a,123b], P. Dondero[120a,120b], J. Donini[34], J. Dopke[30], A. Doria[103a], M.T. Dova[70], A.T. Doyle[53], M. Dris[10], J. Dubbert[88], S. Dube[15], E. Dubreuil[34], E. Duchovni[173], G. Duckeck[99], O.A. Ducu[26a], D. Duda[176], A. Dudarev[30], F. Dudziak[63], L. Duflot[116], L. Duguid[76], M. Dührssen[30], M. Dunford[58a], H. Duran Yildiz[4a], M. Düren[52], A. Durglishvili[51b], M. Dwuznik[38a], M. Dyndal[38a], J. Ebke[99], W. Edson[2], N.C. Edwards[46], W. Ehrenfeld[21], T. Eifert[144], G. Eigen[14], K. Einsweiler[15], T. Ekelof[167], M. El Kacimi[136c], M. Ellert[167], S. Elles[5], F. Ellinghaus[82], N. Ellis[30], J. Elmsheuser[99], M. Elsing[30], D. Emeliyanov[130], Y. Enari[156], O.C. Endner[82], M. Endo[117], R. Engelmann[149], J. Erdmann[177], A. Ereditato[17], D. Eriksson[147a], G. Ernis[176], J. Ernst[2], M. Ernst[25], J. Ernwein[137], D. Errede[166], S. Errede[166], E. Ertel[82], M. Escalier[116], H. Esch[43], C. Escobar[124], B. Esposito[47], A.I. Etienvre[137], E. Etzion[154], H. Evans[60], A. Ezhilov[122], L. Fabbri[20a,20b], G. Facini[30], R.M. Fakhrutdinov[129], S. Falciano[133a], R.J. Falla[77], J. Faltova[128], Y. Fang[33a], M. Fanti[90a,90b], A. Farbin[8], A. Farilla[135a], T. Farooque[12], S. Farrell[164], S.M. Farrington[171], P. Farthouat[30], F. Fassi[168], P. Fassnacht[30], D. Fassouliotis[9], A. Favareto[50a,50b], L. Fayard[116], P. Federic[145a], O.L. Fedin[122,j], W. Fedorko[169], M. Fehling-Kaschek[48], S. Feigl[30], L. Feligioni[84], C. Feng[33d], E.J. Feng[6], H. Feng[88], A.B. Fenyuk[129], S. Fernandez Perez[30], S. Ferrag[53], J. Ferrando[53], A. Ferrari[167], P. Ferrari[106], R. Ferrari[120a], D.E. Ferreira de Lima[53], A. Ferrer[168], D. Ferrere[49], C. Ferretti[88], A. Ferretto Parodi[50a,50b], M. Fiascaris[31], F. Fiedler[82], A. Filipčič[74], M. Filipuzzi[42], F. Filthaut[105], M. Fincke-Keeler[170], K.D. Finelli[151], M.C.N. Fiolhais[125a,125c], L. Fiorini[168], A. Firan[40], J. Fischer[176], W.C. Fisher[89], E.A. Fitzgerald[23], M. Flechl[48], I. Fleck[142], P. Fleischmann[88], S. Fleischmann[176], G.T. Fletcher[140], G. Fletcher[75], T. Flick[176], A. Floderus[80], L.R. Flores Castillo[174,k], A.C. Florez Bustos[160b], M.J. Flowerdew[100], A. Formica[137], A. Forti[83], D. Fortin[160a], D. Fournier[116], H. Fox[71], S. Fracchia[12], P. Francavilla[79], M. Franchini[20a,20b], S. Franchino[30], D. Francis[30], M. Franklin[57], S. Franz[61], M. Fraternali[120a,120b], S.T. French[28], C. Friedrich[42], F. Friedrich[44], D. Froidevaux[30], J.A. Frost[28], C. Fukunaga[157], E. Fullana Torregrosa[82], B.G. Fulsom[144], J. Fuster[168], C. Gabaldon[55], O. Gabizon[173], A. Gabrielli[20a,20b], A. Gabrielli[133a,133b], S. Gadatsch[106], S. Gadomski[49], G. Gagliardi[50a,50b], P. Gagnon[60], C. Galea[105], B. Galhardo[125a,125c], E.J. Gallas[119], V. Gallo[17], B.J. Gallop[130], P. Gallus[127], G. Galster[36], K.K. Gan[110], R.P. Gandrajula[62], J. Gao[33b,g], Y.S. Gao[144,e], F.M. Garay Walls[46], F. Garberson[177], C. García[168], J.E. García Navarro[168], M. Garcia-Sciveres[15], R.W. Gardner[31], N. Garelli[144], V. Garonne[30], C. Gatti[47], G. Gaudio[120a], B. Gaur[142], L. Gauthier[94], P. Gauzzi[133a,133b], I.L. Gavrilenko[95], C. Gay[169], G. Gaycken[21], E.N. Gazis[10], P. Ge[33d], Z. Gecse[169], C.N.P. Gee[130], D.A.A. Geerts[106], Ch. Geich-Gimbel[21], K. Gellerstedt[147a,147b], C. Gemme[50a], A. Gemmell[53], M.H. Genest[55], S. Gentile[133a,133b], M. George[54], S. George[76], D. Gerbaudo[164], A. Gershon[154], H. Ghazlane[136b], N. Ghodbane[34], B. Giacobbe[20a], S. Giagu[133a,133b], V. Giangiobbe[12], P. Giannetti[123a,123b], F. Gianotti[30],

JHEP09(2014)079

B. Gibbard[25], S.M. Gibson[76], M. Gilchriese[15], T.P.S. Gillam[28], D. Gillberg[30], G. Gilles[34], D.M. Gingrich[3,d], N. Giokaris[9], M.P. Giordani[165a,165c], R. Giordano[103a,103b], F.M. Giorgi[20a], F.M. Giorgi[16], P.F. Giraud[137], D. Giugni[90a], C. Giuliani[48], M. Giulini[58b], B.K. Gjelsten[118], I. Gkialas[155,l], L.K. Gladilin[98], C. Glasman[81], J. Glatzer[30], P.C.F. Glaysher[46], A. Glazov[42], G.L. Glonti[64], M. Goblirsch-Kolb[100], J.R. Goddard[75], J. Godfrey[143], J. Godlewski[30], C. Goeringer[82], S. Goldfarb[88], T. Golling[177], D. Golubkov[129], A. Gomes[125a,125b,125d], L.S. Gomez Fajardo[42], R. Gonçalo[125a], J. Goncalves Pinto Firmino Da Costa[137], L. Gonella[21], S. González de la Hoz[168], G. Gonzalez Parra[12], M.L. Gonzalez Silva[27], S. Gonzalez-Sevilla[49], L. Goossens[30], P.A. Gorbounov[96], H.A. Gordon[25], I. Gorelov[104], B. Gorini[30], E. Gorini[72a,72b], A. Gorišek[74], E. Gornicki[39], A.T. Goshaw[6], C. Gössling[43], M.I. Gostkin[64], M. Gouighri[136a], D. Goujdami[136c], M.P. Goulette[49], A.G. Goussiou[139], C. Goy[5], S. Gozpinar[23], H.M.X. Grabas[137], L. Graber[54], I. Grabowska-Bold[38a], P. Grafström[20a,20b], K-J. Grahn[42], J. Gramling[49], E. Gramstad[118], S. Grancagnolo[16], V. Grassi[149], V. Gratchev[122], H.M. Gray[30], E. Graziani[135a], O.G. Grebenyuk[122], Z.D. Greenwood[78,m], K. Gregersen[77], I.M. Gregor[42], P. Grenier[144], J. Griffiths[8], A.A. Grillo[138], K. Grimm[71], S. Grinstein[12,n], Ph. Gris[34], Y.V. Grishkevich[98], J.-F. Grivaz[116], J.P. Grohs[44], A. Grohsjean[42], E. Gross[173], J. Grosse-Knetter[54], G.C. Grossi[134a,134b], J. Groth-Jensen[173], Z.J. Grout[150], K. Grybel[142], L. Guan[33b], F. Guescini[49], D. Guest[177], O. Gueta[154], C. Guicheney[34], E. Guido[50a,50b], T. Guillemin[116], S. Guindon[2], U. Gul[53], C. Gumpert[44], J. Gunther[127], J. Guo[35], S. Gupta[119], P. Gutierrez[112], N.G. Gutierrez Ortiz[53], C. Gutschow[77], N. Guttman[154], C. Guyot[137], C. Gwenlan[119], C.B. Gwilliam[73], A. Haas[109], C. Haber[15], H.K. Hadavand[8], N. Haddad[136e], P. Haefner[21], S. Hageböck[21], Z. Hajduk[39], H. Hakobyan[178], M. Haleem[42], D. Hall[119], G. Halladjian[89], K. Hamacher[176], P. Hamal[114], K. Hamano[170], M. Hamer[54], A. Hamilton[146a], S. Hamilton[162], P.G. Hamnett[42], L. Han[33b], K. Hanagaki[117], K. Hanawa[156], M. Hance[15], P. Hanke[58a], R. Hanna[137], J.B. Hansen[36], J.D. Hansen[36], P.H. Hansen[36], K. Hara[161], A.S. Hard[174], T. Harenberg[176], F. Hariri[116], S. Harkusha[91], D. Harper[88], R.D. Harrington[46], O.M. Harris[139], P.F. Harrison[171], F. Hartjes[106], S. Hasegawa[102], Y. Hasegawa[141], A. Hasib[112], S. Hassani[137], S. Haug[17], M. Hauschild[30], R. Hauser[89], M. Havranek[126], C.M. Hawkes[18], R.J. Hawkings[30], A.D. Hawkins[80], T. Hayashi[161], D. Hayden[89], C.P. Hays[119], H.S. Hayward[73], S.J. Haywood[130], S.J. Head[18], T. Heck[82], V. Hedberg[80], L. Heelan[8], S. Heim[121], T. Heim[176], B. Heinemann[15], L. Heinrich[109], S. Heisterkamp[36], J. Hejbal[126], L. Helary[22], C. Heller[99], M. Heller[30], S. Hellman[147a,147b], D. Hellmich[21], C. Helsens[30], J. Henderson[119], R.C.W. Henderson[71], C. Hengler[42], A. Henrichs[177], A.M. Henriques Correia[30], S. Henrot-Versille[116], C. Hensel[54], G.H. Herbert[16], Y. Hernández Jiménez[168], R. Herrberg-Schubert[16], G. Herten[48], R. Hertenberger[99], L. Hervas[30], G.G. Hesketh[77], N.P. Hessey[106], R. Hickling[75], E. Higón-Rodriguez[168], E. Hill[170], J.C. Hill[28], K.H. Hiller[42], S. Hillert[21], S.J. Hillier[18], I. Hinchliffe[15], E. Hines[121], M. Hirose[117], D. Hirschbuehl[176], J. Hobbs[149], N. Hod[106], M.C. Hodgkinson[140], P. Hodgson[140], A. Hoecker[30], M.R. Hoeferkamp[104], J. Hoffman[40], D. Hoffmann[84], J.I. Hofmann[58a], M. Hohlfeld[82], T.R. Holmes[15], T.M. Hong[121], L. Hooft van Huysduynen[109], J-Y. Hostachy[55], S. Hou[152], A. Hoummada[136a], J. Howard[119], J. Howarth[42], M. Hrabovsky[114], I. Hristova[16], J. Hrivnac[116], T. Hryn'ova[5], P.J. Hsu[82], S.-C. Hsu[139], D. Hu[35], X. Hu[25], Y. Huang[42], Z. Hubacek[30], F. Hubaut[84], F. Huegging[21], T.B. Huffman[119], E.W. Hughes[35], G. Hughes[71], M. Huhtinen[30], T.A. Hülsing[82], M. Hurwitz[15], N. Huseynov[64,b], J. Huston[89], J. Huth[57], G. Iacobucci[49], G. Iakovidis[10], I. Ibragimov[142], L. Iconomidou-Fayard[116], E. Ideal[177], P. Iengo[103a], O. Igonkina[106], T. Iizawa[172], Y. Ikegami[65], K. Ikematsu[142], M. Ikeno[65], Y. Ilchenko[31,aa], D. Iliadis[155], N. Ilic[159], Y. Inamaru[66], T. Ince[100], P. Ioannou[9], M. Iodice[135a], K. Iordanidou[9], V. Ippolito[57], A. Irles Quiles[168], C. Isaksson[167], M. Ishino[67], M. Ishitsuka[158], R. Ishmukhametov[110], C. Issever[119], S. Istin[19a], J.M. Iturbe Ponce[83], J. Ivarsson[80], A.V. Ivashin[129], W. Iwanski[39], H. Iwasaki[65], J.M. Izen[41], V. Izzo[103a], B. Jackson[121], M. Jackson[73], P. Jackson[1], M.R. Jaekel[30], V. Jain[2], K. Jakobs[48], S. Jakobsen[30], T. Jakoubek[126], J. Jakubek[127], D.O. Jamin[152], D.K. Jana[78], E. Jansen[77], H. Jansen[30], J. Janssen[21], M. Janus[171], G. Jarlskog[80], N. Javadov[64,b], T. Javůrek[48], L. Jeanty[15],

JHEP09(2014)079

G.-Y. Jeng[151], D. Jennens[87], P. Jenni[48,o], J. Jentzsch[43], C. Jeske[171], S. Jézéquel[5], H. Ji[174], W. Ji[82], J. Jia[149], Y. Jiang[33b], M. Jimenez Belenguer[42], S. Jin[33a], A. Jinaru[26a], O. Jinnouchi[158], M.D. Joergensen[36], K.E. Johansson[147a], P. Johansson[140], K.A. Johns[7], K. Jon-And[147a,147b], G. Jones[171], R.W.L. Jones[71], T.J. Jones[73], J. Jongmanns[58a], P.M. Jorge[125a,125b], K.D. Joshi[83], J. Jovicevic[148], X. Ju[174], C.A. Jung[43], R.M. Jungst[30], P. Jussel[61], A. Juste Rozas[12,n], M. Kaci[168], A. Kaczmarska[39], M. Kado[116], H. Kagan[110], M. Kagan[144], E. Kajomovitz[45], C.W. Kalderon[119], S. Kama[40], N. Kanaya[156], M. Kaneda[30], S. Kaneti[28], T. Kanno[158], V.A. Kantserov[97], J. Kanzaki[65], B. Kaplan[109], A. Kapliy[31], D. Kar[53], K. Karakostas[10], N. Karastathis[10], M. Karnevskiy[82], S.N. Karpov[64], K. Karthik[109], V. Kartvelishvili[71], A.N. Karyukhin[129], L. Kashif[174], G. Kasieczka[58b], R.D. Kass[110], A. Kastanas[14], Y. Kataoka[156], A. Katre[49], J. Katzy[42], V. Kaushik[7], K. Kawagoe[69], T. Kawamoto[156], G. Kawamura[54], S. Kazama[156], V.F. Kazanin[108], M.Y. Kazarinov[64], R. Keeler[170], R. Kehoe[40], M. Keil[54], J.S. Keller[42], J.J. Kempster[76], H. Keoshkerian[5], O. Kepka[126], B.P. Kerševan[74], S. Kersten[176], K. Kessoku[156], J. Keung[159], F. Khalil-zada[11], H. Khandanyan[147a,147b], A. Khanov[113], A. Khodinov[97], A. Khomich[58a], T.J. Khoo[28], G. Khoriauli[21], A. Khoroshilov[176], V. Khovanskiy[96], E. Khramov[64], J. Khubua[51b], H.Y. Kim[8], H. Kim[147a,147b], S.H. Kim[161], N. Kimura[172], O. Kind[16], B.T. King[73], M. King[168], R.S.B. King[119], S.B. King[169], J. Kirk[130], A.E. Kiryunin[100], T. Kishimoto[66], D. Kisielewska[38a], F. Kiss[48], T. Kitamura[66], T. Kittelmann[124], K. Kiuchi[161], E. Kladiva[145b], M. Klein[73], U. Klein[73], K. Kleinknecht[82], P. Klimek[147a,147b], A. Klimentov[25], R. Klingenberg[43], J.A. Klinger[83], T. Klioutchnikova[30], P.F. Klok[105], E.-E. Kluge[58a], P. Kluit[106], S. Kluth[100], E. Kneringer[61], E.B.F.G. Knoops[84], A. Knue[53], T. Kobayashi[156], M. Kobel[44], M. Kocian[144], P. Kodys[128], P. Koevesarki[21], T. Koffas[29], E. Koffeman[106], L.A. Kogan[119], S. Kohlmann[176], Z. Kohout[127], T. Kohriki[65], T. Koi[144], H. Kolanoski[16], I. Koletsou[5], J. Koll[89], A.A. Komar[95,*], Y. Komori[156], T. Kondo[65], N. Kondrashova[42], K. Köneke[48], A.C. König[105], S. König[82], T. Kono[65,p], R. Konoplich[109,q], N. Konstantinidis[77], R. Kopeliansky[153], S. Koperny[38a], L. Köpke[82], A.K. Kopp[48], K. Korcyl[39], K. Kordas[155], A. Korn[77], A.A. Korol[108,r], I. Korolkov[12], E.V. Korolkova[140], V.A. Korotkov[129], O. Kortner[100], S. Kortner[100], V.V. Kostyukhin[21], V.M. Kotov[64], A. Kotwal[45], C. Kourkoumelis[9], V. Kouskoura[155], A. Koutsman[160a], R. Kowalewski[170], T.Z. Kowalski[38a], W. Kozanecki[137], A.S. Kozhin[129], V. Kral[127], V.A. Kramarenko[98], G. Kramberger[74], D. Krasnopevtsev[97], M.W. Krasny[79], A. Krasznahorkay[30], J.K. Kraus[21], A. Kravchenko[25], S. Kreiss[109], M. Kretz[58c], J. Kretzschmar[73], K. Kreutzfeldt[52], P. Krieger[159], K. Kroeninger[54], H. Kroha[100], J. Kroll[121], J. Kroseberg[21], J. Krstic[13a], U. Kruchonak[64], H. Krüger[21], T. Kruker[17], N. Krumnack[63], Z.V. Krumshteyn[64], A. Kruse[174], M.C. Kruse[45], M. Kruskal[22], T. Kubota[87], S. Kuday[4a], S. Kuehn[48], A. Kugel[58c], A. Kuhl[138], T. Kuhl[42], V. Kukhtin[64], Y. Kulchitsky[91], S. Kuleshov[32b], M. Kuna[133a,133b], J. Kunkle[121], A. Kupco[126], H. Kurashige[66], Y.A. Kurochkin[91], R. Kurumida[66], V. Kus[126], E.S. Kuwertz[148], M. Kuze[158], J. Kvita[114], A. La Rosa[49], L. La Rotonda[37a,37b], C. Lacasta[168], F. Lacava[133a,133b], J. Lacey[29], H. Lacker[16], D. Lacour[79], V.R. Lacuesta[168], E. Ladygin[64], R. Lafaye[5], B. Laforge[79], T. Lagouri[177], S. Lai[48], H. Laier[58a], L. Lambourne[77], S. Lammers[60], C.L. Lampen[7], W. Lampl[7], E. Lançon[137], U. Landgraf[48], M.P.J. Landon[75], V.S. Lang[58a], C. Lange[42], A.J. Lankford[164], F. Lanni[25], K. Lantzsch[30], S. Laplace[79], C. Lapoire[21], J.F. Laporte[137], T. Lari[90a], M. Lassnig[30], P. Laurelli[47], W. Lavrijsen[15], A.T. Law[138], P. Laycock[73], B.T. Le[55], O. Le Dortz[79], E. Le Guirriec[84], E. Le Menedeu[12], T. LeCompte[6], F. Ledroit-Guillon[55], C.A. Lee[152], H. Lee[106], J.S.H. Lee[117], S.C. Lee[152], L. Lee[177], G. Lefebvre[79], M. Lefebvre[170], F. Legger[99], C. Leggett[15], A. Lehan[73], M. Lehmacher[21], G. Lehmann Miotto[30], X. Lei[7], W.A. Leight[29], A. Leisos[155], A.G. Leister[177], M.A.L. Leite[24d], R. Leitner[128], D. Lellouch[173], B. Lemmer[54], K.J.C. Leney[77], T. Lenz[106], G. Lenzen[176], B. Lenzi[30], R. Leone[7], K. Leonhardt[44], S. Leontsinis[10], C. Leroy[94], C.G. Lester[28], C.M. Lester[121], M. Levchenko[122], J. Levêque[5], D. Levin[88], L.J. Levinson[173], M. Levy[18], A. Lewis[119], G.H. Lewis[109], A.M. Leyko[21], M. Leyton[41], B. Li[33b,s], B. Li[84], H. Li[149], H.L. Li[31], L. Li[45], L. Li[33e], S. Li[45], Y. Li[33c,t], Z. Liang[138], H. Liao[34], B. Liberti[134a], P. Lichard[30], K. Lie[166], J. Liebal[21], W. Liebig[14], C. Limbach[21], A. Limosani[87], S.C. Lin[152,u], F. Linde[106], B.E. Lindquist[149], J.T. Linnemann[89], E. Lipeles[121], A. Lipniacka[14], M. Lisovyi[42], T.M. Liss[166],

JHEP09(2014)079

D. Lissauer[25], A. Lister[169], A.M. Litke[138], B. Liu[152], D. Liu[152], J.B. Liu[33b], K. Liu[33b,v], L. Liu[88], M. Liu[45], M. Liu[33b], Y. Liu[33b], M. Livan[120a,120b], S.S.A. Livermore[119], A. Lleres[55], J. Llorente Merino[81], S.L. Lloyd[75], F. Lo Sterzo[152], E. Lobodzinska[42], P. Loch[7], W.S. Lockman[138], T. Loddenkoetter[21], F.K. Loebinger[83], A.E. Loevschall-Jensen[36], A. Loginov[177], C.W. Loh[169], T. Lohse[16], K. Lohwasser[42], M. Lokajicek[126], V.P. Lombardo[5], B.A. Long[22], J.D. Long[88], R.E. Long[71], L. Lopes[125a], D. Lopez Mateos[57], B. Lopez Paredes[140], I. Lopez Paz[12], J. Lorenz[99], N. Lorenzo Martinez[60], M. Losada[163], P. Loscutoff[15], X. Lou[41], A. Lounis[116], J. Love[6], P.A. Love[71], A.J. Lowe[144,e], F. Lu[33a], H.J. Lubatti[139], C. Luci[133a,133b], A. Lucotte[55], F. Luehring[60], W. Lukas[61], L. Luminari[133a], O. Lundberg[147a,147b], B. Lund-Jensen[148], M. Lungwitz[82], D. Lynn[25], R. Lysak[126], E. Lytken[80], H. Ma[25], L.L. Ma[33d], G. Maccarrone[47], A. Macchiolo[100], J. Machado Miguens[125a,125b], D. Macina[30], D. Madaffari[84], R. Madar[48], H.J. Maddocks[71], W.F. Mader[44], A. Madsen[167], M. Maeno[8], T. Maeno[25], E. Magradze[54], K. Mahboubi[48], J. Mahlstedt[106], S. Mahmoud[73], C. Maiani[137], C. Maidantchik[24a], A. Maio[125a,125b,125d], S. Majewski[115], Y. Makida[65], N. Makovec[116], P. Mal[137,w], B. Malaescu[79], Pa. Malecki[39], V.P. Maleev[122], F. Malek[55], U. Mallik[62], D. Malon[6], C. Malone[144], S. Maltezos[10], V.M. Malyshev[108], S. Malyukov[30], J. Mamuzic[13b], B. Mandelli[30], L. Mandelli[90a], I. Mandić[74], R. Mandrysch[62], J. Maneira[125a,125b], A. Manfredini[100], L. Manhaes de Andrade Filho[24b], J.A. Manjarres Ramos[160b], A. Mann[99], P.M. Manning[138], A. Manousakis-Katsikakis[9], B. Mansoulie[137], R. Mantifel[86], L. Mapelli[30], L. March[168], J.F. Marchand[29], G. Marchiori[79], M. Marcisovsky[126], C.P. Marino[170], M. Marjanovic[13a], C.N. Marques[125a], F. Marroquim[24a], S.P. Marsden[83], Z. Marshall[15], L.F. Marti[17], S. Marti-Garcia[168], B. Martin[30], B. Martin[89], T.A. Martin[171], V.J. Martin[46], B. Martin dit Latour[14], H. Martinez[137], M. Martinez[12,n], S. Martin-Haugh[130], A.C. Martyniuk[77], M. Marx[139], F. Marzano[133a], A. Marzin[30], L. Masetti[82], T. Mashimo[156], R. Mashinistov[95], J. Masik[83], A.L. Maslennikov[108], I. Massa[20a,20b], N. Massol[5], P. Mastrandrea[149], A. Mastroberardino[37a,37b], T. Masubuchi[156], T. Matsushita[66], P. Mättig[176], S. Mättig[42], J. Mattmann[82], J. Maurer[26a], S.J. Maxfield[73], D.A. Maximov[108,r], R. Mazini[152], L. Mazzaferro[134a,134b], G. Mc Goldrick[159], S.P. Mc Kee[88], A. McCarn[88], R.L. McCarthy[149], T.G. McCarthy[29], N.A. McCubbin[130], K.W. McFarlane[56,*], J.A. Mcfayden[77], G. Mchedlidze[54], S.J. McMahon[130], R.A. McPherson[170,i], A. Meade[85], J. Mechnich[106], M. Medinnis[42], S. Meehan[31], S. Mehlhase[36], A. Mehta[73], K. Meier[58a], C. Meineck[99], B. Meirose[80], C. Melachrinos[31], B.R. Mellado Garcia[146c], F. Meloni[90a,90b], A. Mengarelli[20a,20b], S. Menke[100], E. Meoni[162], K.M. Mercurio[57], S. Mergelmeyer[21], N. Meric[137], P. Mermod[49], L. Merola[103a,103b], C. Meroni[90a], F.S. Merritt[31], H. Merritt[110], A. Messina[30,x], J. Metcalfe[25], A.S. Mete[164], C. Meyer[82], C. Meyer[31], J-P. Meyer[137], J. Meyer[30], R.P. Middleton[130], S. Migas[73], L. Mijović[21], G. Mikenberg[173], M. Mikestikova[126], M. Mikuž[74], D.W. Miller[31], C. Mills[46], A. Milov[173], D.A. Milstead[147a,147b], D. Milstein[173], A.A. Minaenko[129], I.A. Minashvili[64], A.I. Mincer[109], B. Mindur[38a], M. Mineev[64], Y. Ming[174], L.M. Mir[12], G. Mirabelli[133a], T. Mitani[172], J. Mitrevski[99], V.A. Mitsou[168], S. Mitsui[65], A. Miucci[49], P.S. Miyagawa[140], J.U. Mjörnmark[80], T. Moa[147a,147b], K. Mochizuki[84], V. Moeller[28], S. Mohapatra[35], W. Mohr[48], S. Molander[147a,147b], R. Moles-Valls[168], K. Mönig[42], C. Monini[55], J. Monk[36], E. Monnier[84], J. Montejo Berlingen[12], F. Monticelli[70], S. Monzani[133a,133b], R.W. Moore[3], A. Moraes[53], N. Morange[62], J. Morel[54], D. Moreno[82], M. Moreno Llácer[54], P. Morettini[50a], M. Morgenstern[44], M. Morii[57], S. Moritz[82], A.K. Morley[148], G. Mornacchi[30], J.D. Morris[75], L. Morvaj[102], H.G. Moser[100], M. Mosidze[51b], J. Moss[110], R. Mount[144], E. Mountricha[25], S.V. Mouraviev[95,*], E.J.W. Moyse[85], S. Muanza[84], R.D. Mudd[18], F. Mueller[58a], J. Mueller[124], K. Mueller[21], T. Mueller[28], T. Mueller[82], D. Muenstermann[49], Y. Munwes[154], J.A. Murillo Quijada[18], W.J. Murray[171,130], H. Musheghyan[54], E. Musto[153], A.G. Myagkov[129,y], M. Myska[127], O. Nackenhorst[54], J. Nadal[54], K. Nagai[61], R. Nagai[158], Y. Nagai[84], K. Nagano[65], A. Nagarkar[110], Y. Nagasaka[59], M. Nagel[100], A.M. Nairz[30], Y. Nakahama[30], K. Nakamura[65], T. Nakamura[156], I. Nakano[111], H. Namasivayam[41], G. Nanava[21], R. Narayan[58b], T. Nattermann[21], T. Naumann[42], G. Navarro[163], R. Nayyar[7], H.A. Neal[88], P.Yu. Nechaeva[95], T.J. Neep[83], A. Negri[120a,120b], G. Negri[30], M. Negrini[20a], S. Nektarijevic[49], A. Nelson[164], T.K. Nelson[144], S. Nemecek[126],

JHEP09(2014)079

P. Nemethy[109], A.A. Nepomuceno[24a], M. Nessi[30,z], M.S. Neubauer[166], M. Neumann[176], R.M. Neves[109], P. Nevski[25], P.R. Newman[18], D.H. Nguyen[6], R.B. Nickerson[119], R. Nicolaidou[137], B. Nicquevert[30], J. Nielsen[138], N. Nikiforou[35], A. Nikiforov[16], V. Nikolaenko[129,y], I. Nikolic-Audit[79], K. Nikolics[49], K. Nikolopoulos[18], P. Nilsson[8], Y. Ninomiya[156], A. Nisati[133a], R. Nisius[100], T. Nobe[158], L. Nodulman[6], M. Nomachi[117], I. Nomidis[155], S. Norberg[112], M. Nordberg[30], S. Nowak[100], M. Nozaki[65], L. Nozka[114], K. Ntekas[10], G. Nunes Hanninger[87], T. Nunnemann[99], E. Nurse[77], F. Nuti[87], B.J. O'Brien[46], F. O'grady[7], D.C. O'Neil[143], V. O'Shea[53], F.G. Oakham[29,d], H. Oberlack[100], T. Obermann[21], J. Ocariz[79], A. Ochi[66], M.I. Ochoa[77], S. Oda[69], S. Odaka[65], H. Ogren[60], A. Oh[83], S.H. Oh[45], C.C. Ohm[30], H. Ohman[167], T. Ohshima[102], W. Okamura[117], H. Okawa[25], Y. Okumura[31], T. Okuyama[156], A. Olariu[26a], A.G. Olchevski[64], S.A. Olivares Pino[46], D. Oliveira Damazio[25], E. Oliver Garcia[168], A. Olszewski[39], J. Olszowska[39], A. Onofre[125a,125e], P.U.E. Onyisi[31,aa], C.J. Oram[160a], M.J. Oreglia[31], Y. Oren[154], D. Orestano[135a,135b], N. Orlando[72a,72b], C. Oropeza Barrera[53], R.S. Orr[159], B. Osculati[50a,50b], R. Ospanov[121], G. Otero y Garzon[27], H. Otono[69], M. Ouchrif[136d], E.A. Ouellette[170], F. Ould-Saada[118], A. Ouraou[137], K.P. Oussoren[106], Q. Ouyang[33a], A. Ovcharova[15], M. Owen[83], V.E. Ozcan[19a], N. Ozturk[8], K. Pachal[119], A. Pacheco Pages[12], C. Padilla Aranda[12], M. Pagáčová[48], S. Pagan Griso[15], E. Paganis[140], C. Pahl[100], F. Paige[25], P. Pais[85], K. Pajchel[118], G. Palacino[160b], S. Palestini[30], D. Pallin[34], A. Palma[125a,125b], J.D. Palmer[18], Y.B. Pan[174], E. Panagiotopoulou[10], J.G. Panduro Vazquez[76], P. Pani[106], N. Panikashvili[88], S. Panitkin[25], D. Pantea[26a], L. Paolozzi[134a,134b], Th.D. Papadopoulou[10], K. Papageorgiou[155,l], A. Paramonov[6], D. Paredes Hernandez[34], M.A. Parker[28], F. Parodi[50a,50b], J.A. Parsons[35], U. Parzefall[48], E. Pasqualucci[133a], S. Passaggio[50a], A. Passeri[135a], F. Pastore[135a,135b,*], Fr. Pastore[76], G. Pásztor[29], S. Pataraia[176], N.D. Patel[151], J.R. Pater[83], S. Patricelli[103a,103b], T. Pauly[30], J. Pearce[170], M. Pedersen[118], S. Pedraza Lopez[168], R. Pedro[125a,125b], S.V. Peleganchuk[108], D. Pelikan[167], H. Peng[33b], B. Penning[31], J. Penwell[60], D.V. Perepelitsa[25], E. Perez Codina[160a], M.T. Pérez García-Estañ[168], V. Perez Reale[35], L. Perini[90a,90b], H. Pernegger[30], R. Perrino[72a], R. Peschke[42], V.D. Peshekhonov[64], K. Peters[30], R.F.Y. Peters[83], B.A. Petersen[87], T.C. Petersen[36], E. Petit[42], A. Petridis[147a,147b], C. Petridou[155], E. Petrolo[133a], F. Petrucci[135a,135b], M. Petteni[143], N.E. Pettersson[158], R. Pezoa[32b], P.W. Phillips[130], G. Piacquadio[144], E. Pianori[171], A. Picazio[49], E. Piccaro[75], M. Piccinini[20a,20b], R. Piegaia[27], D.T. Pignotti[110], J.E. Pilcher[31], A.D. Pilkington[77], J. Pina[125a,125b,125d], M. Pinamonti[165a,165c,ab], A. Pinder[119], J.L. Pinfold[3], A. Pingel[36], B. Pinto[125a], S. Pires[79], M. Pitt[173], C. Pizio[90a,90b], M.-A. Pleier[25], V. Pleskot[128], E. Plotnikova[64], P. Plucinski[147a,147b], S. Poddar[58a], F. Podlyski[34], R. Poettgen[82], L. Poggioli[116], D. Pohl[21], M. Pohl[49], G. Polesello[120a], A. Policicchio[37a,37b], R. Polifka[159], A. Polini[20a], C.S. Pollard[45], V. Polychronakos[25], K. Pommès[30], L. Pontecorvo[133a], B.G. Pope[89], G.A. Popeneciu[26b], D.S. Popovic[13a], A. Poppleton[30], X. Portell Bueso[12], G.E. Pospelov[100], S. Pospisil[127], K. Potamianos[15], I.N. Potrap[64], C.J. Potter[150], C.T. Potter[115], G. Poulard[30], J. Poveda[60], V. Pozdnyakov[64], P. Pralavorio[84], A. Pranko[15], S. Prasad[30], R. Pravahan[8], S. Prell[63], D. Price[83], J. Price[73], L.E. Price[6], D. Prieur[124], M. Primavera[72a], M. Proissl[46], K. Prokofiev[47], F. Prokoshin[32b], E. Protopapadaki[137], S. Protopopescu[25], J. Proudfoot[6], M. Przybycien[38a], H. Przysiezniak[5], E. Ptacek[115], E. Pueschel[85], D. Puldon[149], M. Purohit[25,ac], P. Puzo[116], J. Qian[88], G. Qin[53], Y. Qin[83], A. Quadt[54], D.R. Quarrie[15], W.B. Quayle[165a,165b], M. Queitsch-Maitland[83], D. Quilty[53], A. Qureshi[160b], V. Radeka[25], V. Radescu[42], S.K. Radhakrishnan[149], P. Radloff[115], P. Rados[87], F. Ragusa[90a,90b], G. Rahal[179], S. Rajagopalan[25], M. Rammensee[30], A.S. Randle-Conde[40], C. Rangel-Smith[167], K. Rao[164], F. Rauscher[99], T.C. Rave[48], T. Ravenscroft[53], M. Raymond[30], A.L. Read[118], D.M. Rebuzzi[120a,120b], A. Redelbach[175], G. Redlinger[25], R. Reece[138], K. Reeves[41], L. Rehnisch[16], H. Reisin[27], M. Relich[164], C. Rembser[30], H. Ren[33a], Z.L. Ren[152], A. Renaud[116], M. Rescigno[133a], S. Resconi[90a], O.L. Rezanova[108,r], P. Reznicek[128], R. Rezvani[94], R. Richter[100], M. Ridel[79], P. Rieck[16], J. Rieger[54], M. Rijssenbeek[149], A. Rimoldi[120a,120b], L. Rinaldi[20a], E. Ritsch[61], I. Riu[12], F. Rizatdinova[113], E. Rizvi[75], S.H. Robertson[86,i], A. Robichaud-Veronneau[119], D. Robinson[28], J.E.M. Robinson[83],

JHEP09(2014)079

A. Robson[53], C. Roda[123a,123b], L. Rodrigues[30], S. Roe[30], O. Røhne[118], S. Rolli[162], A. Romaniouk[97], M. Romano[20a,20b], G. Romeo[27], E. Romero Adam[168], N. Rompotis[139], L. Roos[79], E. Ros[168], S. Rosati[133a], K. Rosbach[49], M. Rose[76], P.L. Rosendahl[14], O. Rosenthal[142], V. Rossetti[147a,147b], E. Rossi[103a,103b], L.P. Rossi[50a], R. Rosten[139], M. Rotaru[26a], I. Roth[173], J. Rothberg[139], D. Rousseau[116], C.R. Royon[137], A. Rozanov[84], Y. Rozen[153], X. Ruan[146c], F. Rubbo[12], I. Rubinskiy[42], V.I. Rud[98], C. Rudolph[44], M.S. Rudolph[159], F. Rühr[48], A. Ruiz-Martinez[30], Z. Rurikova[48], N.A. Rusakovich[64], A. Ruschke[99], J.P. Rutherfoord[7], N. Ruthmann[48], Y.F. Ryabov[122], M. Rybar[128], G. Rybkin[116], N.C. Ryder[119], A.F. Saavedra[151], S. Sacerdoti[27], A. Saddique[3], I. Sadeh[154], H.F-W. Sadrozinski[138], R. Sadykov[64], F. Safai Tehrani[133a], H. Sakamoto[156], Y. Sakurai[172], G. Salamanna[75], A. Salamon[134a], M. Saleem[112], D. Salek[106], P.H. Sales De Bruin[139], D. Salihagic[100], A. Salnikov[144], J. Salt[168], B.M. Salvachua Ferrando[6], D. Salvatore[37a,37b], F. Salvatore[150], A. Salvucci[105], A. Salzburger[30], D. Sampsonidis[155], A. Sanchez[103a,103b], J. Sánchez[168], V. Sanchez Martinez[168], H. Sandaker[14], R.L. Sandbach[75], H.G. Sander[82], M.P. Sanders[99], M. Sandhoff[176], T. Sandoval[28], C. Sandoval[163], R. Sandstroem[100], D.P.C. Sankey[130], A. Sansoni[47], C. Santoni[34], R. Santonico[134a,134b], H. Santos[125a], I. Santoyo Castillo[150], K. Sapp[124], A. Sapronov[64], J.G. Saraiva[125a,125d], B. Sarrazin[21], G. Sartisohn[176], O. Sasaki[65], Y. Sasaki[156], G. Sauvage[5,*], E. Sauvan[5], P. Savard[159,d], D.O. Savu[30], C. Sawyer[119], L. Sawyer[78,m], D.H. Saxon[53], J. Saxon[121], C. Sbarra[20a], A. Sbrizzi[3], T. Scanlon[77], D.A. Scannicchio[164], M. Scarcella[151], J. Schaarschmidt[173], P. Schacht[100], D. Schaefer[121], R. Schaefer[42], S. Schaepe[21], S. Schaetzel[58b], U. Schäfer[82], A.C. Schaffer[116], D. Schaile[99], R.D. Schamberger[149], V. Scharf[58a], V.A. Schegelsky[122], D. Scheirich[128], M. Schernau[164], M.I. Scherzer[35], C. Schiavi[50a,50b], J. Schieck[99], C. Schillo[48], M. Schioppa[37a,37b], S. Schlenker[30], E. Schmidt[48], K. Schmieden[30], C. Schmitt[82], C. Schmitt[99], S. Schmitt[58b], B. Schneider[17], Y.J. Schnellbach[73], U. Schnoor[44], L. Schoeffel[137], A. Schoening[58b], B.D. Schoenrock[89], A.L.S. Schorlemmer[54], M. Schott[82], D. Schouten[160a], J. Schovancova[25], S. Schramm[159], M. Schreyer[175], C. Schroeder[82], N. Schuh[82], M.J. Schultens[21], H.-C. Schultz-Coulon[58a], H. Schulz[16], M. Schumacher[48], B.A. Schumm[138], Ph. Schune[137], C. Schwanenberger[83], A. Schwartzman[144], Ph. Schwegler[100], Ph. Schwemling[137], R. Schwienhorst[89], J. Schwindling[137], T. Schwindt[21], M. Schwoerer[5], F.G. Sciacca[17], E. Scifo[116], G. Sciolla[23], W.G. Scott[130], F. Scuri[123a,123b], F. Scutti[21], J. Searcy[88], G. Sedov[42], E. Sedykh[122], S.C. Seidel[104], A. Seiden[138], F. Seifert[127], J.M. Seixas[24a], G. Sekhniaidze[103a], S.J. Sekula[40], K.E. Selbach[46], D.M. Seliverstov[122,*], G. Sellers[73], N. Semprini-Cesari[20a,20b], C. Serfon[30], L. Serin[116], L. Serkin[54], T. Serre[84], R. Seuster[160a], H. Severini[112], F. Sforza[100], A. Sfyrla[30], E. Shabalina[54], M. Shamim[115], L.Y. Shan[33a], R. Shang[166], J.T. Shank[22], Q.T. Shao[87], M. Shapiro[15], P.B. Shatalov[96], K. Shaw[165a,165b], P. Sherwood[77], L. Shi[152,ad], S. Shimizu[66], C.O. Shimmin[164], M. Shimojima[101], M. Shiyakova[64], A. Shmeleva[95], M.J. Shochet[31], D. Short[119], S. Shrestha[63], E. Shulga[97], M.A. Shupe[7], S. Shushkevich[42], P. Sicho[126], D. Sidorov[113], A. Sidoti[133a], F. Siegert[44], Dj. Sijacki[13a], J. Silva[125a,125d], Y. Silver[154], D. Silverstein[144], S.B. Silverstein[147a], V. Simak[127], O. Simard[5], Lj. Simic[13a], S. Simion[116], E. Simioni[82], B. Simmons[77], R. Simoniello[90a,90b], M. Simonyan[36], P. Sinervo[159], N.B. Sinev[115], V. Sipica[142], G. Siragusa[175], A. Sircar[78], A.N. Sisakyan[64,*], S.Yu. Sivoklokov[98], J. Sjölin[147a,147b], T.B. Sjursen[14], H.P. Skottowe[57], K.Yu. Skovpen[108], P. Skubic[112], M. Slater[18], T. Slavicek[127], K. Sliwa[162], V. Smakhtin[173], B.H. Smart[46], L. Smestad[14], S.Yu. Smirnov[97], Y. Smirnov[97], L.N. Smirnova[98,ae], O. Smirnova[80], K.M. Smith[53], M. Smizanska[71], K. Smolek[127], A.A. Snesarev[95], G. Snidero[75], S. Snyder[25], R. Sobie[170,i], F. Socher[44], A. Soffer[154], D.A. Soh[152,ad], C.A. Solans[30], M. Solar[127], J. Solc[127], E.Yu. Soldatov[97], U. Soldevila[168], E. Solfaroli Camillocci[133a,133b], A.A. Solodkov[129], O.V. Solovyanov[129], V. Solovyev[122], P. Sommer[48], H.Y. Song[33b], N. Soni[1], A. Sood[15], A. Sopczak[127], B. Sopko[127], V. Sopko[127], V. Sorin[12], M. Sosebee[8], R. Soualah[165a,165c], P. Soueid[94], A.M. Soukharev[108], D. South[42], S. Spagnolo[72a,72b], F. Spanò[76], W.R. Spearman[57], R. Spighi[20a], G. Spigo[30], M. Spousta[128], T. Spreitzer[159], B. Spurlock[8], R.D. St. Denis[53,*], S. Staerz[44], J. Stahlman[121], R. Stamen[58a], E. Stanecka[39], R.W. Stanek[6], C. Stanescu[135a], M. Stanescu-Bellu[42], M.M. Stanitzki[42],

JHEP09(2014)079

S. Stapnes[118], E.A. Starchenko[129], J. Stark[55], P. Staroba[126], P. Starovoitov[42], R. Staszewski[39], P. Stavina[145a,*], G. Steele[53], P. Steinberg[25], B. Stelzer[143], H.J. Stelzer[30], O. Stelzer-Chilton[160a], H. Stenzel[52], S. Stern[100], G.A. Stewart[53], J.A. Stillings[21], M.C. Stockton[86], M. Stoebe[86], G. Stoicea[26a], P. Stolte[54], S. Stonjek[100], A.R. Stradling[8], A. Straessner[44], M.E. Stramaglia[17], J. Strandberg[148], S. Strandberg[147a,147b], A. Strandlie[118], E. Strauss[144], M. Strauss[112], P. Strizenec[145b], R. Ströhmer[175], D.M. Strom[115], R. Stroynowski[40], S.A. Stucci[17], B. Stugu[14], N.A. Styles[42], D. Su[144], J. Su[124], HS. Subramania[3], R. Subramaniam[78], A. Succurro[12], Y. Sugaya[117], C. Suhr[107], M. Suk[127], V.V. Sulin[95], S. Sultansoy[4c], T. Sumida[67], X. Sun[33a], J.E. Sundermann[48], K. Suruliz[140], G. Susinno[37a,37b], M.R. Sutton[150], Y. Suzuki[65], M. Svatos[126], S. Swedish[169], M. Swiatlowski[144], I. Sykora[145a], T. Sykora[128], D. Ta[89], K. Tackmann[42], J. Taenzer[159], A. Taffard[164], R. Tafirout[160a], N. Taiblum[154], Y. Takahashi[102], H. Takai[25], R. Takashima[68], H. Takeda[66], T. Takeshita[141], Y. Takubo[65], M. Talby[84], A.A. Talyshev[108,r], J.Y.C. Tam[175], M.C. Tamsett[78,af], K.G. Tan[87], J. Tanaka[156], R. Tanaka[116], S. Tanaka[132], S. Tanaka[65], A.J. Tanasijczuk[143], K. Tani[66], N. Tannoury[21], S. Tapprogge[82], S. Tarem[153], F. Tarrade[29], G.F. Tartarelli[90a], P. Tas[128], M. Tasevsky[126], T. Tashiro[67], E. Tassi[37a,37b], A. Tavares Delgado[125a,125b], Y. Tayalati[136d], F.E. Taylor[93], G.N. Taylor[87], W. Taylor[160b], F.A. Teischinger[30], M. Teixeira Dias Castanheira[75], P. Teixeira-Dias[76], K.K. Temming[48], H. Ten Kate[30], P.K. Teng[152], J.J. Teoh[117], S. Terada[65], K. Terashi[156], J. Terron[81], S. Terzo[100], M. Testa[47], R.J. Teuscher[159,i], J. Therhaag[21], T. Theveneaux-Pelzer[34], S. Thoma[48], J.P. Thomas[18], J. Thomas-Wilsker[76], E.N. Thompson[35], P.D. Thompson[18], P.D. Thompson[159], A.S. Thompson[53], L.A. Thomsen[36], E. Thomson[121], M. Thomson[28], W.M. Thong[87], R.P. Thun[88,*], F. Tian[35], M.J. Tibbetts[15], V.O. Tikhomirov[95,ag], Yu.A. Tikhonov[108,r], S. Timoshenko[97], E. Tiouchichine[84], P. Tipton[177], S. Tisserant[84], T. Todorov[5], S. Todorova-Nova[128], B. Toggerson[7], J. Tojo[69], S. Tokár[145a], K. Tokushuku[65], K. Tollefson[89], L. Tomlinson[83], M. Tomoto[102], L. Tompkins[31], K. Toms[104], N.D. Topilin[64], E. Torrence[115], H. Torres[143], E. Torró Pastor[168], J. Toth[84,ah], F. Touchard[84], D.R. Tovey[140], H.L. Tran[116], T. Trefzger[175], L. Tremblet[30], A. Tricoli[30], I.M. Trigger[160a], S. Trincaz-Duvoid[79], M.F. Tripiana[70], N. Triplett[25], W. Trischuk[159], B. Trocmé[55], C. Troncon[90a], M. Trottier-McDonald[143], M. Trovatelli[135a,135b], P. True[89], M. Trzebinski[39], A. Trzupek[39], C. Tsarouchas[30], J.C-L. Tseng[119], P.V. Tsiareshka[91], D. Tsionou[137], G. Tsipolitis[10], N. Tsirintanis[9], S. Tsiskaridze[12], V. Tsiskaridze[48], E.G. Tskhadadze[51a], I.I. Tsukerman[96], V. Tsulaia[15], S. Tsuno[65], D. Tsybychev[149], A. Tudorache[26a], V. Tudorache[26a], A.N. Tuna[121], S.A. Tupputi[20a,20b], S. Turchikhin[98,ae], D. Turecek[127], I. Turk Cakir[4d], R. Turra[90a,90b], P.M. Tuts[35], A. Tykhonov[74], M. Tylmad[147a,147b], M. Tyndel[130], K. Uchida[21], I. Ueda[156], R. Ueno[29], M. Ughetto[84], M. Ugland[14], M. Uhlenbrock[21], F. Ukegawa[161], G. Unal[30], A. Undrus[25], G. Unel[164], F.C. Ungaro[48], Y. Unno[65], D. Urbaniec[35], P. Urquijo[87], G. Usai[8], A. Usanova[61], L. Vacavant[84], V. Vacek[127], B. Vachon[86], N. Valencic[106], S. Valentinetti[20a,20b], A. Valero[168], L. Valery[34], S. Valkar[128], E. Valladolid Gallego[168], S. Vallecorsa[49], J.A. Valls Ferrer[168], P.C. Van Der Deijl[106], R. van der Geer[106], H. van der Graaf[106], R. Van Der Leeuw[106], D. van der Ster[30], N. van Eldik[30], P. van Gemmeren[6], J. Van Nieuwkoop[143], I. van Vulpen[106], M.C. van Woerden[30], M. Vanadia[133a,133b], W. Vandelli[30], R. Vanguri[121], A. Vaniachine[6], P. Vankov[42], F. Vannucci[79], G. Vardanyan[178], R. Vari[133a], E.W. Varnes[7], T. Varol[85], D. Varouchas[79], A. Vartapetian[8], K.E. Varvell[151], F. Vazeille[34], T. Vazquez Schroeder[54], J. Veatch[7], F. Veloso[125a,125c], S. Veneziano[133a], A. Ventura[72a,72b], D. Ventura[85], M. Venturi[48], N. Venturi[159], A. Venturini[23], V. Vercesi[120a], M. Verducci[139], W. Verkerke[106], J.C. Vermeulen[106], A. Vest[44], M.C. Vetterli[143,d], O. Viazlo[80], I. Vichou[166], T. Vickey[146c,ai], O.E. Vickey Boeriu[146c], G.H.A. Viehhauser[119], S. Viel[169], R. Vigne[30], M. Villa[20a,20b], M. Villaplana Perez[168], E. Vilucchi[47], M.G. Vincter[29], V.B. Vinogradov[64], J. Virzi[15], I. Vivarelli[150], F. Vives Vaque[3], S. Vlachos[10], D. Vladoiu[99], M. Vlasak[127], A. Vogel[21], M. Vogel[32a], P. Vokac[127], G. Volpi[123a,123b], M. Volpi[87], H. von der Schmitt[100], H. von Radziewski[48], E. von Toerne[21], V. Vorobel[128], K. Vorobev[97], M. Vos[168], R. Voss[30], J.H. Vossebeld[73], N. Vranjes[137], M. Vranjes Milosavljevic[106], V. Vrba[126], M. Vreeswijk[106], T. Vu Anh[48], R. Vuillermet[30], I. Vukotic[31], Z. Vykydal[127],

JHEP09(2014)079

P. Wagner[21], W. Wagner[176], S. Wahrmund[44], J. Wakabayashi[102], J. Walder[71], R. Walker[99], W. Walkowiak[142], R. Wall[177], P. Waller[73], B. Walsh[177], C. Wang[152,aj], C. Wang[45], F. Wang[174], H. Wang[15], H. Wang[40], J. Wang[42], J. Wang[33a], K. Wang[86], R. Wang[104], S.M. Wang[152], T. Wang[21], X. Wang[177], C. Wanotayaroj[115], A. Warburton[86], C.P. Ward[28], D.R. Wardrope[77], M. Warsinsky[48], A. Washbrook[46], C. Wasicki[42], I. Watanabe[66], P.M. Watkins[18], A.T. Watson[18], I.J. Watson[151], M.F. Watson[18], G. Watts[139], S. Watts[83], B.M. Waugh[77], S. Webb[83], M.S. Weber[17], S.W. Weber[175], J.S. Webster[31], A.R. Weidberg[119], P. Weigell[100], B. Weinert[60], J. Weingarten[54], C. Weiser[48], H. Weits[106], P.S. Wells[30], T. Wenaus[25], D. Wendland[16], Z. Weng[152,ad], T. Wengler[30], S. Wenig[30], N. Wermes[21], M. Werner[48], P. Werner[30], M. Wessels[58a], J. Wetter[162], K. Whalen[29], A. White[8], M.J. White[1], R. White[32b], S. White[123a,123b], D. Whiteson[164], D. Wicke[176], F.J. Wickens[130], W. Wiedenmann[174], M. Wielers[130], P. Wienemann[21], C. Wiglesworth[36], L.A.M. Wiik-Fuchs[21], P.A. Wijeratne[77], A. Wildauer[100], M.A. Wildt[42,ak], H.G. Wilkens[30], J.Z. Will[99], H.H. Williams[121], S. Williams[28], C. Willis[89], S. Willocq[85], A. Wilson[88], J.A. Wilson[18], I. Wingerter-Seez[5], F. Winklmeier[115], B.T. Winter[21], M. Wittgen[144], T. Wittig[43], J. Wittkowski[99], S.J. Wollstadt[82], M.W. Wolter[39], H. Wolters[125a,125c], B.K. Wosiek[39], J. Wotschack[30], M.J. Woudstra[83], K.W. Wozniak[39], M. Wright[53], M. Wu[55], S.L. Wu[174], X. Wu[49], Y. Wu[88], E. Wulf[35], T.R. Wyatt[83], B.M. Wynne[46], S. Xella[36], M. Xiao[137], D. Xu[33a], L. Xu[33b,al], B. Yabsley[151], S. Yacoob[146b,am], M. Yamada[65], H. Yamaguchi[156], Y. Yamaguchi[156], A. Yamamoto[65], K. Yamamoto[63], S. Yamamoto[156], T. Yamamura[156], T. Yamanaka[156], K. Yamauchi[102], Y. Yamazaki[66], Z. Yan[22], H. Yang[33e], H. Yang[174], U.K. Yang[83], Y. Yang[110], S. Yanush[92], L. Yao[33a], W-M. Yao[15], Y. Yasu[65], E. Yatsenko[42], K.H. Yau Wong[21], J. Ye[40], S. Ye[25], A.L. Yen[57], E. Yildirim[42], M. Yilmaz[4b], R. Yoosoofmiya[124], K. Yorita[172], R. Yoshida[6], K. Yoshihara[156], C. Young[144], C.J.S. Young[30], S. Youssef[22], D.R. Yu[15], J. Yu[8], J.M. Yu[88], J. Yu[113], L. Yuan[66], A. Yurkewicz[107], B. Zabinski[39], R. Zaidan[62], A.M. Zaitsev[129,y], A. Zaman[149], S. Zambito[23], L. Zanello[133a,133b], D. Zanzi[100], A. Zaytsev[25], C. Zeitnitz[176], M. Zeman[127], A. Zemla[38a], K. Zengel[23], O. Zenin[129], T. Ženiš[145a], D. Zerwas[116], G. Zevi della Porta[57], D. Zhang[88], F. Zhang[174], H. Zhang[89], J. Zhang[6], L. Zhang[152], X. Zhang[33d], Z. Zhang[116], Z. Zhao[33b], A. Zhemchugov[64], J. Zhong[119], B. Zhou[88], L. Zhou[35], N. Zhou[164], C.G. Zhu[33d], H. Zhu[33a], J. Zhu[88], Y. Zhu[33b], X. Zhuang[33a], A. Zibell[175], D. Zieminska[60], N.I. Zimine[64], C. Zimmermann[82], R. Zimmermann[21], S. Zimmermann[21], S. Zimmermann[48], Z. Zinonos[54], M. Ziolkowski[142], G. Zobernig[174], A. Zoccoli[20a,20b], M. zur Nedden[16], G. Zurzolo[103a,103b], V. Zutshi[107], L. Zwalinski[30]

[1] Department of Physics, University of Adelaide, Adelaide, Australia
[2] Physics Department, SUNY Albany, Albany NY, United States of America
[3] Department of Physics, University of Alberta, Edmonton AB, Canada
[4] [(a)] Department of Physics, Ankara University, Ankara; [(b)] Department of Physics, Gazi University, Ankara; [(c)] Division of Physics, TOBB University of Economics and Technology, Ankara; [(d)] Turkish Atomic Energy Authority, Ankara, Turkey
[5] LAPP, CNRS/IN2P3 and Université de Savoie, Annecy-le-Vieux, France
[6] High Energy Physics Division, Argonne National Laboratory, Argonne IL, United States of America
[7] Department of Physics, University of Arizona, Tucson AZ, United States of America
[8] Department of Physics, The University of Texas at Arlington, Arlington TX, United States of America
[9] Physics Department, University of Athens, Athens, Greece
[10] Physics Department, National Technical University of Athens, Zografou, Greece
[11] Institute of Physics, Azerbaijan Academy of Sciences, Baku, Azerbaijan
[12] Institut de Física d'Altes Energies and Departament de Física de la Universitat Autònoma de Barcelona, Barcelona, Spain
[13] [(a)] Institute of Physics, University of Belgrade, Belgrade; [(b)] Vinca Institute of Nuclear Sciences, University of Belgrade, Belgrade, Serbia
[14] Department for Physics and Technology, University of Bergen, Bergen, Norway

JHEP09(2014)079

[15] Physics Division, Lawrence Berkeley National Laboratory and University of California, Berkeley CA, United States of America
[16] Department of Physics, Humboldt University, Berlin, Germany
[17] Albert Einstein Center for Fundamental Physics and Laboratory for High Energy Physics, University of Bern, Bern, Switzerland
[18] School of Physics and Astronomy, University of Birmingham, Birmingham, United Kingdom
[19] [(a)] Department of Physics, Bogazici University, Istanbul; [(b)] Department of Physics, Dogus University, Istanbul; [(c)] Department of Physics Engineering, Gaziantep University, Gaziantep, Turkey
[20] [(a)] INFN Sezione di Bologna; [(b)] Dipartimento di Fisica e Astronomia, Università di Bologna, Bologna, Italy
[21] Physikalisches Institut, University of Bonn, Bonn, Germany
[22] Department of Physics, Boston University, Boston MA, United States of America
[23] Department of Physics, Brandeis University, Waltham MA, United States of America
[24] [(a)] Universidade Federal do Rio De Janeiro COPPE/EE/IF, Rio de Janeiro; [(b)] Federal University of Juiz de Fora (UFJF), Juiz de Fora; [(c)] Federal University of Sao Joao del Rei (UFSJ), Sao Joao del Rei; [(d)] Instituto de Fisica, Universidade de Sao Paulo, Sao Paulo, Brazil
[25] Physics Department, Brookhaven National Laboratory, Upton NY, United States of America
[26] [(a)] National Institute of Physics and Nuclear Engineering, Bucharest; [(b)] National Institute for Research and Development of Isotopic and Molecular Technologies, Physics Department, Cluj Napoca; [(c)] University Politehnica Bucharest, Bucharest; [(d)] West University in Timisoara, Timisoara, Romania
[27] Departamento de Física, Universidad de Buenos Aires, Buenos Aires, Argentina
[28] Cavendish Laboratory, University of Cambridge, Cambridge, United Kingdom
[29] Department of Physics, Carleton University, Ottawa ON, Canada
[30] CERN, Geneva, Switzerland
[31] Enrico Fermi Institute, University of Chicago, Chicago IL, United States of America
[32] [(a)] Departamento de Física, Pontificia Universidad Católica de Chile, Santiago; [(b)] Departamento de Física, Universidad Técnica Federico Santa María, Valparaíso, Chile
[33] [(a)] Institute of High Energy Physics, Chinese Academy of Sciences, Beijing; [(b)] Department of Modern Physics, University of Science and Technology of China, Anhui; [(c)] Department of Physics, Nanjing University, Jiangsu; [(d)] School of Physics, Shandong University, Shandong; [(e)] Physics Department, Shanghai Jiao Tong University, Shanghai, China
[34] Laboratoire de Physique Corpusculaire, Clermont Université and Université Blaise Pascal and CNRS/IN2P3, Clermont-Ferrand, France
[35] Nevis Laboratory, Columbia University, Irvington NY, United States of America
[36] Niels Bohr Institute, University of Copenhagen, Kobenhavn, Denmark
[37] [(a)] INFN Gruppo Collegato di Cosenza, Laboratori Nazionali di Frascati; [(b)] Dipartimento di Fisica, Università della Calabria, Rende, Italy
[38] [(a)] AGH University of Science and Technology, Faculty of Physics and Applied Computer Science, Krakow; [(b)] Marian Smoluchowski Institute of Physics, Jagiellonian University, Krakow, Poland
[39] The Henryk Niewodniczanski Institute of Nuclear Physics, Polish Academy of Sciences, Krakow, Poland
[40] Physics Department, Southern Methodist University, Dallas TX, United States of America
[41] Physics Department, University of Texas at Dallas, Richardson TX, United States of America
[42] DESY, Hamburg and Zeuthen, Germany
[43] Institut für Experimentelle Physik IV, Technische Universität Dortmund, Dortmund, Germany
[44] Institut für Kern- und Teilchenphysik, Technische Universität Dresden, Dresden, Germany
[45] Department of Physics, Duke University, Durham NC, United States of America
[46] SUPA - School of Physics and Astronomy, University of Edinburgh, Edinburgh, United Kingdom
[47] INFN Laboratori Nazionali di Frascati, Frascati, Italy
[48] Fakultät für Mathematik und Physik, Albert-Ludwigs-Universität, Freiburg, Germany

JHEP09(2014)079

[49] Section de Physique, Université de Genève, Geneva, Switzerland
[50] [(a)] INFN Sezione di Genova; [(b)] Dipartimento di Fisica, Università di Genova, Genova, Italy
[51] [(a)] E. Andronikashvili Institute of Physics, Iv. Javakhishvili Tbilisi State University, Tbilisi; [(b)] High Energy Physics Institute, Tbilisi State University, Tbilisi, Georgia
[52] II Physikalisches Institut, Justus-Liebig-Universität Giessen, Giessen, Germany
[53] SUPA - School of Physics and Astronomy, University of Glasgow, Glasgow, United Kingdom
[54] II Physikalisches Institut, Georg-August-Universität, Göttingen, Germany
[55] Laboratoire de Physique Subatomique et de Cosmologie, Université Grenoble-Alpes, CNRS/IN2P3, Grenoble, France
[56] Department of Physics, Hampton University, Hampton VA, United States of America
[57] Laboratory for Particle Physics and Cosmology, Harvard University, Cambridge MA, United States of America
[58] [(a)] Kirchhoff-Institut für Physik, Ruprecht-Karls-Universität Heidelberg, Heidelberg; [(b)] Physikalisches Institut, Ruprecht-Karls-Universität Heidelberg, Heidelberg; [(c)] ZITI Institut für technische Informatik, Ruprecht-Karls-Universität Heidelberg, Mannheim, Germany
[59] Faculty of Applied Information Science, Hiroshima Institute of Technology, Hiroshima, Japan
[60] Department of Physics, Indiana University, Bloomington IN, United States of America
[61] Institut für Astro- und Teilchenphysik, Leopold-Franzens-Universität, Innsbruck, Austria
[62] University of Iowa, Iowa City IA, United States of America
[63] Department of Physics and Astronomy, Iowa State University, Ames IA, United States of America
[64] Joint Institute for Nuclear Research, JINR Dubna, Dubna, Russia
[65] KEK, High Energy Accelerator Research Organization, Tsukuba, Japan
[66] Graduate School of Science, Kobe University, Kobe, Japan
[67] Faculty of Science, Kyoto University, Kyoto, Japan
[68] Kyoto University of Education, Kyoto, Japan
[69] Department of Physics, Kyushu University, Fukuoka, Japan
[70] Instituto de Física La Plata, Universidad Nacional de La Plata and CONICET, La Plata, Argentina
[71] Physics Department, Lancaster University, Lancaster, United Kingdom
[72] [(a)] INFN Sezione di Lecce; [(b)] Dipartimento di Matematica e Fisica, Università del Salento, Lecce, Italy
[73] Oliver Lodge Laboratory, University of Liverpool, Liverpool, United Kingdom
[74] Department of Physics, Jožef Stefan Institute and University of Ljubljana, Ljubljana, Slovenia
[75] School of Physics and Astronomy, Queen Mary University of London, London, United Kingdom
[76] Department of Physics, Royal Holloway University of London, Surrey, United Kingdom
[77] Department of Physics and Astronomy, University College London, London, United Kingdom
[78] Louisiana Tech University, Ruston LA, United States of America
[79] Laboratoire de Physique Nucléaire et de Hautes Energies, UPMC and Université Paris-Diderot and CNRS/IN2P3, Paris, France
[80] Fysiska institutionen, Lunds universitet, Lund, Sweden
[81] Departamento de Fisica Teorica C-15, Universidad Autonoma de Madrid, Madrid, Spain
[82] Institut für Physik, Universität Mainz, Mainz, Germany
[83] School of Physics and Astronomy, University of Manchester, Manchester, United Kingdom
[84] CPPM, Aix-Marseille Université and CNRS/IN2P3, Marseille, France
[85] Department of Physics, University of Massachusetts, Amherst MA, United States of America
[86] Department of Physics, McGill University, Montreal QC, Canada
[87] School of Physics, University of Melbourne, Victoria, Australia
[88] Department of Physics, The University of Michigan, Ann Arbor MI, United States of America
[89] Department of Physics and Astronomy, Michigan State University, East Lansing MI, United States of America
[90] [(a)] INFN Sezione di Milano; [(b)] Dipartimento di Fisica, Università di Milano, Milano, Italy
[91] B.I. Stepanov Institute of Physics, National Academy of Sciences of Belarus, Minsk, Republic of Belarus

JHEP09(2014)079

[92] National Scientific and Educational Centre for Particle and High Energy Physics, Minsk, Republic of Belarus
[93] Department of Physics, Massachusetts Institute of Technology, Cambridge MA, United States of America
[94] Group of Particle Physics, University of Montreal, Montreal QC, Canada
[95] P.N. Lebedev Institute of Physics, Academy of Sciences, Moscow, Russia
[96] Institute for Theoretical and Experimental Physics (ITEP), Moscow, Russia
[97] Moscow Engineering and Physics Institute (MEPhI), Moscow, Russia
[98] D.V.Skobeltsyn Institute of Nuclear Physics, M.V.Lomonosov Moscow State University, Moscow, Russia
[99] Fakultät für Physik, Ludwig-Maximilians-Universität München, München, Germany
[100] Max-Planck-Institut für Physik (Werner-Heisenberg-Institut), München, Germany
[101] Nagasaki Institute of Applied Science, Nagasaki, Japan
[102] Graduate School of Science and Kobayashi-Maskawa Institute, Nagoya University, Nagoya, Japan
[103] [(a)] INFN Sezione di Napoli; [(b)] Dipartimento di Fisica, Università di Napoli, Napoli, Italy
[104] Department of Physics and Astronomy, University of New Mexico, Albuquerque NM, United States of America
[105] Institute for Mathematics, Astrophysics and Particle Physics, Radboud University Nijmegen/Nikhef, Nijmegen, Netherlands
[106] Nikhef National Institute for Subatomic Physics and University of Amsterdam, Amsterdam, Netherlands
[107] Department of Physics, Northern Illinois University, DeKalb IL, United States of America
[108] Budker Institute of Nuclear Physics, SB RAS, Novosibirsk, Russia
[109] Department of Physics, New York University, New York NY, United States of America
[110] Ohio State University, Columbus OH, United States of America
[111] Faculty of Science, Okayama University, Okayama, Japan
[112] Homer L. Dodge Department of Physics and Astronomy, University of Oklahoma, Norman OK, United States of America
[113] Department of Physics, Oklahoma State University, Stillwater OK, United States of America
[114] Palacký University, RCPTM, Olomouc, Czech Republic
[115] Center for High Energy Physics, University of Oregon, Eugene OR, United States of America
[116] LAL, Université Paris-Sud and CNRS/IN2P3, Orsay, France
[117] Graduate School of Science, Osaka University, Osaka, Japan
[118] Department of Physics, University of Oslo, Oslo, Norway
[119] Department of Physics, Oxford University, Oxford, United Kingdom
[120] [(a)] INFN Sezione di Pavia; [(b)] Dipartimento di Fisica, Università di Pavia, Pavia, Italy
[121] Department of Physics, University of Pennsylvania, Philadelphia PA, United States of America
[122] Petersburg Nuclear Physics Institute, Gatchina, Russia
[123] [(a)] INFN Sezione di Pisa; [(b)] Dipartimento di Fisica E. Fermi, Università di Pisa, Pisa, Italy
[124] Department of Physics and Astronomy, University of Pittsburgh, Pittsburgh PA, United States of America
[125] [(a)] Laboratorio de Instrumentacao e Fisica Experimental de Particulas - LIP, Lisboa; [(b)] Faculdade de Ciências, Universidade de Lisboa, Lisboa; [(c)] Department of Physics, University of Coimbra, Coimbra; [(d)] Centro de Física Nuclear da Universidade de Lisboa, Lisboa; [(e)] Departamento de Fisica, Universidade do Minho, Braga; [(f)] Departamento de Fisica Teorica y del Cosmos and CAFPE, Universidad de Granada, Granada (Spain); [(g)] Dep Fisica and CEFITEC of Faculdade de Ciencias e Tecnologia, Universidade Nova de Lisboa, Caparica, Portugal
[126] Institute of Physics, Academy of Sciences of the Czech Republic, Praha, Czech Republic
[127] Czech Technical University in Prague, Praha, Czech Republic
[128] Faculty of Mathematics and Physics, Charles University in Prague, Praha, Czech Republic
[129] State Research Center Institute for High Energy Physics, Protvino, Russia
[130] Particle Physics Department, Rutherford Appleton Laboratory, Didcot, United Kingdom

JHEP09(2014)079

[131] Physics Department, University of Regina, Regina SK, Canada
[132] Ritsumeikan University, Kusatsu, Shiga, Japan
[133] [(a)] INFN Sezione di Roma; [(b)] Dipartimento di Fisica, Sapienza Università di Roma, Roma, Italy
[134] [(a)] INFN Sezione di Roma Tor Vergata; [(b)] Dipartimento di Fisica, Università di Roma Tor Vergata, Roma, Italy
[135] [(a)] INFN Sezione di Roma Tre; [(b)] Dipartimento di Matematica e Fisica, Università Roma Tre, Roma, Italy
[136] [(a)] Faculté des Sciences Ain Chock, Réseau Universitaire de Physique des Hautes Energies - Université Hassan II, Casablanca; [(b)] Centre National de l'Energie des Sciences Techniques Nucleaires, Rabat; [(c)] Faculté des Sciences Semlalia, Université Cadi Ayyad, LPHEA-Marrakech; [(d)] Faculté des Sciences, Université Mohamed Premier and LPTPM, Oujda; [(e)] Faculté des sciences, Université Mohammed V-Agdal, Rabat, Morocco
[137] DSM/IRFU (Institut de Recherches sur les Lois Fondamentales de l'Univers), CEA Saclay (Commissariat à l'Energie Atomique et aux Energies Alternatives), Gif-sur-Yvette, France
[138] Santa Cruz Institute for Particle Physics, University of California Santa Cruz, Santa Cruz CA, United States of America
[139] Department of Physics, University of Washington, Seattle WA, United States of America
[140] Department of Physics and Astronomy, University of Sheffield, Sheffield, United Kingdom
[141] Department of Physics, Shinshu University, Nagano, Japan
[142] Fachbereich Physik, Universität Siegen, Siegen, Germany
[143] Department of Physics, Simon Fraser University, Burnaby BC, Canada
[144] SLAC National Accelerator Laboratory, Stanford CA, United States of America
[145] [(a)] Faculty of Mathematics, Physics & Informatics, Comenius University, Bratislava; [(b)] Department of Subnuclear Physics, Institute of Experimental Physics of the Slovak Academy of Sciences, Kosice, Slovak Republic
[146] [(a)] Department of Physics, University of Cape Town, Cape Town; [(b)] Department of Physics, University of Johannesburg, Johannesburg; [(c)] School of Physics, University of the Witwatersrand, Johannesburg, South Africa
[147] [(a)] Department of Physics, Stockholm University; [(b)] The Oskar Klein Centre, Stockholm, Sweden
[148] Physics Department, Royal Institute of Technology, Stockholm, Sweden
[149] Departments of Physics & Astronomy and Chemistry, Stony Brook University, Stony Brook NY, United States of America
[150] Department of Physics and Astronomy, University of Sussex, Brighton, United Kingdom
[151] School of Physics, University of Sydney, Sydney, Australia
[152] Institute of Physics, Academia Sinica, Taipei, Taiwan
[153] Department of Physics, Technion: Israel Institute of Technology, Haifa, Israel
[154] Raymond and Beverly Sackler School of Physics and Astronomy, Tel Aviv University, Tel Aviv, Israel
[155] Department of Physics, Aristotle University of Thessaloniki, Thessaloniki, Greece
[156] International Center for Elementary Particle Physics and Department of Physics, The University of Tokyo, Tokyo, Japan
[157] Graduate School of Science and Technology, Tokyo Metropolitan University, Tokyo, Japan
[158] Department of Physics, Tokyo Institute of Technology, Tokyo, Japan
[159] Department of Physics, University of Toronto, Toronto ON, Canada
[160] [(a)] TRIUMF, Vancouver BC; [(b)] Department of Physics and Astronomy, York University, Toronto ON, Canada
[161] Faculty of Pure and Applied Sciences, University of Tsukuba, Tsukuba, Japan
[162] Department of Physics and Astronomy, Tufts University, Medford MA, United States of America
[163] Centro de Investigaciones, Universidad Antonio Narino, Bogota, Colombia
[164] Department of Physics and Astronomy, University of California Irvine, Irvine CA, United States of America
[165] [(a)] INFN Gruppo Collegato di Udine, Sezione di Trieste, Udine; [(b)] ICTP, Trieste; [(c)] Dipartimento di Chimica, Fisica e Ambiente, Università di Udine, Udine, Italy

JHEP09(2014)079

[166] Department of Physics, University of Illinois, Urbana IL, United States of America
[167] Department of Physics and Astronomy, University of Uppsala, Uppsala, Sweden
[168] Instituto de Física Corpuscular (IFIC) and Departamento de Física Atómica, Molecular y Nuclear and Departamento de Ingeniería Electrónica and Instituto de Microelectrónica de Barcelona (IMB-CNM), University of Valencia and CSIC, Valencia, Spain
[169] Department of Physics, University of British Columbia, Vancouver BC, Canada
[170] Department of Physics and Astronomy, University of Victoria, Victoria BC, Canada
[171] Department of Physics, University of Warwick, Coventry, United Kingdom
[172] Waseda University, Tokyo, Japan
[173] Department of Particle Physics, The Weizmann Institute of Science, Rehovot, Israel
[174] Department of Physics, University of Wisconsin, Madison WI, United States of America
[175] Fakultät für Physik und Astronomie, Julius-Maximilians-Universität, Würzburg, Germany
[176] Fachbereich C Physik, Bergische Universität Wuppertal, Wuppertal, Germany
[177] Department of Physics, Yale University, New Haven CT, United States of America
[178] Yerevan Physics Institute, Yerevan, Armenia
[179] Centre de Calcul de l'Institut National de Physique Nucléaire et de Physique des Particules (IN2P3), Villeurbanne, France

[a] Also at Department of Physics, King's College London, London, United Kingdom
[b] Also at Institute of Physics, Azerbaijan Academy of Sciences, Baku, Azerbaijan
[c] Also at Particle Physics Department, Rutherford Appleton Laboratory, Didcot, United Kingdom
[d] Also at TRIUMF, Vancouver BC, Canada
[e] Also at Department of Physics, California State University, Fresno CA, United States of America
[f] Also at Tomsk State University, Tomsk, Russia
[g] Also at CPPM, Aix-Marseille Université and CNRS/IN2P3, Marseille, France
[h] Also at Università di Napoli Parthenope, Napoli, Italy
[i] Also at Institute of Particle Physics (IPP), Canada
[j] Also at Department of Physics, St. Petersburg State Polytechnical University, St. Petersburg, Russia
[k] Also at Chinese University of Hong Kong, China
[l] Also at Department of Financial and Management Engineering, University of the Aegean, Chios, Greece
[m] Also at Louisiana Tech University, Ruston LA, United States of America
[n] Also at Institucio Catalana de Recerca i Estudis Avancats, ICREA, Barcelona, Spain
[o] Also at CERN, Geneva, Switzerland
[p] Also at Ochadai Academic Production, Ochanomizu University, Tokyo, Japan
[q] Also at Manhattan College, New York NY, United States of America
[r] Also at Novosibirsk State University, Novosibirsk, Russia
[s] Also at Institute of Physics, Academia Sinica, Taipei, Taiwan
[t] Also at LAL, Université Paris-Sud and CNRS/IN2P3, Orsay, France
[u] Also at Academia Sinica Grid Computing, Institute of Physics, Academia Sinica, Taipei, Taiwan
[v] Also at Laboratoire de Physique Nucléaire et de Hautes Energies, UPMC and Université Paris-Diderot and CNRS/IN2P3, Paris, France
[w] Also at School of Physical Sciences, National Institute of Science Education and Research, Bhubaneswar, India
[x] Also at Dipartimento di Fisica, Sapienza Università di Roma, Roma, Italy
[y] Also at Moscow Institute of Physics and Technology State University, Dolgoprudny, Russia
[z] Also at Section de Physique, Université de Genève, Geneva, Switzerland
[aa] Also at Department of Physics, The University of Texas at Austin, Austin TX, United States of America
[ab] Also at International School for Advanced Studies (SISSA), Trieste, Italy
[ac] Also at Department of Physics and Astronomy, University of South Carolina, Columbia SC, United States of America

JHEP09(2014)079

[ad] Also at School of Physics and Engineering, Sun Yat-sen University, Guangzhou, China
[ae] Also at Faculty of Physics, M.V.Lomonosov Moscow State University, Moscow, Russia
[af] Also at Physics Department, Brookhaven National Laboratory, Upton NY, United States of America
[ag] Also at Moscow Engineering and Physics Institute (MEPhI), Moscow, Russia
[ah] Also at Institute for Particle and Nuclear Physics, Wigner Research Centre for Physics, Budapest, Hungary
[ai] Also at Department of Physics, Oxford University, Oxford, United Kingdom
[aj] Also at Department of Physics, Nanjing University, Jiangsu, China
[ak] Also at Institut für Experimentalphysik, Universität Hamburg, Hamburg, Germany
[al] Also at Department of Physics, The University of Michigan, Ann Arbor MI, United States of America
[am] Also at Discipline of Physics, University of KwaZulu-Natal, Durban, South Africa
[*] Deceased

JHEP09(2014)079